N GT-21-002-080
NGT-80001

# The MPR-300 Reactor System for use in Martian Applications

(NASA-CR-184747) THE MPR-300 REACTOR SYSTEM FOR USE IN MARTIAN APPLICATIONS Final Report (Texas A&M Univ.) 141 p

N89-70330

Unclas
00/73 0189682

by

Ted G. Bagwell
Oscar J. Lessard
John A. Rennie
Sandra M. Sloan
John D. Valentine

Texas A&M Univ.,
College Station

## Table of Contents

# I. Attributes

All project members had an active role in the development of this project. The decision on which project to do, and well as the major decisions of the final project, were a collaborative effort by the entire group. The calculations of the individual systems were divided among the specific group members. Table I.1 basically shows the tasks assigned to each group member.

Table I.1 Member Responsibilities

| | |
|---|---|
| Ted G. Bagwell | • group leader<br>• coordination of activities<br>• reactor thermal-hydraulics |
| Oscar J. Lessard | • core neutronics<br>• materials considerations<br>• background research in gas reactors |
| John A. Rennie | • space logistics<br>• micrometeroid shielding<br>• solar irradiation analysis |
| Sandra M. Sloan | • heat rejection system |
| John Valentine | • cycle thermodynamics<br>• radiation shielding<br>• turbomachinery |

## II. Introduction

The motivation behind the design project was to provide power for propulsion for an unmanned GEO to Mars mission in a 2 to 6 month time span and to provide 6 years of terrestrial power on Mars. Research was conducted on the German HTR reactor, current U.S. government journal articles on particle bed space reactors, and the British MAGNOX carbon dioxide reactor of the 1960's. After this background research it was determined that a carbon dioxide gas cooled pebble fueled reactor would be feasible to meet our initial motivation. The main reasons for this choice were the availability of carbon dioxide on the Martian surface and the small reactor size with high power densities achieved with particulate type fuel.

The design objectives consisted of obtaining an approximate electrical power level of 300 kW in order to provide power for MPD thrusters for the GEO to Mars journey and obtaining a high cycle efficiency in order to keep the reactor thermal power output around 1 MW. The entire system mass objective was under 10,000 kg in order to ensure that the system could feasibly fit on one shuttle payload. This led to the choice of heat pipe radiators for waste heat rejection as the total mass of the heat rejection system was of utmost concern. The reliability provided by a redundant system was another design objective in order to meet mission goals.

The report outline consists of seven different sections which are contained in the body of the report. The first section consists of neutronics which calculates flux distributions and fuel requirements. The second section is made up of thermal-hydraulics considerations for calculating reactor core temperature and pressure characteristics. Section three consists of the thermodynamic cycle calculations which defines states and arrives at an overall cycle efficiency. The turbomachinery selections can be seen in section four. The heat pipe radiators for waste heat rejection are explained in section five. The sixth section contains the shadow shield configuration necessary to protect electronic components from radioactivity. Section seven is comprised of propulsion and space logistics in order to succesfully complete the GEO to Mars mission.

# III. Body

# 1. NEUTRONICS

## Introduction:

A pebble bed nuclear space reactor is needed to supply power for propulsion and instrumentation from GEO to Mars and to supply terrestrial power on the Martian surface. The entire lifetime of the reactor is limited to seven years. The power required is one megawatt thermal.

The concept of the pebble bed reactor is based on a combination of the German HTR and recent research on the fixed particle bed space reactor. The advantages of this type of reactor are its small size and its high power density due to the large surface area of the fuel particles [1]. The gas coolant will be carbon dioxide because of the availability of this gas on the Martian surface. The Martian atmosphere is over 80% $CO_2$ . The use of $CO_2$ in a reactor is based on the British MAGNOX reactor of the 1960's [2]. The only serious problems encountered with this design is the carbon dioxide and graphite corrosion activation at temperatures exceeding 810K.

The conceptual design of the pebble bed reactor can be seen in figure 1.1. The turbine-compressor drive shaft goes through the center of the reactor and $BeO/B_4C$ control drums are used for reactivity control. The fuel is a BISO type consisting of UN fuel and a PyC cladding. A very thin coating of stainless steel makes up the outer surface of the fuel pebble in case temperatures exceed the 810K discussed above. It can be observed that this is an axial flow pebble bed reactor.

## General Assumptions:

Certain assumptions were made before neutronics calculations could be accomplished. Since the reactor core consisted of an annular cylindrical shape, it was difficult to choose a corresponding computer code for neutronics calculations. It was finally decided that a two group approximation using a finite difference approach would be used. This allowed one to determine the radial flux profile by breaking the center turbine-compressor, the reactor vessel walls, the reactor core, and the control drums into separate regions for neutron flux approximations. The axial

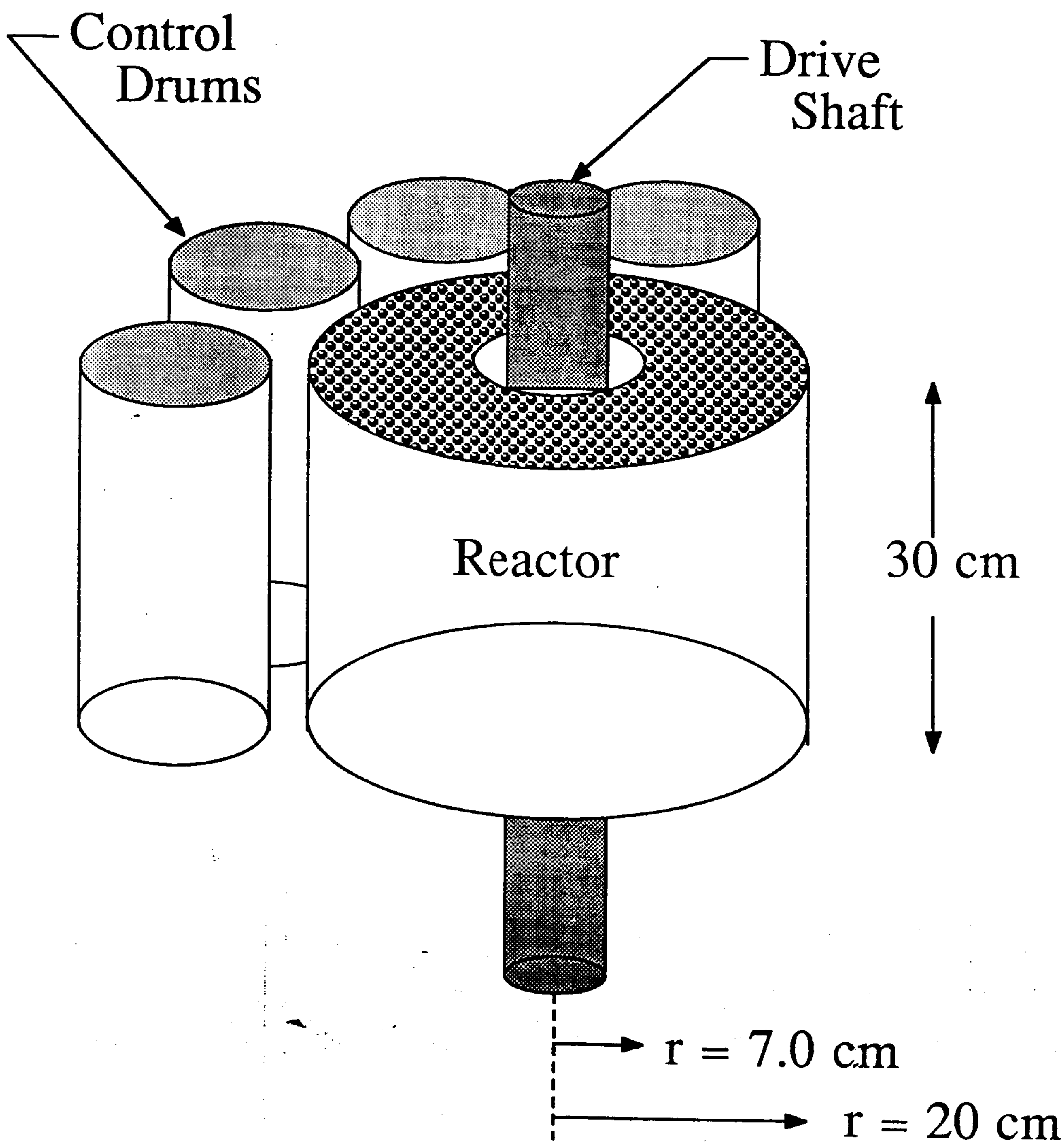


Figure 1.1 Conceptual Reactor Design

neutron flux distribution was then assumed to be a cosine shape which is the normal case for cylindrical geometry.

The gas coolant voiding in the reactor core was assumed to be 37%. This is true as long as the annular radius is larger than five fuel pebble diameters [3]. The other 63% of the reactor core volume was assumed to consist of equal volumes of fuel and cladding. This was considered a reasonable estimate as the fuel radius was 79% of the entire fuel pebble radius. This should allow sufficient fission product gathering in the BISO fuel pebble. The fuel pebble concept can be seen in figure 1.2.

The center turbine-compressor shaft was used as it was our intention to have a reactor diameter equalling that of the turbine and compressor. This would allow for a jet engine type arrangement where the turbine and compressor are welded directly to the reactor vessel. This would also allow for reduced piping and reduced overall area required for the reactor assembly.

The choice of the center shaft made it necessary for one to have an intermediate reactor instead of a fast reactor. This reactor type was chosen to keep the fast neutron flux as low as possible on the surface of the shaft. Neutron embrittlement could become a serious problem if the center shaft is exposed to high neutron fluxes.

These are a few of the general assumptions needed before neutronics modelling could be considered. Many other minor assumptions will be discussed in the text as deemed necessary.

**Neutron Flux Modelling:**

The DIF2DK two group, one dimensional diffusion theory code supplied in the NUEN 429, Spring 1987 course was used for neutronics modelling. The two group equations as solved by the computer code are written as [4]:

$$\nabla \cdot D_1 \nabla \phi_1 - \Sigma_{a_1} \phi_1 - \Sigma_{1\to 2} \phi_1 + \frac{1}{K_{eff}} \left( \nu \Sigma_{f_1} \phi_1 + \nu \Sigma_{f_2} \phi_2 \right) = 0 \quad (1.1)$$

and

$$\nabla \cdot D_2 \nabla \phi_2 - \Sigma_{a_2} \phi_2 + \Sigma_{1\to 2} \phi_1 = 0 \quad (1.2)$$

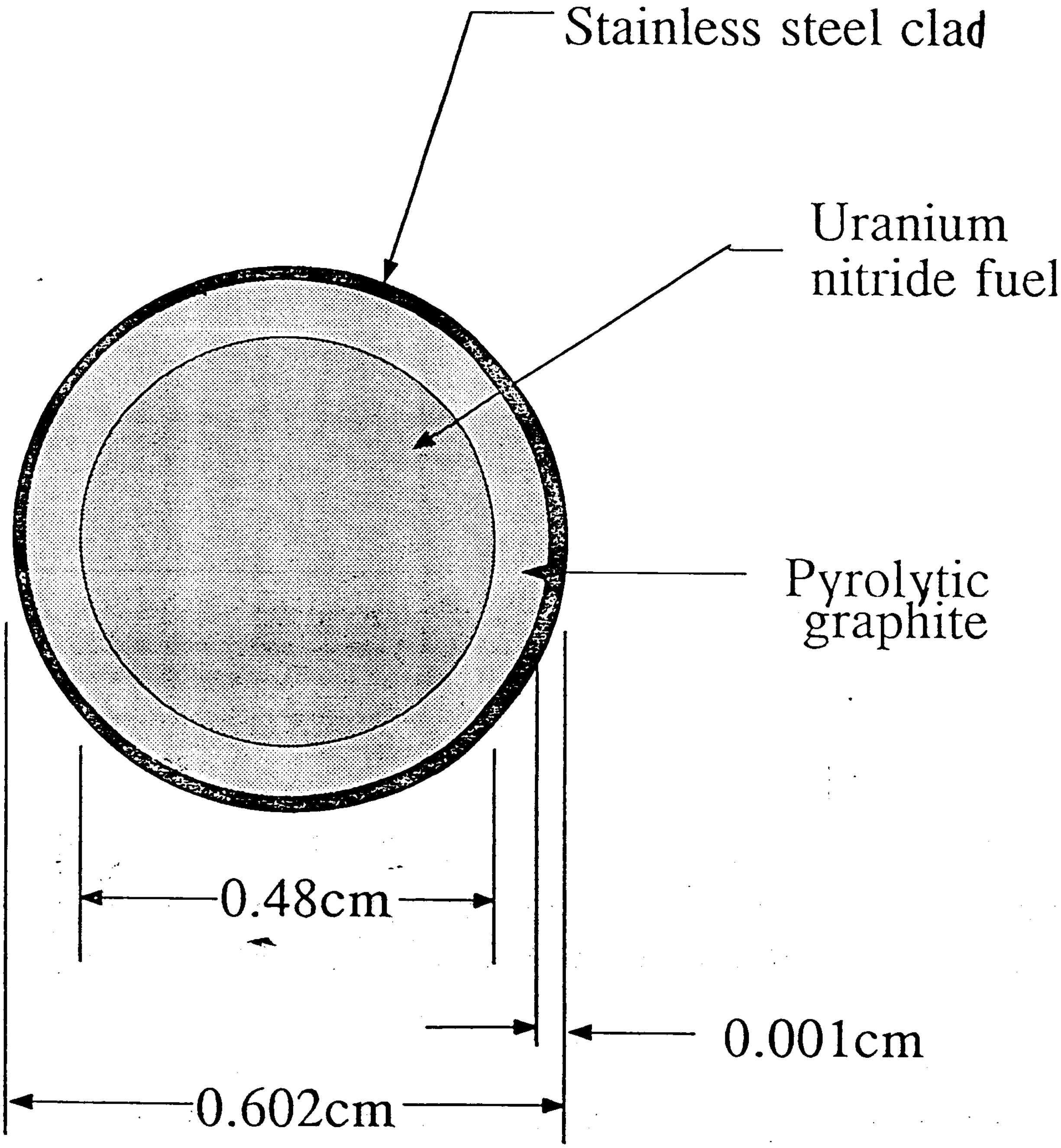


Figure 1.2 Pebble Fuel Design

where :

$D_1$ = fast group diffusion coefficient
$D_2$ = thermal group diffusion coefficient
$K_{eff}$ = multiplication factor
$\Sigma_{a_1}$ = macroscopic fast group absorption cross section
$\Sigma_{a_2}$ = macroscopic thermal absorption cross section
$\Sigma_{1\to 2}$ = macroscopic slowing down cross section
$\Sigma_{f_1}$ = macroscopic fission cross section (fast)
$\Sigma_{f_2}$ = macroscopic fission cross section (thermal)
$\nu$ = neutrons released per fission
$\phi_1$ = fast neutron flux
$\phi_2$ = thermal neutron flux

The code was slightly modified to accept the inputed thermal power and energy per fission to calculate the actual neutron flux values in the radial direction. The equations used were:

$$A = \frac{P}{K \sum_{i=1}^{N} \left( \nu \Sigma_{f_i} \frac{\Delta_i}{2} + \nu \Sigma_{f_{i+1}} \frac{\Delta_{i+1}}{2} \right) \tilde{\phi}_i} \quad (1.3) \qquad \text{and} \qquad \phi_i = a \tilde{\phi}_i \quad (1.4)$$

where : $P$ = power in MeV
$K$ = energy per fission
$\tilde{\phi}_i$ = normalized flux
$\phi_i$ = actual flux
$\nu$ = neutrons released per fission
$\Sigma_f$ = macroscopic fission cross section
$i$ = number of intervals in finite difference approach

A finite difference approach is used to solve the two group problem. This allows one to define different material regions and the input of DIF2DK requires the neutronic properties of each of these regions. These properties are the diffusion coefficient and the macroscopic absorption, slowing down, and nu-fission cross sections.

A computer code called START was written to solve for the properties needed for the DIF2DK input deck. The microscopic absorption, slowing down, nu-fission, and transport cross sections are required in order to calculate the properties needed. In order to come up with the two group microscopic cross sections, it was necessary to use the computer code ANISN to collapse the 27 group cross sections. For this intermediate reactor the thermal group was defined from 0 to 1 ev and the fast group was defined from 1 ev to infinity. This is an accepted energy group distribution for an intermediate reactor [5]. The code START calculates the required number densities from the given material densities in order to determine the macroscopic cross sections as follows:

$$N = \frac{\rho A_o}{M} \qquad (1.5)$$

where :

$N$ = atom number density

$A_o$ = Avogadro's number $(6.02 \times 10^{23})$

$\rho$ = density

$M$ = atomic or molecular weight

The diffusion coefficient is determined by:

$$D = \frac{1}{3 \Sigma_{tr}} \qquad (1.6)$$

where :

$D$ = diffusion coefficient

$\Sigma_{tr}$ = macroscopic transport cross section

The detailed input deck of START can be seen in table 1.1 and the output description can be seen in table 1.2.

The START program is capable of accepting different fuel enrichments, fuel and cladding volume ratios, and fraction of BeO seen in the control drum compared to $B_4C$ in the radial direction. The output of START is then used as the input to DIF2DK. The input deck of DIF2DK is desribed in table 1.3. The stainless steel reactor vessel walls and the center turbine-compressor

**Table 1.1**
**Input Deck of START**

The order of microscopic cross section input is as follows:
absorption, slowing down, nu-fission, and transport

Line 1: Oxygen-16, fast
Line 2: Oxygen-16, thermal
Line 3: Uranium-235, fast
Line 4: Uranium-235, thermal
Line 5: Uranium-238, fast
Line 6: Uranium-238, thermal
Line 7: Carbon-12, fast
Line 8: Carbon-12, thermal
Line 9: Iron, fast
Line 10: Iron, thermal
Line 11: Beryllium-9, fast
Line 12: Beryllium-9, thermal
Line 13: Boron, fast
Line 14: Boron, thermal
Line 15: Nitrogen, fast
Line 16: Nitrogen, thermal

**Table 1.2:**
**Output of START**

Line 1: Macroscopic absorption cross sections in the following order:
U-235 fast, U-235 thermal, U-238 fast, U-238 thermal
Line 2: Macroscopic nu-fission cross sections in the same order

The remaining lines have the following output order:
diffusion coefficient, macroscopic absorption cross section, macroscopic slowing down cross section, macroscopic nu-fission cross section

Line 3: Reactor core properties, fast
Line 4: Reactor core properties, thermal
Line 5: Reactor vessel walls and center shaft properties, fast
Line 6: Reactor vessel walls and center shaft properties, thermal
Line 7: Control drum properties, fast
Line 8: Control drum properties, thermal

**Table 1.3:**
**Input Deck of DIF2DK**

Line 1: # of regions, # of materials, fractional convergence criterion, thermal power (Mev), energy per fission

Line 2: geometry (2-cylinder), left B.C. (1-symmetry), right B.C. (0-zero flux at extr. boundary)

Line 3: region #1, material in region, # intervals in region, region thickness

Line 4: same as above for region #2

Line 5: same as above for region #3

Line 6: same as above for region #4

Line 7: material #1, fast diffusion coefficient, fast macroscopic absorption cross section, fast macroscopic slowing down cross section, fast macroscopic nu-fission cross section

Line 8: same as line 7 for thermal properties

Line 9: same as above for material #2 fast properties

Line 10: same as above for material #2 thermal properties

Line 11: same as above for material #3 fast properties

Line 12: same as above for material #3 thermal properties

** regions

1) center shaft and inner vessel wall
2) reactor core
3) outer vessel wall
4) control drums

** materials

1) homogeneous reactor core
2) iron
3) contol drums (BeO/$B_4C$)

shaft were assumed to be iron for neutron cross section purposes. The reactor core was assumed to be a homogeneous mixture of equal volume PyC cladding and UN fuel and a volume fraction of 0.37 of $CO_2$ gas. The control drums were assumed to be one region with the option of varying the amounts of BeO and $B_4C$. The output of the DIF2DK program consists of the normalized fast and thermal neutron fluxes, the actual fluxes and the value of Keff. START and DIF2DK program listings can be seen in appendices 1.1 and 1.2 respectively.

### Neutron Flux Calculations:

The initial inputs of the DIF2DK program consisted of a 7 cm region of center shaft and inner vessel wall (3 cm shaft radius and 4 cm inner vessel wall region), a 10 cm region of reactor core, a 3 cm region of outer vessel wall, and a 20 cm region of control drums. The fuel enrichment and annular core radius were varied numerous times and it was finally determined that a fuel enrichment of 5.6% resulted in a 12.8 cm annular core radius for criticality or Keff equal to one. An infinite reflector (control drum) was approached with a region equal to 10 cm. This was a good result as it produced a reactor assembly of about 65 cm in total diameter which compares favorably well with turbine and compressor diameters. It was also a favorable result when considering the magnitude of the neutron flux at the center drive shaft surface. The thermal and fast flux profiles can be seen in figures 1.3 and 1.4 respectively. The fast flux at the surface of the shaft was less than 4E14 and the thermal flux was less than 2E13. These flux values do not produce any neutron embrittlement problems for the steel shaft.

The ratio of the fast flux to thermal flux throughout the reactor core was on the order of 15 to 1 with the peak fast flux in the core being 7.3E14 and the peak thermal flux being 4.7E13. The peak to average flux ratio for both thermal and fast fluxes was on the order of 1.12. The average flux ratio was calculated by averaging the 20 data points within the core. This peak to average flux ratio and the average fluxes were passed on for thermohydraulic considerations. The equation used to break the power into fast and thermal components is given by:

$$q''' = K\left[(\Sigma_{f28}\,\phi_1 + \Sigma_{f25}\,\phi_1)_{fast} + (\Sigma_{f28}\,\phi_2 + \Sigma_{f25}\,\phi_2)_{slow}\right] \quad (1.7)$$

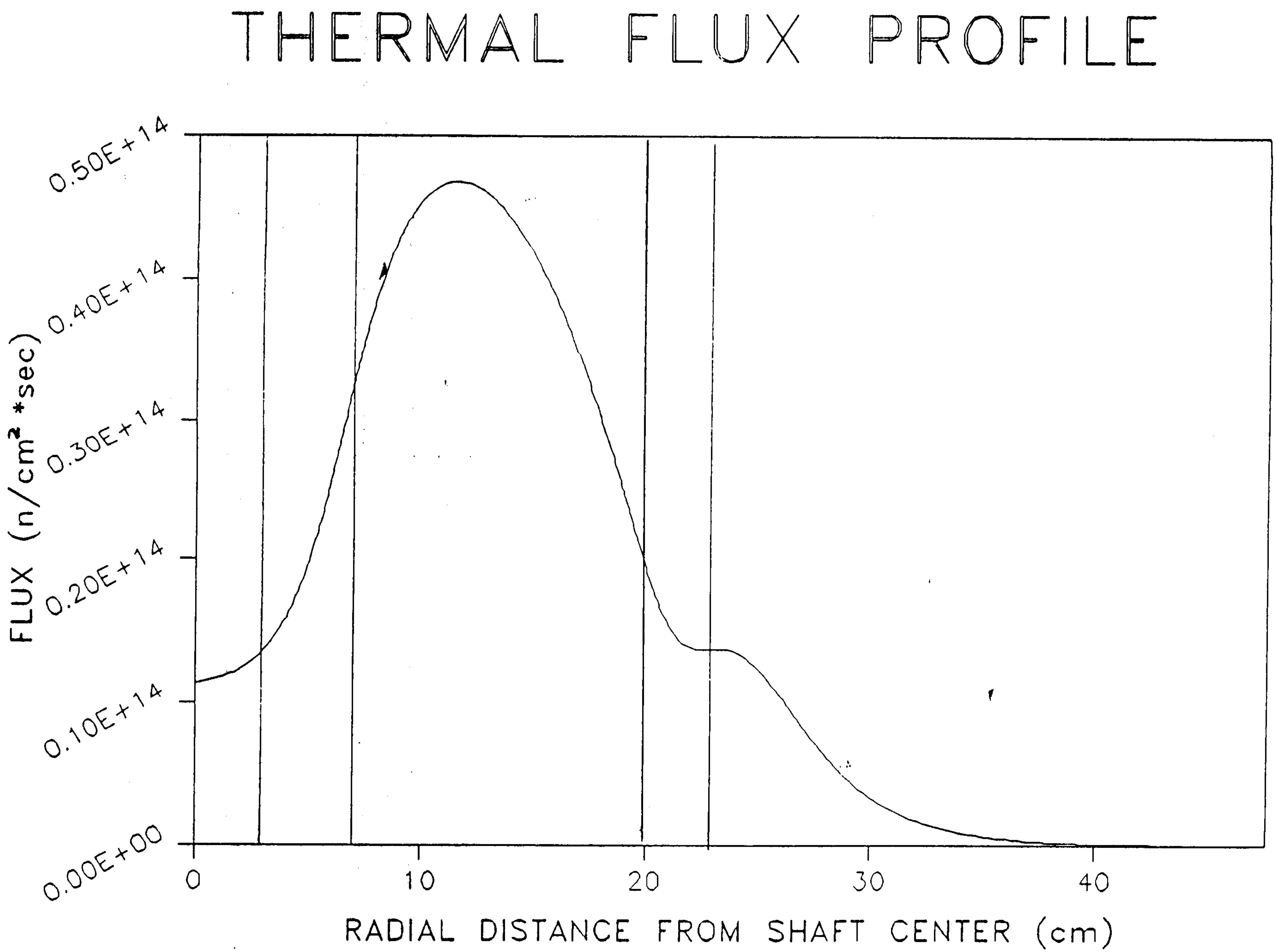


Figure 1.3 Thermal Flux Profile

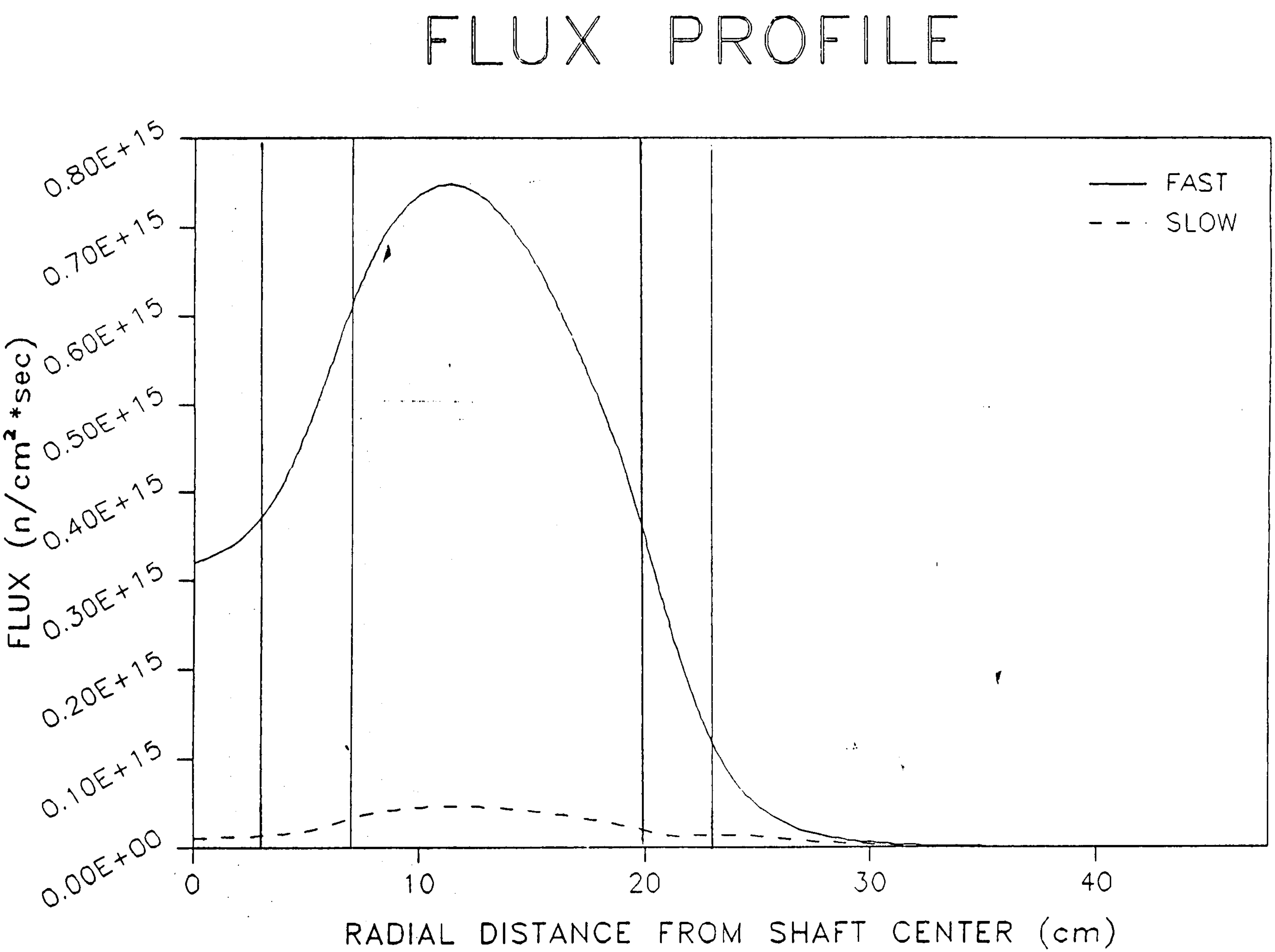


Figure 1.4 Fast and Thermal Flux Profile

where :

$q'''$ = power density

$K$ = energy released per fission

$\Sigma_{f28}$ = macrosiopic fission cross section of U-238

$\Sigma_{f25}$ : macroscopic fission cross section of U-235

$\phi_1$ = fast flux

$\phi_2$ = thermal flux

After performing the calculation it was observed that 91% of the power is generated by the thermal flux as is expected even though the fast flux magnitude is much greater.

The method used to account for fuel burnup during the seven year lifetime will be to increase the fuel enrichment. The axial flux distribution will be of the cosine shape as discussed previously for cylindrical geometry. The annular radius of 12.8 cm of the core can be turned into an equivalent cylinder radius by assuming that the volume of the annular core is equal to the volume of a cylinder. The equivalent cylinder radius becomes 18.5 cm. With a reactor height of 30 cm, the height to diameter ratio of the reactor core becomes 30/37 or 0.81. This value compares well to the other HTGR reactors which have height to diameter ratios of 0.75 to 0.90. A complete summary of reactor parameters can be seen in table 1.4.

**Fuel Burnup Considerations:**

The burnup of U-235 in the UN fuel in the reactor core is due to consumption by fission and parasitic absorption of U-235 by radioactive capture. Assuming a thermal reactor, the equation used to calculate the burnup of U-235 is given by [6]:

$$\text{Consumption rate} = 1.05\,(1+\alpha)\,P \quad \text{g/day} \qquad (1.8)$$

**Table 1.4:**
**Reactor Parameters**

| | |
|---|---|
| Thermal Output | 1 MWt |
| Electrical Output | 300 kWe |
| Power Density | 3.1 W/cm$^3$ |
| Active Core Volume | 32,330 cm$^3$ |
| CO2 fraction | 0.37 |
| UN fraction | 0.315 |
| PyC fraction | 0.315 |
| Peak to Average Flux Ratio | 1.12 |
| Power Production | |
| Thermal Flux | 91% |
| Fast Flux | 9% |
| Control Drum Diameter | 10 cm |
| Reactor core annular radius | 12.8 cm |
| Central Shaft Diameter | 6 cm |
| Reactor Vessel Wall Diameter | |
| inner | 4 cm |
| outer | 3 cm |
| Peak Fluxes | |
| thermal | 4.7E13 |
| fast | 7.3E14 |
| Reactor Height | 30 cm |
| Height to diameter ratio | 0.81 |

where :

$\alpha$ = 0.169 which is the radiative capture or parasitic absorption factor

$P$ = power in MeV

The value of alpha accounts for the parasitic absorptions and is 0.169 for U-235. Using the above equation it can be seen that 3.16 kg of U-235 will be consumed during the seven year lifetime. Since 7.61 kg of U-235 is available for the 5.6% enriched reactor fuel, it can be calculated that an 8.0% enriched fuel is needed for a total of 10.77 kg of U-235 at reactor startup. Detailed calculations on fuel burnup can be seen in appendix 1.3. The value of Keff at startup using DIF2DK and the 8.0% enriched fuel is 1.228.

**Poisoning Considerations:**

Since this is an intermediate reactor, the fission product poisoning of Xenon-135 and Samarium-149 can be neglected. This is true as the buildup of these fission products is negligible in an intermediate space reactor.

**Decay Heat Considerations:**

After a few days of reactor operation, the beta and gamma radiation emitted from decaying fission products amounts to approximately seven percent of the total thermal power output of the reactor. For the one megawatt reactor, the amount of power available at shutdown due to decay heat will be slightly less than 70 watts of thermal power. Recall that 91% of the power produced is from the thermal spectrum. At any time after shutdown, the ratio of power due to decay heat to the original power is given by[7]:

$$* \quad \frac{P(t_0, t_s)}{P_0} = \frac{P(t_s)}{P_0} - \frac{P(t_0 + t_s)}{P_0} \qquad (1.9)$$

where :

$P$ = power

$P_0$ = original power before shutdown

$t_o$ = finite time of reactor operation

$t_s$ = time since reactor shutdown

* Use Figure 8.3 of "Introduction to Nuclear Engineering" by Lamarsh to obtain results

The use of this equation along with the guidance in Lamarsh [7] results in an available power of about 14 watts at one hour after shutdown. This decay heat has been considered and should not be of much concern because of the low power output of the pebble bed space reactor. A method of cooling could be accomplished by circulating the gas coolant through the core after shutdown.

**Fuel Considerations:**

The fuel pebble is 0.602 cm in diameter and is composed of equal volumes of 8.0% enriched uranium nitride fuel and pyrolitic graphite cladding thus forming a BISO type fuel pebble. The PyC was chosen because of its outstanding heat transfer and fission product gathering characteristics as revealed by previous space reactor design work [1]. A thin coat of stainless steel is placed on the outer surface of the fuel pebble in case the coolant temperature in the core exceeds 810K [8]. At this temperature the $CO_2$ coolant and PyC cladding of the fuel will undergo corrosion activation. The equal volumes of fuel and cladding result in the fuel radius being 79% of the entire fuel radius. This provides plenty of fission product gathering when comparing the fuel pebble to other BISO fuels. After simple volume and number density calculations (see appendix 1.3), a list of fuel characteristics was created in table 1.5.

**Control Drums and Reactivity Control:**

The BeO and $B_4C$ control drums serve as a means for reactivity control. There are a total of seventeen 10 cm diameter drums surrounding the reactor core. 120° of the drum is made up of the boron absorber and the other 240° is made up of the beryllium reflector. The drums are capable of

**Table 1.5:**
**Fuel Characteristics**

| | |
|---|---|
| UN Fuel Mass | 145.7 kg |
| Fuel Enrichment | 8.0% |
| Mass of U-235 | 10.8 kg |
| critical mass at startup | 7.6 kg |
| fuel burnup | 3.2 kg |
| Specific Power | 6.86 kW/kg UN |
| # of Fuel Pebbles | 180,000 |
| Pebble Diameter | 0.602 cm |

adding positive or negative reactivity by letting the reactor core see either the reflector or absorber in the radial direction. Any combination of reflector and absorber is possible with the control drum method.

The reactor also has a mechanism to inject a poison boron dust to cause reactor shutdown as the boron in the control drums may or may not have the capability of shutting down the reactor especially just after startup.

### Other Materials Considerations:

The top and bottom of the reactor core are constructed with a porous grate to allow maximum carbon dioxide flow with enough support to hold the fuel pebbles in place. The thermohydraulics section will discuss these grates in more detail.

The center turbine-compressor drive shaft design is limited by the temperature, the neutron flux at its surface, and the speed of rotation. The maximum temperature will be less than 1000K and the maximum surface flux will be 4E14. These two factors along with normal turbine and compressor drive shaft rotation will allow for the use of almost any ordinary steel. The shaft will be made of a high quality steel of 6 cm in diameter. This should allow for no malfunctions of the shaft due to fatigue or shearing stresses over the seven year lifetime of the system.

The radius of the inner reactor vessel wall is 4 cm thick and the outer vessel wall is 3 cm thick. The extra 1 cm of the inner wall is used to help reduce the neutron flux at the drive shaft surface.

### Masses of the Reactor System:

The masses of the reactor system were calculated using the volumes and densities as follows:

$$m = V\rho \qquad (L.10)$$

where :

$m$ = mass
$\rho$ = density of reactor component
$V$ = volume of reactor component

The sample calculations can be seen in appendix 1.3 and the masses of the reactor system can be seen in table 1.6. The mass of the control drum drive assembly was assumed to equal the mass of the 17 control drums. This appeared to be a conservative estimate.

**Conclusion and Recommendations:**

The pebble bed space reactor has been designed after many iterations of optimization and appears to have a good chance of becoming reality. Future work would consist of even more iterations of the entire system and more in depth studies of the effects and reliability of the center drive shaft. A smaller reactor system with higher fuel enrichments may be a possible alternative also.

**Table 1.6:**
**Reactor System Masses**

| | |
|---|---|
| UN fuel | 145.7 kg |
| PyC cladding | 16.3 kg |
| $CO_2$ | 0.02 kg |
| Steel shaft, vessel walls | 131.0 kg |
| Control drums | 114.5 kg |
| Control drum drive assembly | 114.5 kg |
| Total reactor system | 522 kg |

## References:


1) J.R. Powell and T.E. Potts, "FBR and RBR Particle Bed Space Reactors", BNL-33058, 8 pages, Aug 1983.

2) G.R. Bainbridge and T.N. Marsham, "Three Generations of Nuclear Power Stations", (United Kingdom Atomic Energy Authority, Risley, England), J. Inst. Fuel, 41, 280-8, Jul 1968.

3) S. T. Robinson, " The Pebble Bed Reactor ", Proceedings of the Symposium on Gas Cooled Reactors, Journal of the Franklin Institute, Lancaster, Pa, p. 94, 1960.

4) DIF2DK Computer Code, Dr. Parrish, NUEN 429, Spring 1987.

5) ANL-5800, Nuclear Reactor Constants, USAEC , p. 581, Jul 1963.

6) J.R. Lamarsh, "Introduction to Nuclear Engineering", Chap 3, p. 78, Addison-Wesley Publishing Company, Reading Mass., 1983.

7) Lamarsh, Chap 8, p.350-2.

8) J.K. Pickard, "Nuclear Power Reactors", Chap 8, p. 310-2, D. Van Nostrand Company Inc, Princeton NJ, 1957.

Appendix 1.1

DIF2DK Code

```
         4         3     .0001        1.0      200.0
         2         1         0
         1         2         7          7
         2         1        20       12.8
         3         2         3          3
        -4         3        20         25
         1    .84061    .16336     .01806     .06709
         1    .38590    .10622        0.0    1.09040
         2    .55914    .01214     .02300        0.0
         2    .30157    .18987        0.0        0.0
         3    .59471    .00038     .09287        0.0
         3    .49701    .00067        0.0        0.0
```

```
C
C-------------------------------------------------------------------
C
C        THIS PROGRAM WILL SOLVE THE TWO GROUP-ONE
C        DIMENSIONAL FINITE DIFFERENCE APPROXIMATION
C        TO THE DIFFUSION EQUATION.  THE NEUTRON SOURCE
C        IS DUE ONLY TO FISSION AND THEREFORE THE SOLUTION
C        CONSISTS OF DETERMINING KEFF(LARGEST EIGENVALUE) AND
C        THE NORMALIZED FLUX(FUNDAMENTAL MODE)SHAPE.
C        SEVERAL MATERIALS AND BOTH  VACUUM AND SYMMETRY
C        BOUNDARY CONDITIONS ARE ALLOWED. UP TP 20 REGIONS
C        CAN BE USED WITH SLAB,CYLINDER,AND SPHERE GEOMETRIES.
C
C-------------------------------------------------------------------
C
C        LIST OF PARAMETERS
C
C-------------------------------------------------------------------
C        M = NUMBER OF MATERIALS BEING CONSIDERED (MAX=20)
C       TH = THICKNESS OF MATERIAL SECTIONS
C      INT = NUMBER OF MESH INTERVALS PER MATERIAL
C       DM = DIFFUSION COEFFICIENT
C     SIGA = ABSORPTION CROSS SECTION
C      FIS = NU TIMES FISSION CROSS SECTION
C        D = EXTRAPOLATION LENGTH
C      XKN = NEW K-EFFECTIVE APPROX.
C      XKO = OLD K-EFFECTIVE APPROX.
C    XLAMN = NEW EIGENVALUE APPROX.
C    XLAMO = OLD EIGENVALUE APPROX.
C    FLUXN = NEW FLUX APPROX.
C    FLUXO = OLD FLUX APPROX.
C     IBNL = INDICATOR FOR LEFT BOUNDARY CONDITION
C     IBNR = INDICATOR FOR RIGHT BOUNDARY CONDITION
C
C
C-------------------------------------------------------------------
C-------------------------------------------------------------------
C
C     SIZE IS LIMITED TO 100 MESH INTERVALS
C
C-------------------------------------------------------------------
C-------------------------------------------------------------------
C
C-------------------------------------------------------------------
C
C        READ IN INITIAL VALUES FOR PROBLEM DESCRIPTION
```

1.1

```
C     ASSIGN VALUES TO THE MESH
C
C-----------------------------------------------------------------
C
      NPTS=0
      DO 101 L=1,NREG
 101  NPTS=NPTS+INT(L)
      NPTS=NPTS+1
      NPTS1=NPTS-1
      DO 102 L=1,NREG
 102  DT(L)=TH(L)/INT(L)
      X(1)=0.0
      L2=1
      DO 103 L=1,NREG
      LXX=INT(L)
      DO 104 L1=1,LXX
      J=MR(L)
      L2=L2+1
      X(L2)=X(L2-1)+DT(L)
      DIFC(L2)=DM(1,J)
      SABS(L2)=SIGA(1,J)
      STR(L2)=SIG12(1,J)
      XNF(L2)=FIS(1,J)
      DIFT(L2)=DM(2,J)
      SABT(L2)=SIGA(2,J)
      XNT(L2)=FIS(2,J)
      DX(L2)=X(L2)-X(L2-1)
 104  CONTINUE
 103  CONTINUE
      WRITE(6,7171)
      WRITE(6,466)
      DIFC(1)=0.0
      SABS(1)=0.0
      STR(1)=0.0
      XNF(1)=0.0
      DO 488 I=1,NPTS
 488  WRITE(6,467)I,X(I),DIFC(I),SABS(I),STR(I),XNF(I)
 467  FORMAT(I4,F14.4,2X,D12.5,2X,D12.5,2X,D12.5,2X,D12.5)
 466  FORMAT(//'  PT',6X,'POSTION',5X,'DIFF COEF',5X,'ABS XSECT'
     1 ,7X,' SIG1-2',2X,'NU SIGF XSCT'//)
      WRITE(6,7172)
      WRITE(6,4668)
      DIFT(1)=0.0
      SABT(1)=0.0
      XNT(1)=0.0
C
      DO 4883 I=1,NPTS
 4883 WRITE(6,4675)I,X(I),DIFT(I),SABT(I),XNT(I)
 4675  FORMAT(I4,F14.4,2X,D12.5,2X,D12.5,2X,D12.5)
 4668 FORMAT(//'  PT',6X,'POSITION',5X,'DIFF COEF',5X,'ABS XSECT'
     1 ,2X,'NU SIGF XSCT'//)
      DO 3333 J=2,NPTS
 3333 SABS(J)=SABS(J)+STR(J)
C
C-----------------------------------------------------------------
C
C     CALCULATE RIGHT AND LEFT VOLUMES AND AREAS FOR EACH
C
C     MESH POINT
C
C-----------------------------------------------------------------
```

```
      YN1=SABS(L)*DLV(L)+SABS(L+1)*DRV(L)+YN1
 99   YD1=(XNF(L)+XNT(L)*R)*DLV(L)+(XNF(L+1)+XNT(L+1)*R)
     1  *DRV(L)+YD1
      FLUXO(NPTS)=1.0
      FLUXP(NPTS)=1.0
      FLUOT(NPTS)=STR(NPTS)/SABT(NPTS)
C
      TOTVOL=TOTVOL+DLV(NPTS)
      YN1=YN1+SABS(2)*DRV(1)
      YD1=YD1+(XNF(2)+XNT(2)*FLUOT(2))*DRV(1)
      YN1=YN1+SABS(NPTS)*DLV(NPTS)
      YD1=YD1+(XNF(NPTS)+XNT(NPTS)*FLUOT(NPTS)/FLUXO(NPTS))*DLV(NPTS)
      XLAMI=YN1/YD1
      XLAMO=XLAMI
      XKO=1./XLAMO
C
      ICNT=0
 599  CONTINUE
      ICNT=ICNT+1
      CALL ALOADF(A,IGEO,IBNL,IBNR,NPTS,DX,DLV,DRV,DLA,DRA,DIFC,
     1 SABS,XNF,XNT,XLAMO,X,B1,FLUXO,FLUOT)
      CALL TRIDG(A,NPTS,101)
      DO 206 I=1,NPTS
 206  FLUXN(I)=A(I,4)
C-----------------------------------------------------------------
C
C     USE OF POWER METHOD TO FIND NEW LAMDA VALUE
C
C-----------------------------------------------------------------
C
      XNUM=0.0
      XDEN=0.0
      DO 150 I=1,NPTS
      XNUM=B1(I)*FLUXN(I)*B1(I)*FLUXO(I)+XNUM
 150  XDEN=(B1(I)**2)*FLUXN(I)**2+XDEN
      XLAMN = XLAMO*XNUM/XDEN
      XKN=1./XLAMN
C
C-----------------------------------------------------------------
C
C     CHECK FOR CONTINUED ITERATIONS
C
C-----------------------------------------------------------------
C
      ERROR = DABS((XKN-XKO)/XKN)
      XKO=1./XLAMN
      XLAMO = XLAMN
      FLXAV=0.0
      DO 210 I = 1,NPTS
 210  FLXAV=FLUXN(I)*(DLV(I)+DRV(I))+FLXAV
      FLXAV=FLXAV/TOTVOL
      DO 211 I=1,NPTS
 211  FLUXO(I)=FLUXN(I)/FLXAV
      FERRM=0.0
      DO 4001 I=1,NPTS
      FERR=DABS((FLUXP(I)-FLUXO(I))/FLUXO(I))
      IF(FERR.GT.FERRM) FERRM=FERR
 4001 CONTINUE
      CALL ALOADT(A,IGEO,IBNL,IBNR,NPTS,DX,DLV,DRV,DLA,DRA,DIFT,
     1 SABT,STR,X,FLUXO)
C
```

```
      WRITE(6,500)
      DO 745 I=1,NPTS
        WRITE(6,600)I,X(I),FLUXF(I),FLUXT(I)
 745  CONTINUE
      STOP
      END
      SUBROUTINE TRIDG(A,N,NDIM)
      IMPLICIT REAL*8(A-H,O-Z)
      DIMENSION A(NDIM,4)
      DO 10 I=2,N
      A(I,1) = A(I,1)/A(I-1,2)
      A(I,2) = A(I,2)-A(I,1)*A(I-1,3)
      A(I,4) = A(I,4)-A(I,1)*A(I-1,4)
 10   CONTINUE
      NM1=N-1
      A(N,4)=A(N,4)/A(N,2)
      DO 20 J=1,NM1
      I= NM1+1-J
      A(I,4)=(A(I,4)-A(I,3)*A(I+1,4))/A(I,2)
 20   CONTINUE
      RETURN
      END
C
C
C
      SUBROUTINE ALOADF(A,IGEO,IBNL,IBNR,NPTS,DX,DLV,DRV,DLA,DRA,
     1  DIFC,SABS,XNF,XNT,XLAMO,X,B1,FLUXO,FLUOT)
      IMPLICIT REAL*8(A-H,O-Z)
      DIMENSION A(101,4),DX(101),DLV(101),DRV(101),DLA(101),DRA(101)
     1 ,DIFC(101),SABS(101),XNF(101),XNT(101),X(101),B1(101),
     2  FLUXO(101),FLUOT(101)
C
C------------------------------------------------------------------
C
C     LOAD THE REQD MATRICES
C
C------------------------------------------------------------------
C
      PI=3.1415927
      NPTS1=NPTS-1
      DA1=1.0
      DANPTS=1.0
      IF(IGEO.EQ.2)DA1=0.0
      IF(IGEO.EQ.3)DA1=0.0
      IF(IGEO.EQ.2)DANPTS=2.0*PI**(NPTS)
      IF(IGEO.EQ.3)DANPTS=4.*PI*X(NPTS)**2
      A(1,1)=0.0
      A(NPTS,3)=0.0
      DO 105 L=2,NPTS1
      R=FLUOT(L)/FLUXO(L)
      A(L,2)=DIFC(L)/DX(L)*DLA(L)+DIFC(L+1)/DX(L+1)*DRA(L)+SABS(L)*
     1DLV(L)+SABS(L+1)*DRV(L)
      A(L,1)=-DIFC(L)/DX(L)*DLA(L)
      A(L,3)=-DIFC(L+1)/DX(L+1)*DRA(L)
      A(L,4)=XLAMO*((XNF(L)+XNT(L)*R)*DLV(L)+(XNF(L+1)+XNT(L+1)
     1   *R)*DRV(L))
      B1(L)=A(L,4)/XLAMO
 105  A(L,4)=A(L,4)*FLUXO(L)
      IF(IBNL.EQ.1) A(1,2)=DIFC(2)/DX(2)*DRA(1)+SABS(2)*DRV(1)
      IF(IBNL.EQ.1) A(1,3)=-DIFC(2)/DX(2)*DLA(2)
      IF(IBNR.EQ.0) A(NPTS,2)=1./(.71*3.)*DANPTS+DIFC(NPTS)/DX(NPTS)
```

```
      IF(IBNR.EQ.O)A(NPTS,4)=STR(NPTS)*DLV(NPTS)*FLUXO(NPTS)
      IF(IBNR.EQ.1)A(NPTS,4)=STR(NPTS)*DLV(NPTS)*FLUXO(NPTS)
      RETURN
      END
```

```
   NO OF REG    NO OF MAT     REL ERR    POWER(MEV)    MEV/FISSION
        4            3        0.00010      1.00000     200.00000

***   CYLINDRICAL GEOMETRY   ***

 LEFT BC EQUALS ZERO CURRENT (SYMMETRY)
 RIGHT BC EQUALS ZERO FLUX AT EXTR. BNDRY (VACUUM)

   REG NO     MAT NO     NO INT        THICK

        1          2          7 0.70000D+01
        2          1         20 0.12800D+02
        3          2          3 0.30000D+01
        4          3         20 0.25000D+02

 CROSS SECTIONS FOR GROUP 1

   MAT NO     DIF COEF      SIG ABS     SIG TRFR     NU SGFIS

        1 0.84061D+00 0.16336D+00 0.18060D-01 0.67090D-01
        2 0.55914D+00 0.12140D-01 0.23000D-01 0.00000D+00
        3 0.59471D+00 0.38000D-03 0.92870D-01 0.00000D+00

 CROSS SECTIONS FOR GROUP 2

   MAT NO     DIF COEF      SIG ABS     SIG TRFR     NU SGFIS

        1 0.38590D+00 0.10622D+00 0.00000D+00 0.10904D+01
        2 0.30157D+00 0.18987D+00 0.00000D+00 0.00000D+00
        3 0.49701D+00 0.67000D-03 0.00000D+00 0.00000D+00

THE VALUE FOR KEFF IS     1.2278809
```

| | | | |
|---|---|---|---|
| 1 | 0.00 | 0.213162E+15 | 0.110393E+14 |
| 2 | 1.00 | 0.216512E+15 | 0.112207E+14 |
| 3 | 2.00 | 0.226699E+15 | 0.117759E+14 |
| 4. | 3.00 | 0.244210E+15 | 0.127442E+14 |
| 5 | 4.00 | 0.269872E+15 | 0.142008E+14 |
| 6 | 5.00 | 0.304908E+15 | 0.162761E+14 |
| 7 | 6.00 | 0.350994E+15 | 0.191953E+14 |
| 8 | 7.00 | 0.410352E+15 | 0.233600E+14 |
| 9 | 7.64 | 0.437340E+15 | 0.256529E+14 |
| 10 | 8.28 | 0.460268E+15 | 0.274565E+14 |
| 11 | 8.92 | 0.478993E+15 | 0.288538E+14 |
| 12 | 9.56 | 0.493512E+15 | 0.299007E+14 |
| 13 | 10.20 | 0.503897E+15 | 0.306369E+14 |
| 14 | 10.84 | 0.510264E+15 | 0.310914E+14 |
| 15 | 11.48 | 0.512758E+15 | 0.312868E+14 |
| 16 | 12.12 | 0.511537E+15 | 0.312420E+14 |
| 17 | 12.76 | 0.506769E+15 | 0.309733E+14 |
| 18 | 13.40 | 0.498629E+15 | 0.304958E+14 |
| 19 | 14.04 | 0.487295E+15 | 0.298241E+14 |
| 20 | 14.68 | 0.472945E+15 | 0.289731E+14 |
| 21 | 15.32 | 0.455757E+15 | 0.279579E+14 |
| 22 | 15.96 | 0.435901E+15 | 0.267953E+14 |
| 23 | 16.60 | 0.413536E+15 | 0.255034E+14 |
| 24 | 17.24 | 0.388804E+15 | 0.241036E+14 |
| 25 | 17.88 | 0.361809E+15 | 0.226212E+14 |
| 26 | 18.52 | 0.332605E+15 | 0.210875E+14 |
| 27 | 19.16 | 0.301163E+15 | 0.195432E+14 |
| 28 | 19.80 | 0.267329E+15 | 0.180428E+14 |
| 29 | 20.80 | 0.194950E+15 | 0.169884E+14 |
| 30 | 21.80 | 0.137934E+15 | 0.208692E+14 |
| 31 | 22.80 | 0.919491E+14 | 0.334831E+14 |
| 32 | 24.05 | 0.548836E+14 | 0.442703E+14 |
| 33 | 25.30 | 0.328016E+14 | 0.486219E+14 |
| 34 | 26.55 | 0.196270E+14 | 0.492851E+14 |
| 35 | 27.80 | 0.117563E+14 | 0.478756E+14 |
| 36 | 29.05 | 0.704866E+13 | 0.453414E+14 |
| 37 | 30.30 | 0.422988E+13 | 0.422360E+14 |
| 38 | 31.55 | 0.254041E+13 | 0.388800E+14 |
| 39 | 32.80 | 0.152688E+13 | 0.354562E+14 |
| 40 | 34.05 | 0.918350E+12 | 0.320662E+14 |
| 41 | 35.30 | 0.552692E+12 | 0.287640E+14 |
| 42 | 36.55 | 0.332809E+12 | 0.255755E+14 |
| 43 | 37.80 | 0.200487E+12 | 0.225106E+14 |
| 44 | 39.05 | 0.120789E+12 | 0.195699E+14 |
| 45 | 40.30 | 0.727292E+11 | 0.167493E+14 |
| 46 | 41.55 | 0.436838E+11 | 0.140415E+14 |
| 47 | 42.80 | 0.260431E+11 | 0.114382E+14 |
| 48 | 44.05 | 0.151989E+11 | 0.893082E+13 |
| 49 | 45.30 | 0.832974E+10 | 0.651045E+13 |
| 50 | 46.55 | 0.366054E+10 | 0.416855E+13 |
| 51 | 47.80 | 0.242961E-13 | 0.189698E+13 |

Appendix 2

START Code

```
0.0,0.39,0.0,3.27
.0002,0.0,0.0,3.641
11.15,.132,75.45,49.82
95.0,0.0,1264.2,621
15.5,.1786,.2031,24.08
2.44,0.0,0.0,11.44
0.0,0.554,0.0,3.682
.003,0.0,0.0,4.437
.1433,.2714,0.0,7.033
2.24,0.0,0.0,13.04
.0053,.8857,0.0,4.427
.009,0.0,0.0,5.569
41.82,.5146,0.0,44.83
669.3,0.0,0.0,672.77
0.0,0.20,0.0,2.0
.0001,0.0,0.0,9.5
C-------------------------------------------------------------------
C
C     CALCULATES THE REQUIRED TERMS FOR THE TWO GROUP EQUATIONS IN LAMARSH
C     AFTER INPUTING THE COLLAPSED TWO GROUP CROSS SECTIONS SUPPLIED BY
C     THE CODE ANASIN.
C
C-------------------------------------------------------------------

C-------------------------------------------------------------------
C
C      VARIABLES:
C         1 - FAST GROUP
C         2 - SLOW GROUP
C         D__ - DIFFUSION COEFFICIENT
C         SIGA__ - MICROSCOPIC ABSORPTION CROSS SECTION
C         SIGS__ - MICROSCOPIC SLOWING DOWN CROSS SECTION
C         SIGF__ - MICROSCOPIC NU*FISSION CROSS SECTION
C         SIGT__ - MICROSCOPIC TRANSPORT CROSS SECTION
C         EA,ES,EF - MACROSCOPIC CROSS SECTIONS
C         O - OXYGEN
C         C - CARBON (GRAPHITE)
C        *N - NITROGEN
C         BE - BERRYLIUM
C         BO - BORON
C         25 - U-235
C         28 - U-238
C         FE - IRON (STAINLESS STEEL)
C         C - STAINLESS STELL SHAFT AND VESSEL WALL
C         F,FL - FUEL
C         R - CONTROL DRUMS
C
C------------------------------------------------------------------

      DIMENSION DC(2),EAC(2),ESC(2),EFC(2),DF(2),EAF(2),ESF(2),
     * EFF(2),DR(2),EAR(2),ESR(2),EFR(2),ETC(2),ETF(2),ETR(2),
     * SIGAO(2),SIGA25(2),SIGA28(2),SIGAC(2),SIGAFE(2),SIGABE(2),
     * SIGABO(2),SIGSO(2),SIGS25(2),SIGS28(2),SIGSC(2),SIGSFE(2),
     * SIGSBE(2),SIGSBO(2),SIGFO(2),SIGF25(2),SIGF28(2),SIGFC(2),
     * SIGFFE(2),SIGFBE(2),SIGFBO(2),SIGTO(2),SIGT25(2),SIGT28(2),
     * SIGTC(2),SIGTFE(2),SIGTBE(2),SIGTBO(2),SIGAN(2),SIGSN(2),
     * SIGFN(2),SIGTN(2)
      OPEN(UNIT=1,FILE='INSTART.DAT',STATUS='OLD')
      OPEN(UNIT=2,FILE='OUTSTART.DAT',STATUS='NEW')

C
```

```
      AWFL=(235.04394*ENR)+(238.05082*(1.0-ENR))+14.0067
      AWG=32.0+12.011
      AWC=12.011
      AWFE=55.85
      AWBEO=25.02
      AWB4C=55.26
C-------------------------------------------------------------------
C
C     CALCULATE THE NUMBER DENSITIES
C
C-------------------------------------------------------------------
      AD25=((.6023*RHOFL)/AWFL)*VOLF*ENR
      AD28=((.6023*RHOFL)/AWFL)*VOLF*(1.0-ENR)
      ADNF=((.6023*RHOFL)/AWFL)*VOLF
      ADOG=((.6023*RHOG)/AWG)*VOLG*2.0
      ADCG=((.6023*RHOG)/AWG)*VOLG
      ADC=((.6023*RHOC)/AWC)*VOLC
      ADFE=((.6023*RHOFE)/AWFE)
      ADBE=((.6023*RHOBEO)/AWBEO)*VOLBE
      ADB4=((.6023*RHOB4C)/AWB4C)*VOLBO*4.0
      ADOBE=((.6023*RHOBEO)/AWBEO)*VOLBE
      ADCB4=((.6023*RHOB4C)/AWB4C)*VOLBO
C----------------------------------------------------------------------
C
C    CALCULATE AND PRINT MACROSCOPIC ABSORPTION AND NU-FISSION CROSS
C    SECTIONS FOR THE U-235 AND U-238
C
C----------------------------------------------------------------------
      EA251=AD25*SIGA25(1)
      EA252=AD25*SIGA25(2)
      EA281=AD28*SIGA28(1)
      EA282=AD28*SIGA28(2)
      EF251=AD25*SIGF25(1)
      EF252=AD25*SIGF25(2)
      EF281=AD28*SIGF28(1)
      EF282=AD28*SIGF28(2)
      WRITE(*,*) EA251,EA252,EA281,EA282
      WRITE(*,*) EF251,EF252,EF281,EF282
C----------------------------------------------------------------------
C
C    CALCULATE AND PRINT PARAMETERS NEEDED FOR THE LAMARSH TWO GROUP EQUATIONS
C
C----------------------------------------------------------------------
      DO 100 I=1,2
      EAF(I)=(AD25*SIGA25(I))+(AD28*SIGA28(I))+(ADNF*SIGAN(I))+
     *       (ADOG*SIGAO(I))+(ADCG*SIGAC(I))+(ADC*SIGAC(I))
      ESF(I)=(AD25*SIGS25(I))+(AD28*SIGS28(I))+(ADNF*SIGSN(I))+
     *       (ADOG*SIGSO(I))+(ADCG*SIGSC(I))+(ADC*SIGSC(I))
      ETF(I)=(AD25*SIGT25(I))+(AD28*SIGT28(I))+(ADNF*SIGTN(I))+
     *       (ADOG*SIGTO(I))+(ADCG*SIGTC(I))+(ADC*SIGTC(I))
      DF(I)=1.0/(3.0*ETF(I))
      EFF(I)=(AD25*SIGF25(I))+(AD28*SIGF28(I))
  100 CONTINUE

      DO 200 I=1,2
      EAC(I)=ADFE*SIGAFE(I)
```

| | | | |
|---|---|---|---|
| 9.6170716E-03 | 8.1939183E-02 | 0.1537438 | 2.4202248E-02 |
| 6.5076955E-02 | 1.090395 | 2.0145397E-03 | 0.0000000E+00 |
| 0.8406107 | 0.1633609 | 1.8055988E-02 | 6.7091495E-02 |
| 0.3859047 | 0.1062184 | 0.0000000E+00 | 1.090395 |
| 0.5591469 | 1.2146703E-02 | 2.3004992E-02 | |
| 0.3015706 | 0.1898717 | 0.0000000E+00 | |
| 0.5947114 | 3.8594622E-04 | 9.2896529E-02 | |
| 0.4970135 | 6.6994439E-04 | 0.0000000E+00 | |

# Appendix 1.3

## Sample Calculations

## FUEL BURNUP

critical radius = 12.8 cm (annular from 7 to 19.8 cm)

$\pi(7)^2(30) = 4618\ cm^3$ $\pi(19.8)^2(30) = 36{,}949\ cm^3$

- volume of annular core = 36,949 − 4618 = 32,331 $cm^3$
- cross sectional area of core (axial)

  $= \pi(19.8)^2 - \pi(7)^2 = 1231.6\ cm^2 - 153.9\ cm^2 = 1077.7\ cm^2$

- volume of UN = $(0.315)(32{,}331\ cm^3) = 10{,}184\ cm^3$ of UN
- mass of UN = $10{,}184\ cm^3 \times 14.31\ g/cm^3 = 145.74$ Kg of UN
- mass of U-235 (5.6% enriched) at startup for criticality

| | | | |
|---|---|---|---|
| 5.6% | U-235 | .056 (235.04) | = 13.1625 |
| 94.4% | U-238 | .944 (238.05) | = 224.9580 |
| | N | | = 14.0067 |
| | | | 252.13 |

$W/o$ U-235 $= \dfrac{13.1625}{252.13} = .0522 = 5.2\%$

(.0522)(145.74 Kg UN) = 7.61 Kg U-235

- mass of U-235 burned up during lifetime

  $1.05(1+\alpha)P$ g/day = 1.23 g/day  $\alpha = 0.169$, $P = 1\ MW_t$

  1.23 g/day × 365 day/yr × 7 yr = 3.16 Kg

- mass of U-235 needed for 7 year lifetime

  7.61 Kg + 3.16 Kg = 10.77 Kg of U-235

- new fuel enrichment

$\dfrac{10.77\ Kg}{145.74\ Kg} = .0739\ W/o$

| | | |
|---|---|---|
| ?(1) | (235.0439) = | 18.632 |
| ?(2) | (238.0508) = | 219.180 |
| N | = | 14.007 |
| | | 251.82 |

?(1) = .0793

?(2) = .9207

7.93% ≈ 8.0% enriched fuel

POWER PRODUCTION

$$q''' = K\left[(\Sigma_{f28}\phi + \Sigma_{f25}\phi)_{fast} + (\Sigma_{f28}\phi + \Sigma_{f25}\phi)_{slow}\right]$$

$K = 200$ MeV / fission

$\bar{\Phi}_f = 6.7 \times 10^{15}$ n/cm²·sec

$\bar{\Phi}_s = 4.1 \times 10^{14}$ n/cm²·sec

$\Sigma_{f28}$ fast $= 5.37 \times 10^{-5}$ cm⁻¹

$\Sigma_{f28}$ slow $= 0$

$\Sigma_{f25}$ fast $= 1.90 \times 10^{-3}$ cm⁻¹

$\Sigma_{f25}$ slow $= 3.32 \times 10^{-1}$ cm⁻¹

$$q''' = 200\left[(3.596\times10^{11} + 1.2708\times10^{13}) + (0 + 1.3606\times10^{14})\right]$$

$$= 200\left[(1.307\times10^{13}) + (1.361\times10^{14})\right]$$

9% thermal      91% fast

$$q''' = 2.982\times10^{16}\ \frac{\text{MeV}}{\text{cm}^3\cdot\text{sec}} \times \frac{1.6\times10^{-13}\ \text{J}}{\text{MeV}} \times 32{,}331\ \text{cm}^3$$

$$= 1003\ \text{KW} = 1.003\ \text{MW}$$

EQUIVALENT REACTOR RADIUS

volume of annular core = volume of cylindrical core

$$32{,}331\ \text{cm}^3 = \pi r^2 h$$

$$r^2 = \frac{32{,}331}{\pi h} \qquad h = 30\text{cm}$$

$$r = \sqrt{\frac{32{,}331}{\pi h}}$$

$$r = 18.5\ \text{cm}$$

REACTOR MASSES

use mass = volume x density

volumes based on $\pi r^2 h$ for cylinder volumes

| material | densities | volumes | mass |
|---|---|---|---|
| UN fuel | 14.31 g/cm$^3$ | 10,184 cm$^3$ | 145.7 Kg |
| PyC clad | 1.60 g/cm$^3$ | 10,184 cm$^3$ | 16.3 Kg |
| Stainless steel | 7.86 g/cm$^3$ | 16,663 cm$^3$ | 131.0 Kg |
| $CO_2$ gas | .0019 g/cm$^3$ | 11,962 cm$^3$ | 0.02 Kg |
| BeO (67%) | 3.025 g/cm$^3$ | 40,055 cm$^3$ | 114.5 Kg |
| $B_4C$ (33%) | 2.52 g/cm$^3$ | | |
| Drive Assembly | | | 114.5 Kg |
| | | TOTAL | 522.0 Kg |

# 2. REACTOR THERMAL-HYDRAULICS

The reactor thermal-hydraulics are incorporated into the code PEB, which was created specifically for this project. This code models the steady state pressure drop and temperature rise for a pebble bed reactor system in one diminsion, using a rough finite difference technique. PEB assumes constant mass flow rate as input by the user. The four basic calculations performed by the code are: the pressure drop across the inlet and outlet grid plates, the pressure drop across the core, the fluid temperature rise across the core, and the fuel pebble centerline temperature. The code is written in standard fortran 77 and uses SI units. A code listing is given in Appendix 2.1.

## PROPERTY ASSUMPTIONS

The $CO_2$ coolant was assumed to be an ideal gas. This conclusion is based on the principle of coresponding states[1]. The principle of corresponding states predicts that a gas will behave ideally if its reduced temperature is approximately 2.0 and its reduced pressure is approximately 1.0. Since our reduced states are approximately correct, the ideal gas law will correctly model our system.

Four gas properties are needed for the PEB code; the density, the thermal conductivity, the constant pressure specific heat, and the viscosity. The density of the gas is found using the ideal gas relation,

$$\rho = \frac{P}{RT} \tag{2.1}$$

where P is the pressure, R is the gas constant, and T is the temperature. The thermal conductivity, constant pressure specific heat, and the viscosity were approximated as a linear function of temperature from experimental data[2]. The three correlations used are shown in equations 2.2, 2.3, and 2.4.

$$K = 7.781X10^{-5}\,T(^{o}K) - 6.59X10^{-3}\,(W/m\,^{o}K) \qquad (2.2)$$

$$C_p = 0.634\,T(^{o}K) + 683.5\ \ (J\,/\,kg\,^{o}K) \qquad (2.3)$$

$$\mu = 3.783X10^{-8}\,T(^{o}K) + 3.894X10^{-6}\,(N\,s\,/\,m^2) \qquad (2.4)$$

The material property necessary for the code is the thermal conductivity. For our system, there are three materials: stainless steel 316, pyrolytic carbon, and uranium nitride. Equations 2.5, 2.6, and 2.7 show the relations used.

$$K_{UN} = 1.864\,T^{\,0.361} \qquad (2.5)^3$$

$$K_{Py\,C} = 4.256 - 0.0027\,T \qquad (2.6)^2$$

$$K_{SS} = 9.248 + 0.0157\,T \qquad (2.7)^2$$

## REACTOR INLET AND OUTLET GRID PRESSURE DROP

The pressure drop across the two grids was approximated by a correlatation predicting the pressure drop across a grid with rounded edges[4]. The correlation predicts a head loss $\Delta H$,

$$\Delta H = \frac{2\,\zeta}{\rho\,\omega_1^2} \qquad (2.8)$$

where $\rho$ is the density of the fluid, $\omega_1$ is the inlet velocity, and $\zeta$ is given by equation 2.9,

$$\zeta = \frac{(\sqrt{\zeta'(1-\bar{f})} + 1 - \bar{f})^2}{\bar{f}^2} \qquad (2.9)$$

where $\zeta'$ is a function of the porisity of the grid. Our calculations assumed a conservative constant value of 0.44 for $\zeta'$. $\bar{f}$ is the flow area fraction, defined to be the ratio of the grate flow area divided by the inlet flow area, or for the grate in Figure 2.1,

$$\bar{f}_{inlet} = \frac{\pi}{4}\left(\frac{D}{P}\right)^2 \qquad (2.10)$$

$$\bar{f}_{outlet} = \frac{\pi}{4\varepsilon}\left(\frac{D}{P}\right)^2 \qquad (2.11)$$

where $\varepsilon$ is the porisity of the particle bed. Using these correlations, the pressure drop across the two plates were calculated in the PEB code.

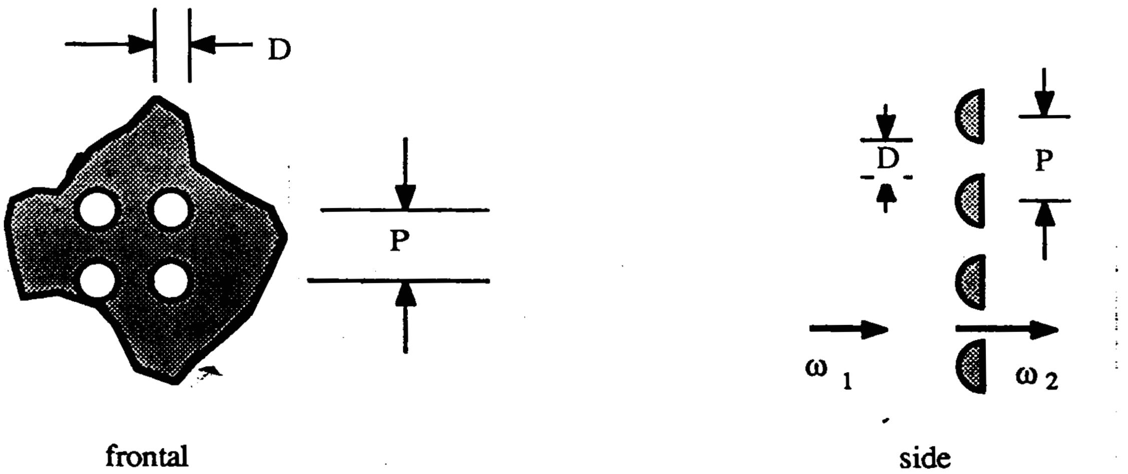


Figure 2.1 Sectional View of Core Grid Plates

## CORE PRESSURE DROP

The pressure drop across a cell, $\Delta P$, was approximated by the correlation[5],

$$\Delta P = \psi \frac{H}{d_h} \frac{\rho}{2} u_p^2 \tag{2.12}$$

where H is the height of the bed, $\rho$ is the density of the fluid, and $u_p$ is the mean velocity of the gas in the gaps at that cell. The hydraulic diameter $d_h$ is given by,

$$d_h = d \frac{\varepsilon}{1 - \varepsilon} \tag{2.13}$$

where d is the diameter of the individual pebble and $\varepsilon$ is the porisity of the bed. The function, $\psi$, is a function of the Reynolds number, $R_e$ and $\varepsilon$, as is shown in equation 2.14.

$$\psi = 320\left(\frac{R_e}{1 - \varepsilon}\right)^{-1} + 6\left(\frac{R_e}{1 - \varepsilon}\right)^{-0.1} \tag{2.14}$$

## FLUID TEMPERATURE RISE

The heat transfer through the core was found by applying conservation of energy in steady state. The form of the energy conservation equation, assuming $q'_s$ is the linear heat generation rate, is given in equation 2.15.

$$q'_s = \dot{m}\, c_p \,\text{Area}\, (T_{out} - T_{in}) \tag{2.15}$$

The PEB code assumes that $c_p$ is a constant at $T_{in}$ and divides the core region into a set number of cells, as specified by the user. The total heat produced in the core is input by the user, then PEB subdivides the total power to all of the cells in a sinusoidal pattern.The linear heat source, q', is assumed to be a sinusoidal source, with zero power produced at the actual edge of the reactor. Although this is not entirely correct, it does well enough for our calculations, since the total amount of energy deposited in the fluid will be the same. Also, this source shape will overestimate the fuel temperature in the center of the reactor, which is a safety plus. With the inlet temperature and the heat generation rate known for the cell, the cell outlet temperature can be found using equation 2.15. The PEB code then uses the outlet temperature of cell i to be the inlet temperature of cell i+1, thus it is a rough finite difference code.

FUEL CENTER TEMPERATURE

To find the temperature in the center of the individual pebbles, $T_c$, three basic thermal resistances are calculated, the thermal resistance across the convection surface, the thermal resistance across the layers of cladding, and the thermal resistance through the fuel itself. The center fuel temperature is then found by using the equation 2.16, where Q is the heat generated in one pebble.

$$T_c = T_{bulk} + Q( R_{conv} + R_{clad} + R_{fuel}) \qquad (2.16)$$

The thermal resistance across the convection surface can be found using the Nusselt number correlation for a packed sphere bed[5],

$$Nu_d = \frac{h\,D}{k_c} = f_\varepsilon Nu_s \qquad (2.17)$$

where h is the heat transfer coefficient, D is the diameter of an individual pellet, $k_c$ is the conductivity of the gas, $f_\varepsilon$ is the arrangement factor, and $Nu_s$ is the Nusselt number for a single ball. The arangement factor, $f_\varepsilon$, is given by equation 2.18.

$$f_{\varepsilon} = 1 + 1.5\,(\,1 - \varepsilon\,) \tag{2.18}$$

The Nusselt number for a singe sphere is given in terms of a laminar and a turbulent Nusselt number,

$$Nu_s = 2 + \sqrt{Nu_l^2 + Nu_t^2} \tag{2.19}$$

The turbulent and laminar Nusselt number are in turn given by the following empirical correlations,

$$Nu_l = 0.66\left(\frac{Re}{\varepsilon}\right)^{0.5}(Pr)^{0.33} \tag{2.20}$$

$$Nu_t = \frac{0.037\left(\frac{Re}{\varepsilon}\right)^{0.8} Pr}{1 + 2.443\left(\frac{Re}{\varepsilon}\right)^{-0.1}\left(Pr^{0.667} - 1\right)} \tag{2.21}$$

With the Nusselt number known for the pebble, the heat transfer coefficient, h, can be determined from the Nusselt number correlation in equation 2.22.

$$h = \frac{Nu\, k_c}{D} \tag{2.22}$$

Since the thermal resistance through the cladding then will be equal to,

$$R_{conv} = \frac{T_{surface} - T_{bulk}}{Q} \tag{2.23}$$

and

$$h = \frac{q''}{T_{surface} - T_{bulk}} \tag{2.24}$$

then,

$$R_{conv} = \frac{1}{Nu\, k_c\, \pi\, D} \tag{2.25}$$

where r is the radius of the pebble. The resistance through N layers of cladding will be equal to,

$$R_{clad} = \frac{\sum_{n=1}^{N-2} \frac{1}{k_{n+1}} \left( \frac{1}{r_n} - \frac{1}{r_{n+1}} \right)}{4\pi} \tag{2.26}$$

where the subscripts are shown in figure 2.2.

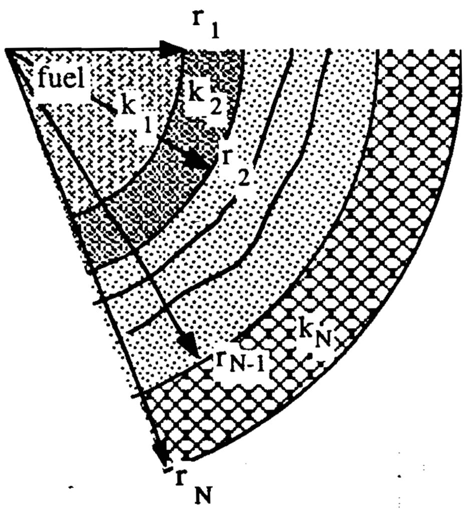


Figure 2.2 Cutaway of fuel pellet showing node numbering

The thermal resistance through the fuel itself can be calculated using the 1-D conduction equation with a source term. The solution to this is given in equation 2.27.

$$R_{fuel} = \frac{1}{8\, k_1\, r_1\, \pi} \tag{2.27}$$

Using equation 2.16, 2.25, 2.26, and 2.27, the final solution for the centerline fuel temperature will be,

$$T_{center} = T_{bulk} + Q\left(\frac{1}{Nu\, k_c \pi D} + \frac{\sum_{n=1}^{N-2} \frac{1}{k_{n+1}}\left(\frac{1}{r_n} - \frac{1}{r_{n+1}}\right)}{4\pi} + \frac{1}{8\, k_1 r_1 \pi}\right) \tag{2.28}$$

- In axial flow pebble beds, there is a signifigant amount of radial conduction and radiation that will occur. This phenomenon was not accounted for in our calculations, due to the complexity of the problem. However, the radial heat transfer regime will only serve to " spread out " the heat source, thus our calculations are still conservative in that our temperature distribution will appear to be more peaked in the radial direction.

## PEB INPUT AND OUTPUT DESCRIPTION

The input to the PEB code, shown in Table 2.1, is quite simple. Most of the input is self explanitory, except the material number. This number corresponds to an identification number contained in PEB. 50 is pyrolytic carbon, 61 is SS-316, and 82 is uranium nitride. Also, the apture of the core plate refers to the ratio of D to P in Figure 2.1. One of the actual input decks to PEB is contained in Appendix 2.2.

Table 2.1 PEB Input description

| line # | | | |
|---|---|---|---|
| 1 | # of cells (NAX) | # of layers in a pellet (NLAY) | total reactor length |
| | | | |
| 2 | inlet temperature | inlet pressure | mass flow rate |
| | | | |
| 3 | total reacor power | | |
| | | | |

| | | | | |
|---|---|---|---|---|
| 4 | inner radius of | outer radius of | porisity of | apture of |
| | core region | core region | bed | core plate |
| | | | | |
| 5 | radius of fuel | fuel material number | | |
| | | | | |
| 6 | radius of first clad | first clad material number | | |
| 7 | radius of second clad | second clad material number | | |
| . | . | . | | |
| . | . | . | | |
| . | . | . | | |
| NLAY+4 | radius of last clad | last clad material number | | |

An example PEB output is given in Appendix 2.3. The output is clearly labelled, therefore no explination will be given.

RESULTS

The thermal-hydraulic calculations in PEB were carried out to determine the size of the reactor, the size of the pebbles, the apture in the core grid plate, and the mass flow rate through the core. All calculations were performed with the limiting parameters being that the fluid outlet temperature could not exceed 900 $^{o}K$ and the fuel centerline temperature could not exceed 1800 $^{o}K$. With these limiting margins, no serious interactions or material degredation will occur. In the determination of the entire core size, a corroborative effort with the neutronics personnel had to be maintained, since the overall core size affects both fields. In the end, however, there was a large margin in which to work with and thus no severe problems were encountered. The size of the individual pebbles was strictly a thermal-hydralics problem. If the pebbles are too large, the center temperature will exceed the design criterion. Also, if the pebbles are too small, there will be the possibility of signifigant manufacturing problems and too large of a pressure drop. Since we did not know the extent of the manufacturing problems, the centerline fuel temperature was raised to a maximum. The massflow rate was adjusted to obtain an outlet temperature of approximately 850 $^{o}K$. Previous experiments[6] have shown that the porisity of the particle bed will be 0.37, if the ratio of the core radius to the pebble radius is greater than 5. Since our reactor radius is on the order of 10 cm and the pebbles are less than a centimeter in size, we could safely assume that the porisity is a constant 0.37. The inlet temperature was assumed to be 500 $^{o}$K and the inlet pressure was assumed to be 6.9 MPa.

After several interations, the pebble size was found to be 0.6 cm in diameter. The mass flow rate was 2.43 kg/s. The core size was found by the neutronics personnel. The final actual input conditions are the ones listed in Appendix 2.2. With these input conditions, the output in Appendix 2.3 was generated. These results are displayed graphically in Figures 2.3, 2.4, 2.5, and 2.6.

Figure 2.3 shows the total pressure drop across the reactor. Notice that most of the pressure losses are incurred at the inlet and outlet grid plate. Since this does not make intuitive sense, there is a significant possibility that the correlation in equation 2.12 is either incorrect or is used inapropriately. First, this is probably not the exact plate geometry that will be used, however this should not be a large factor. The one factor that was overassumed was the $\zeta'$ factor. However, in the end result, the pressure drop was assumed to be that of Figure 2.3, since this will be conservative.

Figure 2.4 shows the fluid temperature rise through the core. The outlet temperature was found to be about 868 $^{o}$K, which is within our design criterion. Figure 2.5 shows the fuel center temperature as a function of axial location. Two curves are shown, the uppermost being the hot channel temperature distribution and the lower one being the average channel temperature distribution. Both curves have a maximum of less than 1400 $^{o}$K, which is well below the design criterion. Figure 2.6 shows two curves, the average center fuel temperature and the fluid temperature as a function of core axial distance. The calculations came out quite well, since the two curves had nearly the same value at the outlet.

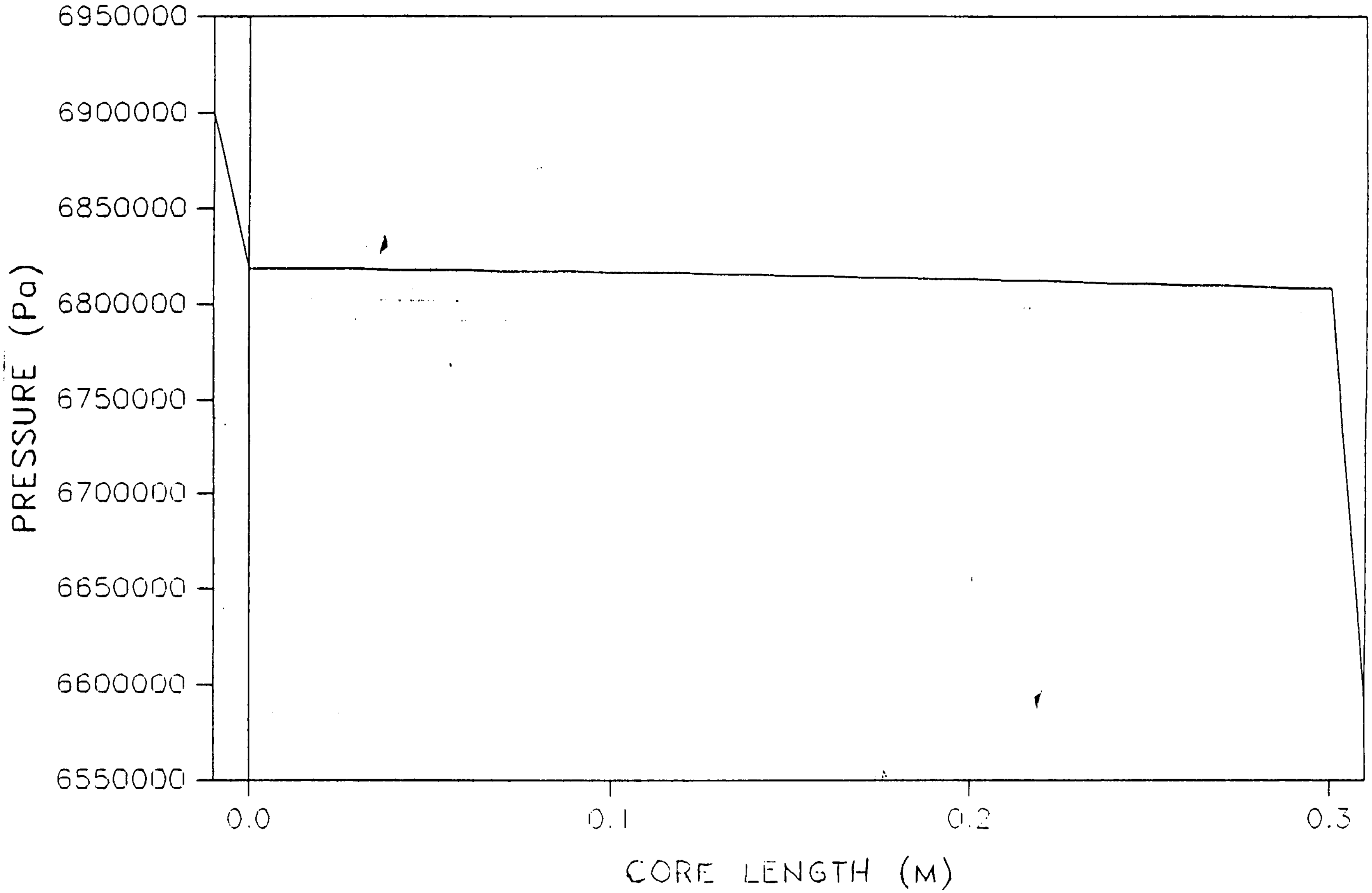


Figure 2.3 Pressure Drop Across the Core

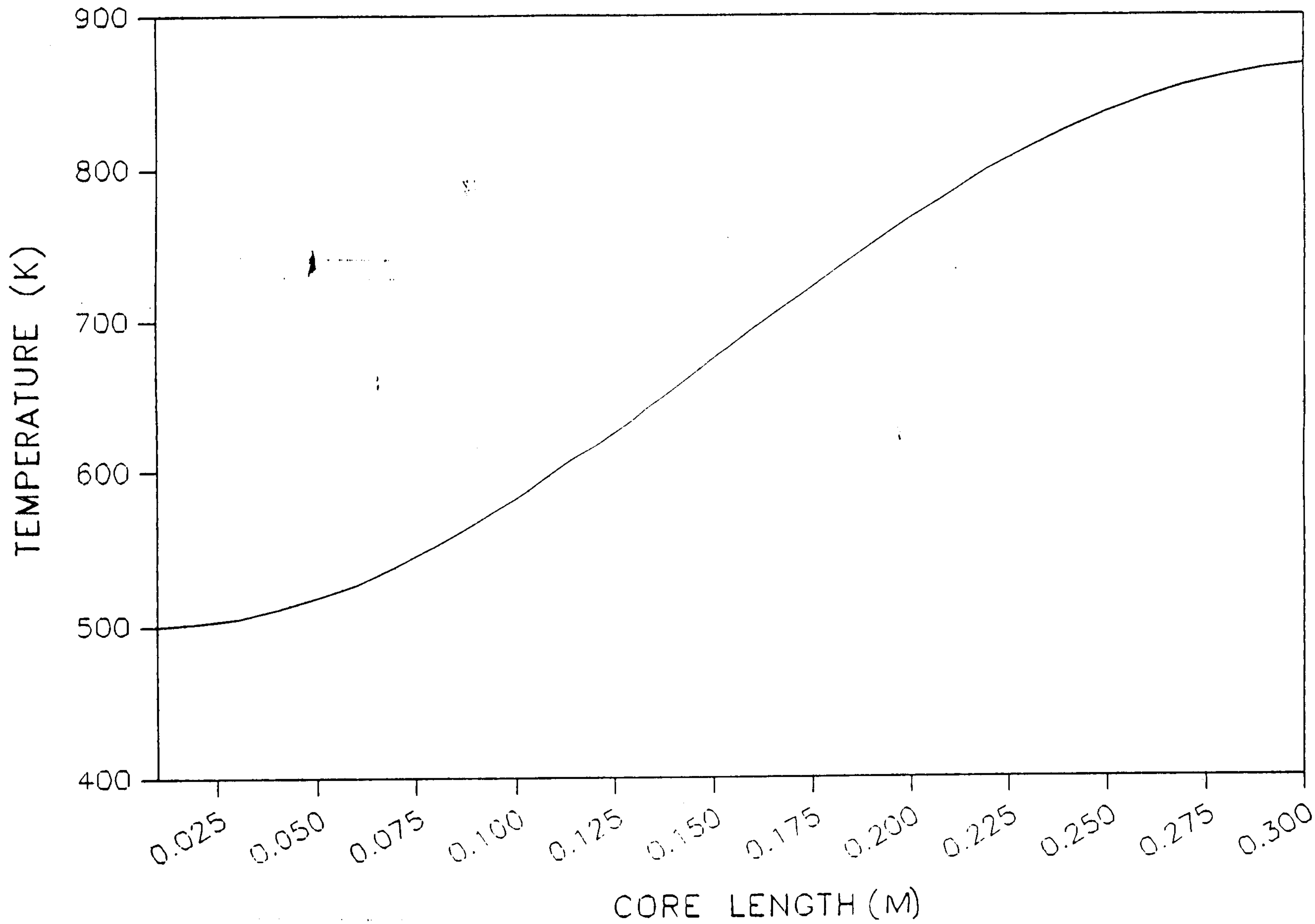


Figure 2.4 Fluid Temperature Rise Across the Core

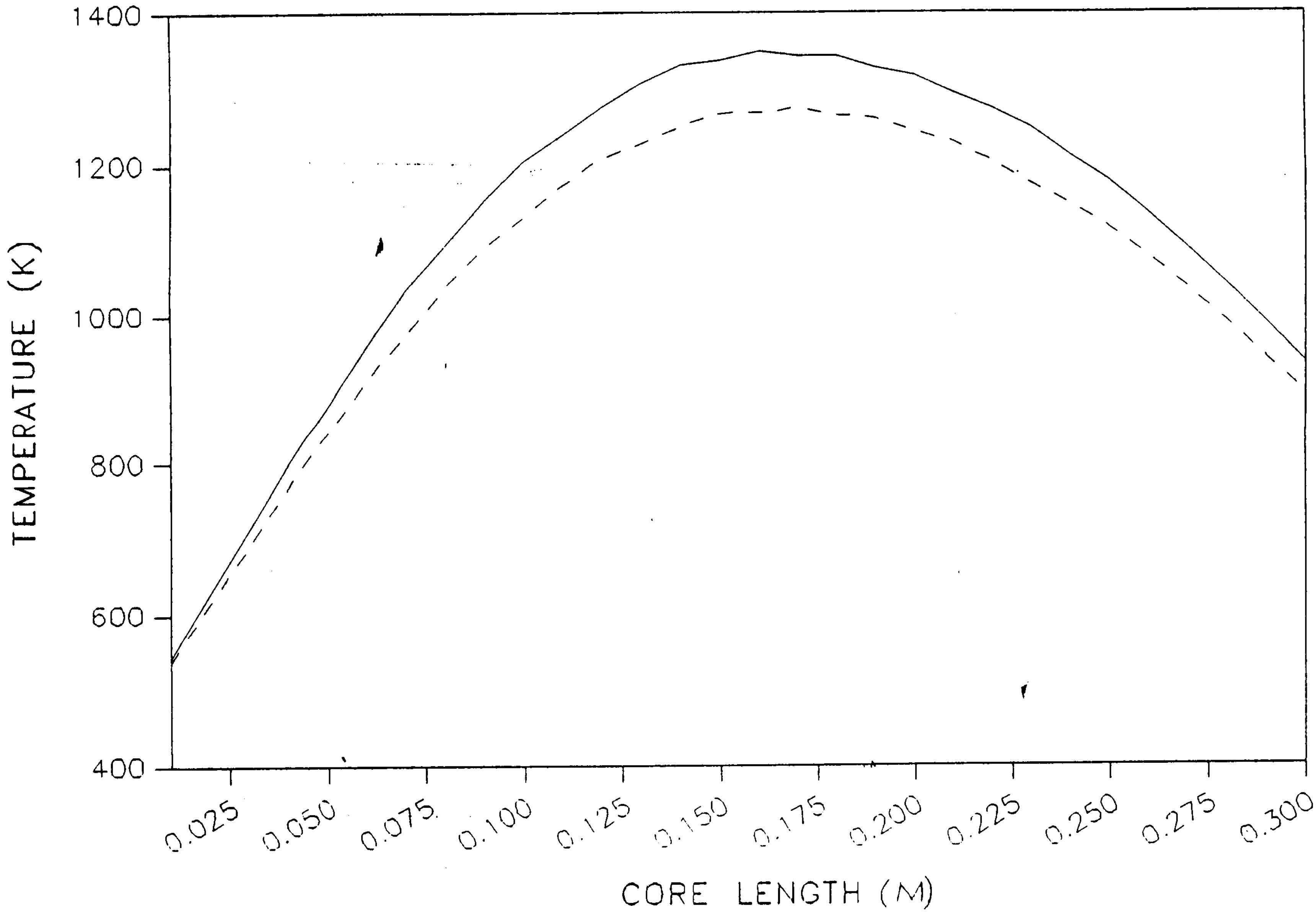


Figure 2.5 Maximum and Average Fuel Center Temperature

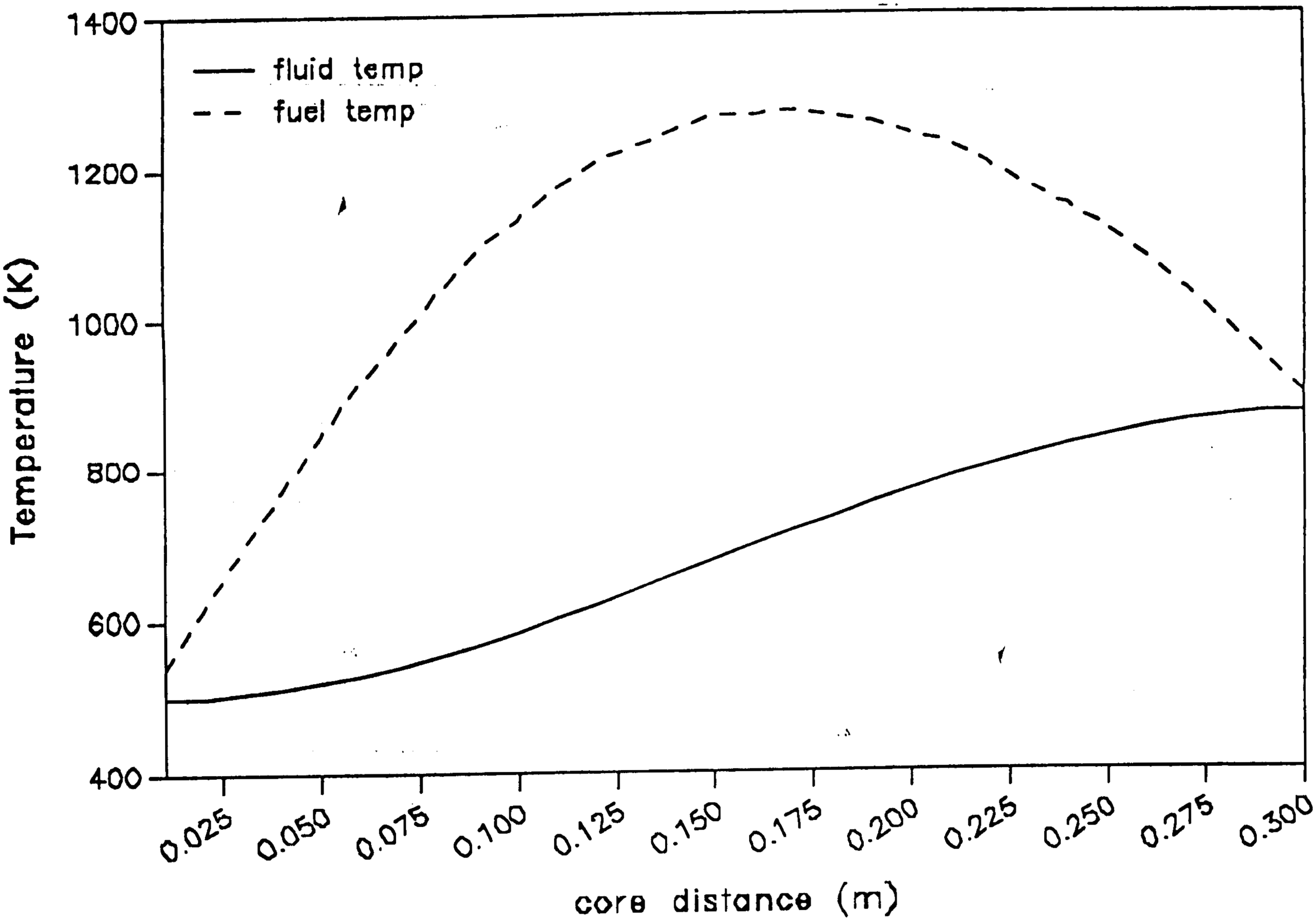


Figure 2.6 Fluid and Fuel Center Temperature Across the Core

## REFERENCES


1. Wark, K., "Thermodynamics," McGraw-Hill Book Company, New York, p 137, 1983.

2. Incropera, F. P. and DeWitt, D. P., "Fundamentals of Heat and Mass Transfer," John Wiley & Sons, New York, 1985, Appendix A.

3 Thomas, J. K. and Hayes, S. L., " Material Property and Irradiation Performance Correlations for Nitride Fuels," Fifth Symposium for Space Nuclear Power Systems, Albuqeurque, NM, 1988.

4. Chik, I. E. Idel, " Handbook of Hydraulic Resistance, Coefficients of Local Resitance, and of Friction," Gosudarstvennoe Energeticheskoe Izdatel'stvo, Moskva - Leningrad, 1960.

5. French, H. " Heat Transfer and Fluid Flow in Nuclear Systems," Pergamon Press, New York, 1987, Chapter 5, part 2.

6. S. T. Robinson, " The Pebble Bed Reactor ", Proceedings of the Symposium on Gas Cooled Reactors, Journal of the Franklin Institute, Lancaster, Pa, p. 94, 1960.

# Appendix 2.1 PEB Code Listing

```
C23456789 123456789 123456789 123456789 123456789 123456789 123456789 123456789
      PROGRAM MAIN
C
C  CREATED BY TED G. BAGWELL TO MODEL THERMAL-HYDRAULIC CONDITIONS IN
C    A PEBBLE BED REACTOR SYSTEM
C
C  VARIABLE LIST
C   APTUR      = THE APTURE RATIO OF THE INLET AND OUTLET CORE OUTLET PLATES
C   CLEN       = CELL LENGTH (m)
C   DIA        = DIAMETER OF FUEL PELLET (m)
C   KOND(I,T) = THERMAL CONDUCTIVITY OF A MATERIAL W/ ID I AND TEMP T (W/(mK))
C               I = 61 IS SS316
C               I= 82 IS UN
C   RMASFLO    = MASS FLOW (kg/s)
C   NAX        = NO. OF AXIAL CELLS
C   NLAY       = NO. OF LAYERS IN FUEL
C   PIN        = INLET PRESSURE (Pa)
C   PORIS      = PORISITY OF THE BED
C   PRESS(N)   = PRESSURE @ CELL N (Pa)
C   QSOUR(N)   = HEAT GENERATED IN CELL N  (W)
C   R          = MOLECULAR GAS CONSTANT
C   RAD1       = INNER RADIUS OF ANULAR (?) CORE (m)
C   RAD2       = OUTER RADIUS OF ANULAR     CORE (m)
C   RADIUS(M) = RADIUS @ FUEL PELLET INTERFACE (M)
C               RADIUS(1) IS THE ACTUAL FUEL RADIUS
C   RLEN       = TOTAL LENGTH OF THE REACTOR (m)
C   TCOND(T)   = THE THERMAL CONDUCTIVITY OF THE FLUID @ TEMP = T (W/(mK))
C   TEMP(N,1) = FUEL CENTERLINE TEMP @ CELL N (K)
C   TEMP(N,2) = FLUID TEMP @ CELL N (K)
C   TIN        = INLET TEMPERATURE (K)
C   XAREA      = CROSS SECTIONAL AREA OF CORE
C
C
      PARAMETER R=188.9
      PARAMETER PI=3.14
      PARAMETER MAXCEL=100
C
C   DATA
C
      COMMON/THERMAL/ TIN,PIN,VELIN,TEMP(MAXCEL,2),PRESS(MAXCEL),
     &VEL(MAXCEL),QSOUR(MAXCEL),RMASFLO
      COMMON/GEOM/ DIA,NAX,NLAY,PORIS,CLEN,XAREA,RADIUS(MAXCEL),
     &MID(MAXCEL),APTUR
C
C   INPUT
C
      OPEN(UNIT=11,FILE='IN.DAT',STATUS='OLD')
      OPEN(UNIT=12,FILE='OUT.DAT',STATUS='NEW')
      OPEN(UNIT=13,FILE='FUELT.DAT',STATUS='NEW')
      OPEN(UNIT=14,FILE='FLUIDT.DAT',STATUS='NEW')
      OPEN(UNIT=15,FILE='PRESS.DAT',STATUS='NEW')
      READ(11,*)NAX,NLAY,RLEN
      READ(11,*)TIN,PIN,RMASFLO
      READ(11,*)QTOT
      READ(11,*)RAD1,RAD2,PORIS,APTUR
      READ(11,*)(RADIUS(I),MID(I),I=1,NLAY)
      XAREA = PI*(RAD2**2.0-RAD1**2.0)
C
      WRITE(12,*)'NAX  NLAY  RLEN'
      WRITE(12,*)NAX,NLAY,RLEN
      WRITE(12,*)'TIN  PIN  MASFLO'
```

```
C
C23456789 123456789 123456789 123456789 123456789 123456789 123456789 123456789
C
      SUBROUTINE PLATEPD(P1,P2,T1,K)
C
      PARAMETER MAXCEL=100
      PARAMETER PI=3.14
C
      COMMON/THERMAL/ TIN,PIN,VELIN,TEMP(MAXCEL,2),PRESS(MAXCEL),
     &VEL(MAXCEL),QSOUR(MAXCEL),RMASFLO
      COMMON/GEOM/ DIA,NAX,NLAY,PORIS,CLEN,XAREA,RADIUS(MAXCEL),
     &MID(MAXCEL),APTUR
C
      IF(K.EQ.1)FACT=PORIS
      IF(K.EQ.2)FACT=1.0
C
      ZETAP = 0.44
      AREAR = PI*APTUR**2.0/(4.0*FACT)
      QUO = (RMASFLO/(FACT*XAREA))**2.0*DENS(T1,P1)
      DP = 0.5*QUO*(((ZETAP*(1.0-AREAR))**0.5+(1.0-AREAR))/AREAR)**
     &     2.0
      P2=P1-DP
C
      RETURN
      END
C
C23456789 123456789 123456789 123456789 123456789 123456789 123456789 123456789
C
      SUBROUTINE PRESR(N)
C
      PARAMETER R=188.9
      PARAMETER PI=3.14
      PARAMETER MAXCEL=100
C
C    DATA
C
      COMMON/THERMAL/ TIN,PIN,VELIN,TEMP(MAXCEL,2),PRESS(MAXCEL),
     &VEL(MAXCEL),QSOUR(MAXCEL),RMASFLO
      COMMON/GEOM/ DIA,NAX,NLAY,PORIS,CLEN,XAREA,RADIUS(MAXCEL),
     &MID(MAXCEL),APTUR
C
      FACT1=RYNOLD(N-1)/(1-PORIS)
      PSI=320.0*FACT1**-1.0+6.0*FACT1**-0.1
      DP = (PSI*CLEN*(1.0-PORIS)*RMASFLO**2.0)/(2.0*
     &  RADIUS(NLAY)*PORIS**3.0*DENS(TEMP(N,2),PRESS(N-1))*XAREA**2.0)
      PRESS(N)=PRESS(N-1)-DP
      RETURN
      END
C
C23456789 123456789 123456789 123456789 123456789 123456789 123456789
C
      SUBROUTINE TFLUID(N)
C
      PARAMETER R=188.9
      PARAMETER PI=3.14
      PARAMETER MAXCEL=100
C
C    DATA
C
      COMMON/THERMAL/ TIN,PIN,VELIN,TEMP(MAXCEL,2),PRESS(MAXCEL),
     &VEL(MAXCEL),QSOUR(MAXCEL),RMASFLO
```

```
C
      NUSLAM=0.66*FACT1**0.5*FACT2**0.333
      NUSTURB=0.037*FACT1**0.8*FACT2/(1.0+2.443*FACT1**-0.1*
     &(FACT2**0.667-1.0))
C
      NUSS=2.0+SQRT(NUSLAM**2.0+NUSTURB**2.0)
C
      NUSSLT=(1.0+1.5*(1-PORIS))*NUSS
C
      RETURN
      END
C
C23456789 123456789 123456789 123456789 123456789 123456789 123456789
C
      FUNCTION PRANDL(N)
C
      PARAMETER R=188.9
      PARAMETER PI=3.14
      PARAMETER MAXCEL=100
C
C   DATA
C
      COMMON/THERMAL/ TIN,PIN,VELIN,TEMP(MAXCEL,2),PRESS(MAXCEL),
     &VEL(MAXCEL),QSOUR(MAXCEL),RMASFLO
      COMMON/GEOM/ DIA,NAX,NLAY,PORIS,CLEN,XAREA,RADIUS(MAXCEL),
     &MID(MAXCEL),APTUR
      PRANDL=SPHEAT(TEMP(N,2))*VISC(TEMP(N,2))/TCOND(TEMP(N,2))
C
      RETURN
      END
C
C23456789 123456789 123456789 123456789 123456789 123456789 123456789
C
      FUNCTION RYNOLD(N)
C
C
      PARAMETER R=188.9
      PARAMETER PI=3.14
      PARAMETER MAXCEL=100
C
C   DATA
C
      COMMON/THERMAL/ TIN,PIN,VELIN,TEMP(MAXCEL,2),PRESS(MAXCEL),
     &VEL(MAXCEL),QSOUR(MAXCEL),RMASFLO
      COMMON/GEOM/ DIA,NAX,NLAY,PORIS,CLEN,XAREA,RADIUS(MAXCEL),
     &MID(MAXCEL),APTUR
C
      RYNOLD=RMASFLO*RADIUS(NLAY)/(XAREA*PORIS*VISC(TEMP(N,2)))
C
      RETURN
      END
C
C23456789 123456789 123456789 123456789 123456789 123456789 123456789 123456789
C
      FUNCTION VISC(T)
C
C FROM INCROPTERA & DEWITT
C
      VISC = 3.783E-8*T+3.894E-6
C
      RETURN
```

## Appendix 2.2 PEB Code Input

```
30    3  0.3
500.0 6.9E6 2.43
1.0E6
0.07 0.196 0.375 0.6
0.00312   82
0.0039    50
0.004   61
```

# Appendix 2.1 PEB Code Output

```
NAX  NLAY  RLEN
         30          3  0.3000000
TIN  PIN  MASFLO
  500.0000       6900000.       2.430000
QTOT
  1000000.
RAD1 RAD2 PORIS APTUR
 7.0000000E-02  0.1960000      0.3750000       0.6000000
 CROSS SECTIONAL AREA   0.1052402
FUEL PELLET DATA
RADIUS  MID
 3.1200000E-03            82  3.8999999E-03          50  4.0000002E-03          61
 PRESSURE OUT OF INLET =     6819191.
RMASFLO
  2.430000
 POS  TFUEL   TFLUID   PRESSURE  DENS
 1.0000001E-02   538.8765       500.0000       6819191.       72.19894
 2.0000001E-02   615.8722       501.1426       6818941.       72.03169
 3.0000003E-02   692.4456       504.5212       6818689.       71.54668
 4.0000003E-02   770.9007       510.0877       6818434.       70.76326
 5.0000004E-02   842.2253       517.7615       6818175.       69.71183
 6.0000006E-02   914.4991       527.4313       6817911.       68.43110
 7.0000008E-02   974.9374       538.9583       6817641.       66.96487
 8.0000006E-02   1036.378       552.1797       6817364.       65.35880
 9.0000004E-02   1091.851       566.9126       6817078.       63.65759
 0.1000000       1131.411       582.9578       6816784.       61.90282
 0.1100000       1173.516       600.1045       6816481.       60.13141
 0.1200000       1209.238       618.1339       6816167.       58.37484
 0.1300000       1228.035       636.8229       6815843.       56.65900
 0.1400000       1251.129       655.9481       6815509.       55.00433
 0.1500000       1268.404       675.2880       6815163.       53.42632
 0.1600000       1269.245       694.6263       6814807.       51.93622
 0.1700000       1275.444       713.7536       6814439.       50.54170
 0.1800000       1266.192       732.4696       6814061.       49.24753
 0.1900000       1262.288       750.5845       6813673.       48.05624
 0.2000000       1244.129       767.9199       6813275.       46.96865
 0.2100000       1230.816       784.3102       6812868.       45.98436
 0.2200000       1204.700       799.6031       6812451.       45.10212
 0.2300000       1175.313       813.6599       6812027.       44.32017
 0.2400001       1149.172       826.3564       6811595.       43.63645
 0.2500001       1117.865       837.5826       6811156.       43.04882
 0.2600001       1078.105       847.2433       6810712.       42.55518
 0.2700000       1035.755       855.2584       6810263.       42.15359
 0.2800000       991.0170       861.5621       6809811.       41.84240
 0.2900000       944.0694       866.1039       6809355.       41.62019
 0.3000000       895.6300       868.8483       6808898.       41.48594
 PRESSURE OUT OF CORE =    6582291.
```

# 3. BRAYTON CYCLE

## INTRODUCTION

The Brayton cycle utilizes super-heated vapor throughout the cycle, the fluid does not boil and does not operate in the liquid-vapor dome.This requires that turbomachinery have high component efficiency to compensate for the work of compression that is introduced. An actual Brayton cycle temperature-entropy diagram is shown in Figure 3.1, for the system shown in Figure 3.2. The direct-closed cycle uses the primary working fluid for the entire cycle and circulates the same gas repeatedly. Energy is added to the gas in the reactor, the gas is then expanded through the turbine, the waste heat is rejected by the heat pipe radiator, and finally compressed by the compressor. The reactor, turbine, and heat pipe radiator all have significant pressure losses in the Brayton cycle due to the working fluid being gaseous. Also the pressure losses within the ducting may be significant for the same reason.

Carbon dioxide was chosen as a working fluid for this particular design for several reasons. First, the misson is proposed to spend most of its time on the Martian surface and the primary constituent of the Martian atmosphere is carbon dioxide. Therefore, in case of a minor loss of coolant there would be an abundant suppply to refurbish the system. Also, in case of a major loss of coolant, the reactor would be flooded with atmospheric gas, in this case the adverse affects would be minimized by the fact that carbon dioxide is both the coolant and atmospheric fluid. Carbon dioxide is also an extremely suitable fluid for material, thermal, and nuclear designs because of inertness, good heat transfer characteristics , and low absorption cross section. Finally, the departure of carbon dioxide from perfect gas laws results in less work of compression, this increases the cycle efficiency (1).

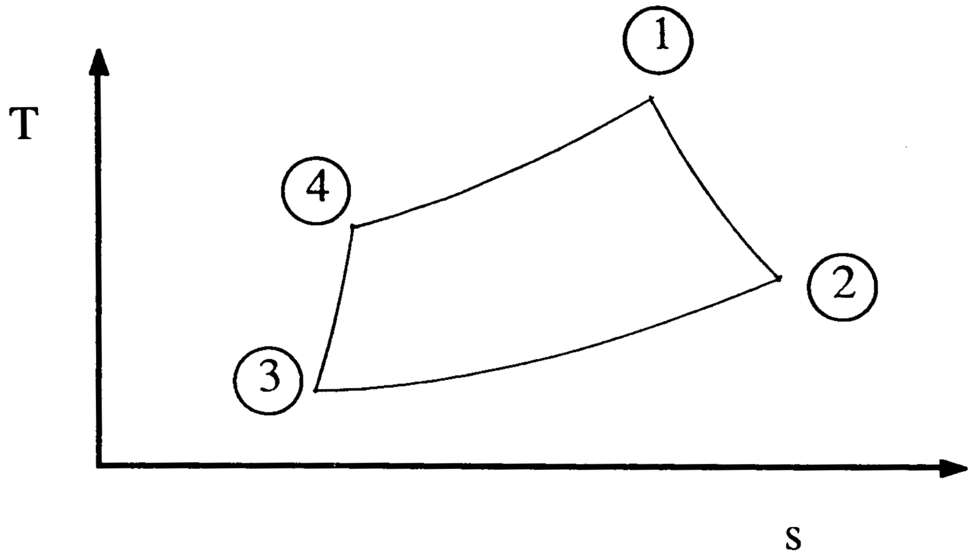


Figure 3.1 Brayton Cycle Temperature-Entropy Diagram

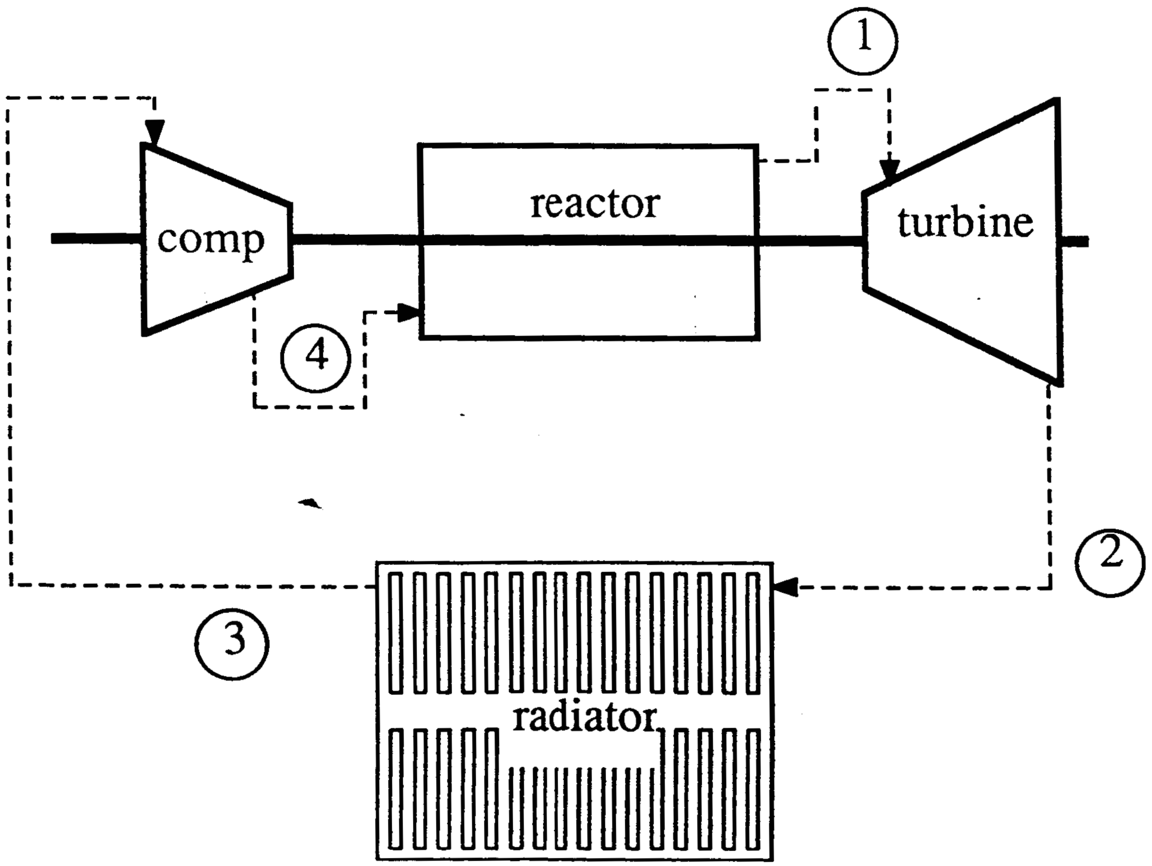


Figure 3.2 System Brayton Cycle

THEORY

In order to evaluate the performance of a Brayton cycle the standard overall cycle efficiency, $\eta$, must be determined from Equation 3.1,

$$\eta = \frac{W_{net}}{Q_{in}} \tag{3.1}$$

where $Q_{in}$ is the heat added to the system by the reactor and $W_{net}$ is the net work done by the system and is calculated by Equation 3.2:

$$W_{net} = W_T - W_C \tag{3.2}$$

where $W_T$ is the work produced by the turbine and $W_C$ is the work necessary to run the compressor. The turbomachinery is not ideal and therefore each component's performance is determined by the efficiency of that component. The turbine efficiency ( $\eta_T$) is represented by Equation 3.3:

$$\eta_T = \frac{\text{Actual Work}}{\text{Ideal Work}} \tag{3.3}$$

whereas, the compressor efficiency ( $\eta_C$ ) is the inverse as in Equation 3.4:

$$\eta_c = \frac{\text{Ideal Work}}{\text{Actual Work}} \tag{3.4}$$

These efficiencies for the turbomachinery are given for the given working fluid and thermodynamic conditions and thus by calculating the ideal work, the actual work can be determined. Equation 3.5 is used to calculate the actual work necessary to drive the compressor ($W_c$) :

$$W_C = \frac{c_p T_3}{\eta_c}(r_p^{(\gamma-1)/\gamma} - 1) \qquad (3.5)$$

where $c_p$ is the specific heat at constant pressure, $T_3$ is the compressor inlet temperature, $\gamma$ is the ratio of specific heat at constant pressure to that at constant volume, and $r_p$ is the compressor pressure ratio. The work that the turbine and is defined by Equation 3.6:

$$W_T = \eta_t c_p T_1 [1 - \frac{\beta}{r_p^{(\gamma-1)/\gamma}}] \qquad (3.6)$$

where $T_1$ is the reactor outlet temperature, and $\beta$ is the pressure losses between the compressor and turbine and is defined by Equation 3.7:

$$\beta = \left(\frac{P_4}{P_1} \cdot \frac{P_2}{P_3}\right)^{(\gamma-1)/\gamma} \qquad (3.7)$$

In Equation 3.7 the pressures are at state 1, the reactor outlet, state 2, the turbine outlet, and states 3 and 4, the inlet and outlet of the compressor.

Once the net work is determined by subtracting Equation 3.5 from 3.6, the heat input by the reactor ($Q_{in}$) is the last necessary calculation for determining the cycle efficiency. Equation 8 is used to calculate $Q_{in}$:

$$Q_{in} = c_p T_1 [(\frac{T_1}{T_3} - 1) - \frac{1}{\eta_c}(r_p^{(\gamma-1)/\gamma} - 1)] \qquad (3.8)$$

where the states are described above.

The work and heat input and output can also be calculated by $c_p \Delta T$ across each component if all of the temperatures around the cycle are known and the gas displays ideal characteristics throughout:

$$Q_{in} = c_p (T_1 - T_4) \tag{3.9}$$

$$Q_{out} = c_p (T_2 - T_3) \tag{3.10}$$

$$W_T = c_p (T_1 - T_2) \tag{3.11}$$

$$W_C = c_p (T_4 - T_3) \tag{3.12}$$

where $Q_{out}$ is the heat removed from the system by the heat pipe radiator (2).

## RESULTS

In order to evaluate the closed-direct Brayton cycle several assumptions were made. It was assumed that the pressure losses in the ducting would be insignificant compared to the losses across the components, that the working fluid performs ideally throughout the system, that the specific heat at constant pressure remained constant around the cycle, and that carbon dioxide is closely approximated by argon in the turbomachinery. The last assumption allows for the use of $\eta_C = \eta_T = 0.86$ (3), while the third assumption results in the use of $r_p$ =1.22 kJ/kg-K and $\gamma$ =1.290 for the entire cycle analysis. The last assumption also allows for the use of $r_p$ =1.90, and a turbine pressure ratio of 1.75 (4).

After defining the reactor inlet and outlet states and considering the above assumptions the pressures at the turbine outlet and compressor inlet were found using the turbine and compressor ratios. Once all of the pressures are known $\beta$ can be calculated and was found to be $\beta$ =1.0188 . Using Equation 3.6 the turbine work was calculated to be $W_T$ = 513 kW, then rearranging Equation 3.11 the turbine outlet temperature was determined to be $T_2$ = 677 K. Considering that our net work must be 300 kWe, for propulsion prurposes, the work to run the compressor was found to be 213 kW. Rearranging Equation 3.12 the compressor inlet temperature was calculated to be 428 K. Table 3.1 list the temperatures and pressures around the system and Table 3.2 list the energy balance and cycle efficiency ( $\eta$ =28.9%).

The assumptions made produced an overall cycle efficiency somewhat higher than expected without a recuperator in the system. However, carbon dioxide is an excellent working fluid and thus the system seems to be a feasible and beneficial design for the specific application it is intended for.

Table 3.1 System Thermodynamic States

| State | Temperature (K) | Pressure (MPa) |
| --- | --- | --- |
| 1 | 850 | 6.58 |
| 2 | 677 | 3.76 |
| 3 | 428 | 3.63 |
| 4 | 500 | 6.90 |

Table 3.2 System Energy Balance

$Q_{in}$ = 1038 kW

$Q_{out}$ = 738 kW

$W_T$ = 513 kW

$W_C$ = 213 kW

$\eta$ = 28.9 %

REFERENCES


1. English, R. E. : Power Generation from Nuclear Reactors in Aerospace Applications. NASA TM 83342, Nov. 1982.

2. Rust, J. H. : Nuclear Power Plant Engineering. Georgia Institute of Technology, 1979.

3. Blumenberg, J. ; Ruppe, H. O. : Comparison of Nuclear and Solar Power Plants with Turboelectric Generators for Application in Space. Technical University of Munich D-8000, Apr. 1983.

4. English, R. E. : Power Generation from Nuclear Reactors in Aerospace Applications. NASA TM 83342, Nov. 1982.

## 4. TURBOMACHINERY

Optimizing the cycle efficiency was a primary concern in choosing the turbine and compressor for this system. However, a consideration of equal importance was chooosing turbomachinery that utilized the system's unique design. The use of carbon dioxide as the primary working fluid for the system constrained the availability of information and the applicability of previously tested systems.

Cycle efficiency optimization for turbine and compressor considerations means achieving the maximum efficiency for both components with minimum mass. In order to accomplish this the turbine needs to have as high an inlet temperature as possible and the compressor pressure ratio ($r_p$) optimized. According to calculations by Blumenberg and Ruppe (1) component efficiencies of $\eta_T$=0.86 and $\eta_C$=0.86 can be expected for the turbine and compressor, respectively, for the system characteristics under consideration. For tests typical of the system under consideration compressor pressure ratios of $r_p$=1.90 were found to be optimum by English (2). The combined mass of these two components and the rotating shaft connecting them is estimated to be 215 kilograms by English.

The system's unique design (Figure 4.1), most significantly having the heat source located between the turbine and compressor on the shaft is perfect for the use of axial flow turbomachinery. Outlet flow from the reactor can more easily be derected to an axial flow turbine (Figure 4.2) for this design. Likewise, both inlet and outlet flow of the compressor is more easily directed for this design with axial flow (Figure 4.3). Axial flow turbomachinery has the advantage of higher efficiency over radial flow, but have the disadvantage of a smaller pressure rise per unit mass in the compressor. These effects balance themselves out and the design concern becomes the factor that makes the axial flow turbomachinery the best alternative for this specific design.

Not much research has been conducted in the area of carbon dioxide turbomachinery and therefore the parameters taken in references 1 and 2 may have some error. Since no available data on turbomachinery could be found for carbon dioxide the efficiencies for both components were taken from data for an argon working fluid at similar conditions. Argon and carbon dioxide have

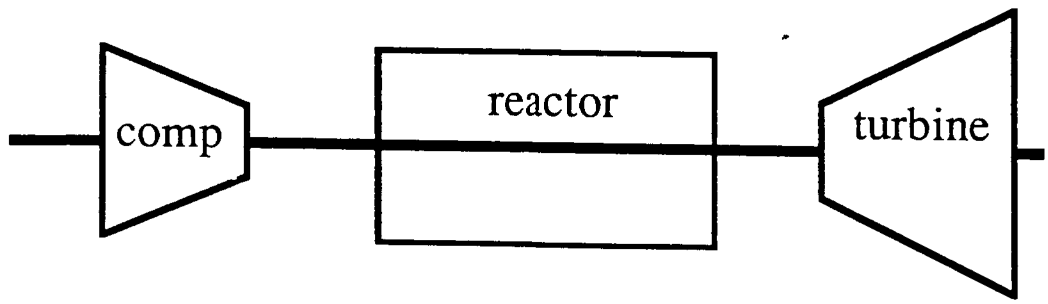


Figure 4.1 Reactor and Turbomachinery Schematic

CS-40265

Figure 4.2 Axial Flow Turbine

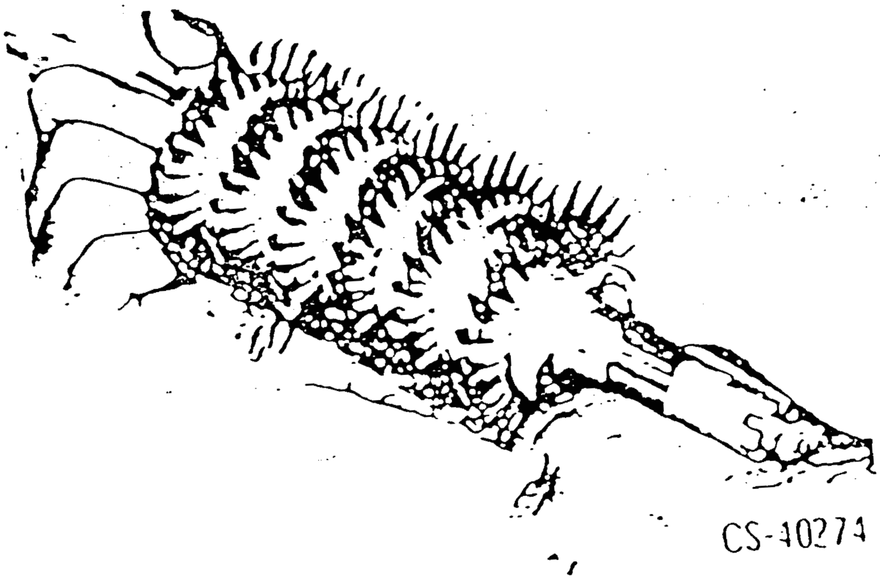


Figure 4.3 Axial Flow Compressor

similar atomic masses, 40 and 44 amu respectively, and therefore the approximation is good as long as the carbon dioxide does not dissociate. At the temperatures under consideration dissociation has a very low probability and thus the approximation should be good as far as turbomachinery is concerned.

## References


1. Blumenberg, J. ; and Ruppe, H. O. : Comparison of Nuclear and Solar Power Plants with Turboelectric Generators for Application in Space. Technical University of Munich D-8000, Apr. 1983.

2. English, R. E. : Power Generation from Nuclear Reactors in Aerospace Applications. NASA TM 83342, Nov. 1982.

# 5. HEAT REJECTION SYSTEM

## 5.1 Introduction

Heat rejection techniques for space reactor systems are distinctly different from those used in terrestrial reactor systems. Terrestrial reactors reject heat by convection to the atmosphere through such mechanisms as cooling towers and to bodies of water such as cooling ponds or rivers. Space power systems can employ neither of these techniques for dissipating waste heat. The only viable mode of heat rejection for space power systems is that of radiation to the surrounding space. Space power systems cannot employ convective heat rejection systems because they operate in a virtual vacuum.

There are two operable types of radiator systems available for space power systems. The first system employs a continous fluid loop which serpentinely winds through the radiator, such as the pumped fluid radiator used on the Shuttle (Pearson and Dabrowski, p. 806). The second type employs a heat pipe radiator system which transfers heat from the reactor coolant to heat pipes. A heat pipe radiator system was chosen for the space power system under discussion.

The decision to use heat pipes was based on safe operating criteria for a long duration of unmanned operation. The continuous fluid loop design has the disadvantage that if the radiator sustains meteroid damage, there is a great probability that the entire cooling loop will be lost. To compensate for this, redundancy and isolation valves must be built into the radiator system. This addition increases system mass and reduces reliability, both critical requirements for space operation of long duration. The heat pipe radiator system is a more reliable system because each heat pipe operates independently of the other heat pipes in the radiator. If one heat pipe sustains meteroid damage, the other heat pipes and cycle fluid are unaffected. The reactor coolant flows through a main manifold which can be shielded for meteroid protection. By including sufficient heat pipe elements to account for losses from meteroid damage and shielding the manifold, the heat pipe radiator has a high level of reliability. In the system under discussion, it was also crucial to have high levels of reliability in the radiator because one of the design criteria was that the power system also be operable on the planet of Mars. The winds on Mars are equivalent to 20 mile per hour winds on earth and dust storms are common. This criteria again pointed toward the use of a heat pipe radiator to insure safe operation of the planet of Mars due to the independent operation of each heat pipe unit.

## 5.2 Principles of Operation

The structure of a heat pipe is shown in Figure 5.1. The main regions are the evaporator section and the condenser section. The pipe itself consists of the pipe wall, the wick, and the working fluid. The heat pipe operates on the principle of capillary forces. In order for the heat pipe to operate properly, the maximum capillary pumping head must be greater than the total pressure drop in the pipe, which is made up of the pressure drop required to return the liquid from the condenser to the evaporator and the pressure drop necessary to cause the vapor to flow from the evaporator to the condenser and the gravitational head.

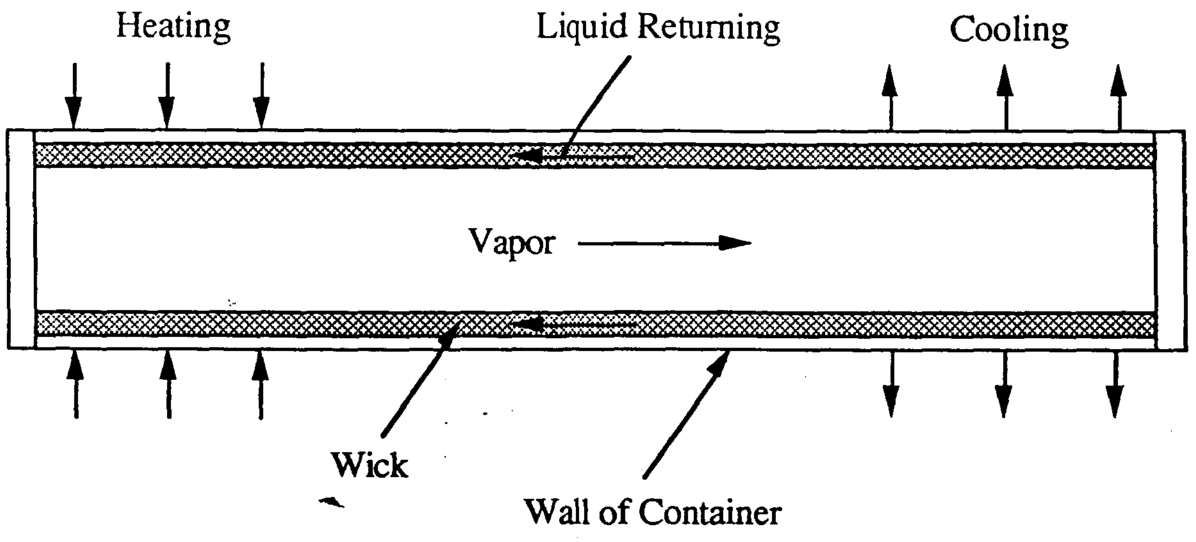


Figure 5.1 - Diagram of Heat Pipe

Energy is transferred to the working fluid of the pipe in the evaporator region. The working fluid begins to evaporate and the vapor moves toward the condenser section of the pipe. When cooled the fluid condenses in the condenser region. Capillary forces in the wick return the condensate to the evaporator region.

Several characteristics of heat pipes are:

1. can operate in any orientation, evaporator position is not restricted (Dunn and Reay, p. 1)
2. very high effective thermal conductance
3. a near isothermal surface of low thermal impedance, the condenser surface of heat pipe will tend to operate at uniform temperature (Dunn and Reay, p. 3).

In space the latent heat produced when the fluid condenses is dissipated by radiation to the surrounding space. In order to increase the area of radiative heat transfer, fins can be attached to the heat pipe. Since radiative heat transfer is proportional to $T^4$, the quantity of energy radiated is larger at higher temperatures. Thus, from the heat transfer standpoint, it is best to reject energy at the highest temperature possible.

## 5.3 Selection of Materials

### 5.3.1. Working Fluid

The working fluid of the heat pipe was chosen to be sodium. Of primary importance was the useful temperature range of the working fluid. The heat pipe radiator design criteria specified that it should operate in the range of 400-800 K. The two working fluids considered whose useful range fell between these two values were potassium and sodium. Two other working fluids, mercury and cesium, had operating ranges which were compatible with the design criteria. Mercury was not considered due to its toxicity and cesium was not considered due to its high cost. The principle criteria for deciding upon a working fluid were latent heat, thermal conductivity, demonstrated radial heat flux capability, and liquid surface tension. The corresponding properties for sodium and potassium are shown in Table 5.1.

Table 5.1 - Properties for Sodium and Potassium

| Fluid | Latent Heat | Thermal Conductivity | Radial Heat Flux Capability | Liquid Surface Tension |
|---|---|---|---|---|
| Na | 4400 kJ/kg | 70 W/m $^{o}$C | 200-1250 W/cm$^2$ | 1.5 N/m x 10 |
| K | 2050 kJ/kg | 49 W/m $^{o}$C | 150-250 W/cm$^2$ | 9.0 N/m x 10$^2$ |

Another means of comparing working fluids is provided by the Merit number, which is given by:

$$M = \rho_l \sigma_l L / \mu_l$$

where $\rho_l$ is the density of the liquid working fluid
$\sigma_l$ is the surface tension
$L$ is the enthalpy of vaporization or latent heat
$\mu_l$ is the viscosity of the liquid working fluid.

Sodium was chosen over potassium because it has superior qualities over the temperature range of interest as shown in Table 5.1 and because it has a higher merit number than potassium. When the Merit numbers at the boiling points of both fluids are compared, the Merit number for sodium is and order of magnitude larger than that of potassium (Dunn and Reay, p. 91).

5.3.2. Container

The container material was selected to be stainless steel (SS 304). The criteria for the container were compatability with the working fluid, strength, and thermal conductivity. The thermal conductivities of several materials are shown in Table 5.2.

Table 5.2 - Properties of Container Materials

| Material | Thermal Conductivity (W/m $^{o}$C) |
|---|---|
| Aluminum | 205 |
| Copper | 394 |
| Stainless Steel 304 | 17.3 |

Aluminum and copper both had significantly higher thermal conductivity than stainless steel, but stainless steel was the only material which was compatible with sodium. Stainless steel is also a stronger material than aluminum or copper, which contributes to the reliability of the system.

5.3.3. Wick

The wick material chosen was a stainless steel mesh, specifically 508 x 3600 mesh s/s twill. The primary criteria for wick material was demonstrated radial heat flux capability with the working fluid. Various types of wicks have been tested with sodium as the working fluid. The results are shown in Table 5.3 (Dunn and Reay, p. 95).

Table 5.3 - Wick Performance with Sodium

| Wick Material | Radial Heat Flux ($W/cm^2$) |
|---|---|
| s/s mesh | 230 |
| various | 200-400 |
| 3 x 65 mesh s/s | 214 |
| 508 x 3600 mesh s/s twill | 1250 |

The 508 x 3600 mesh s/s twill had the highest demonstrated radial heat flux capacity. This particular mess twill has a small pore radius, resulting in a large maximum capillary head being generated which aids axial flow.

5.3.4. Fin

Aluminum was chosen to be the fin material. The criteria used for selecting a fin material was strength, weight, and thermal conductivity. Materials considered were aluminum and copper. Stainless steel was also considered since the heat pipes themselves were to be fabricated from it. The thermal conductivities of these three materials are shown in Table 5.2. The densities of the materials are shown in Table 5.4 (Chi, p. 230).

Table 5.4 - Density of Fin Materials

| Material | Density |
|---|---|
| Aluminum | 2700 $kg/m^3$ |
| Copper | 9000 $kg/m^3$ |
| SS 304 | 7850 $kg/m^3$ |

The ultimate tensile strength was compared and stainless steel had the highest, followed by aluminum, which had a slightly higher ultimate tensile strength than copper over the temperature range of interest, 500-800 K (Chi, p. 231). Although stainless steel was strongest, it was eliminated because of its very low thermal conductivity and high density. The ratio of thermal conductivity to density was computed for aluminum and copper. The ratio was 7.6 X $10^{-2}$ for aluminum and 4.4 X $10^{-2}$ for copper. Thus, aluminum was chosen since it had the greatest strength and the largest ratio of thermal conductivity to density.

### 5.3.5. Coating of Heat Pipe Radiator

The energy radiated by a surface is proportional to the emissivity of the surface material. Since the area required is inversely proportional to the emissivity, the mass of the system can be reduced if the emissivity of the surface is increased. A method to increase the emissivity of a surface whose material does not have a large enough emissivity is to coat the surface with a material which has a greater emissivity. Coatings considered were $Al_2O_3$, $ZrO_2$, and MgO. $Al_2O_3$ was chosen because it had the highest value of emissivity over the temperature range of interest. Its emissivity ranged from 0.85-0.95 (Dieckamp, p. 112). Both the heat pipe and radiator are coated with $Al_2O_3$.

## 5.4. Calculations

A basic diagram of the proposed heat pipe system is shown in Figure 5.2. Hot gas enters one end of the radiator system, flows through the manifold into which the evaporator section of heat pipes protrude, and exits at a lower temperature. The purpose of the calculations was to determine the temperature of each heat pipe unit and thus the energy dissipated by that unit, on which basis the number of heat pipes necessary to dissipate the required amount of heat could be found.

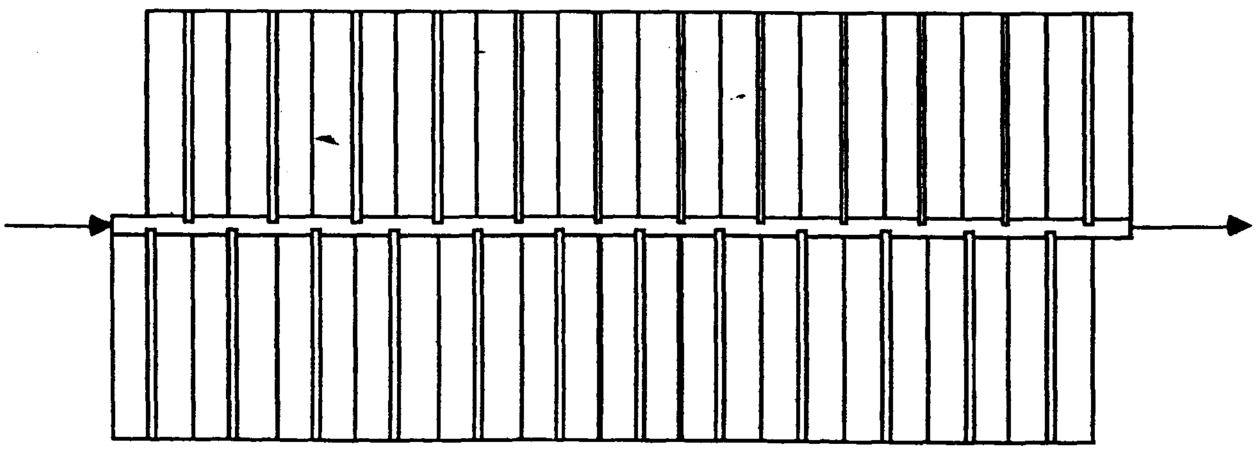

Figure 5.2 - Section of Heat Pipe Radiator System

### 5.4.1. Basic Energy Equation

The equation used to calculate the energy dissipated by each heat pipe was:

$$Q(z) = \varepsilon\,\sigma\,A_{hp}\,(T_{hp}(z)^4 - T^4) + \eta\,\varepsilon\,\sigma\,A_f\,(T_{hp}(z)^4 - T^4)$$

where $Q(z)$ = energy dissipated by a heat pipe unit

$\varepsilon$ = emissivity of the coating

$\sigma$ = Stefan-Boltzmann constant, 5.670 X $10^{-8}$ W/m$^2$ K$^4$

$\eta$ = fin efficiency

$A_{hp}$ = surface area of the heat pipe

$A_f$ = surface area of the fin

$T_{hp}(z)$ = operating temperature of the heat pipe (position dependent)

$T$ = ambient temperature.

A computer code was written which uses this equation to find the number of heat pipes necessary to dissipate a given amount of heat when the inlet and exit temperatures are specified. The code calculates the operating temperature of each heat pipe unit, the amount of heat dissipated by each unit, and finally, the number of heat pipe units needed and the total radiator mass.

### 5.4.2. Assumptions

Several simplifying assumptions were made before the equation above was used in the program. These assumptions were:

1. $\eta = 0.5$, a conservative estimate since fin efficiency is likely to be above this value because the fins are relatively small in width

2. $\varepsilon = 0.85$, a conservative estimate since it is the lower end of the range of 0.85-0.95

3. each heat pipe is isothermal (see 5.2. Priniciples of Operation)

4. the fins operate at the same temperature as the heat pipe; a reasonable assumption considering that the fins are not very wide and aluminum has a high thermal conductivity

5. the temperature of each heat pipe is the temperature of the gas with which it is in contact in the manifold; a reasonable assumption considering that the evaporator region will be completely submersed in the gas and will have numerous small fins protruding into the gas flow to improve convective heat transfer

6. the ambient temperature in space is 0 K.

5.4.3. Preliminary Calculations

Preliminary calculations were necessary to determine the area of the fins and the surface of the heat pipe. Given that the radius of the heat pipes was to be 1.5 cm and the length was to be 4 m, the area was calculated as follows:

$$A_{hp} = 2\,\pi\, r\, h = 2\,\pi\,(.015 \text{ m})\,(4 \text{ m}) = 0.377 \text{ m}^2.$$

The fin area was calculated given that the length was the same as that of the heat pipe, 4 m, and that the width was 0.1 m. The product of length times width was multiplied by two to account for the fin radiating from both sides.

$$A_f = 2\, l\, w = 2\,(4 \text{ m})\,(0.1 \text{ m}) = 0.8 \text{ m}^2$$

Based on the assumptions and the preliminary calculations, the basic equation can be simplified to the following form:

$$Q = \varepsilon\,\sigma\,(T_{hp}(z))^4\,(A_{hp} + \eta\, A_f)$$

$$Q = 3.74 \text{ X } 10^{-11} \text{ kW/K}^4\,(T_{hp}(z))^4.$$

An additional preliminary calculation was undertaken to insure that the heat pipe capability was not going to be exceeded given the operating conditions. The first heat pipe unit in the system dictated the limitations because it would be operating at the highest temperature and rejecting the largest amount of heat. The limiting radial heat flux was estimated to be 800 kW/cm$^2$ (see Table 5.1). This value is reasonably conservative because it falls in the middle of the demonstrated radial heat flux range, but is below that actually demonstrated for the chosen mesh. The heat dissipated by the first heat pipe at the maximum operating temperature was determined:

$$Q_1 = 5.34 \text{ X } 10^{-11} \text{ kW/K}^4 \, (800 \text{ K})^4 = 21.87 \text{ kW}.$$

The maximum length of evaporator section which could protrude into the gas flow and still maintain the radial heat flux below its limiting value was calculated as follows, assuming that $Q_1$ was 25 kW to insure conservatism:

$$25.0 \text{ kW} / 2 \pi r h_e = 0.8 \text{ kW/cm}^2$$

$$h_e = 25.0 \text{ kW} / (0.8 \text{ kW/cm}^2 \times 2 \times \pi \times 1.5 \text{ cm}) = 3.32 \text{ cm}.$$

Thus, the evaporator section can protrude 3.32 cm into the gas flow in the manifold without exceeding the limiting radial heat flux value.

5.4.4. Mass Calculation

The mass of the unit was calculated in the computer code by multiplying the necessary number of heat pipe units by the weight of an individual heat pipe unit. The weight of the unit has three main components: the container, the fluid, and the fin. The mass of the wick can be neglected compared to the masses of these three components. The mass of a unit can then be calculated as follows:

$$\text{mass} = \pi h (r_o^2 - r_i^2) \rho_{ss} + 0.5 \pi h (r_i^2 - r_w^2) \rho_{Na} + h w t \rho_{Al}$$

where $h$ = length of the unit, 4 m

$r_o$ = outer radius of the heat pipe container, .015 m

$r_i$ = inner radius of the heat pipe container, .0135m

$r_w$ = inner radius of the wick, .0125 m

$w$ = fin width, 0.1 m

$t$ = fin thickness, 3 mm

$\rho_{ss} = 7850 \text{ kg/m}^3$

$\rho_{Na} = 900 \text{ kg/m}^3$

$\rho_{Al} = 2700 \text{ kg/m}^3$

and the 0.5 factor in the second term accounts for the fact that the wick is half full of the working fluid.

The result is that the mass of a single heat pipe unit, consisting of the heat pipe and fin is 7.607 kg.

5.4.5. The Program

The program written to do the heat pipe calculations allows the user to input the inlet temperature, the outlet temperature, and the amount of heat to be dissipated. It uses the basic energy equation and the unit mass formulation to determine the size of the system necessary. A listing of the program is provided in Appendix 5.1.

5.4.5.1. Mass Flow Rate

Using the specified inlet and outlet temperatures and the amount of heat to be rejected, the mass flow rate necessary is calculated from:

$$Q = m\,c\,(T_i - T_o)$$

where $m$ = mass flow rate

$c$ = specific heat of the gas.

Although the specific heat actually varies with temperature, the relationship is fairly linear (Incropera and DeWitt, p. 768). Thus, to calculate the mass flow rate the inlet and outlet temperatures are averaged and the specific heat for the average temperature obtained.

5.4.5.2. Algorithm

The basic algorithm of the program begins with the calculation of the heat loss by the first pipe using the basic energy equation. The temperature of the gas after it transfers heat to the first pipe is then calculated using:

$$T_2 = T_1 - Q / (m \times c)$$

This temperature is used to calculate the heat rejection by the second pipe. Since the heat pipe units are arranged in a series configuration, the temperature of the fluid immediately after it transfers heat to the first pipe is the temperature of the gas when it reaches the next pipe. This process is repeated for additional heat pipes until the specified amount of heat is rejected or the specified outlet temperature is reached. The number of heat pipes necessary is then multiplied by the unit mass to determine the system mass.

5.4.5.3. Environment

The code has the capability of calculating radiator size for three environments, in space, on the surface of Mars, and buried underground on Mars. Since the only mechanism for energy loss in space is radiation, the basic energy equation can be used unaltered. On Mars energy is lost through convection and radiation. The basic energy equation must be modified with a term to account for convection. The value used for ambient temperature temperature on Mars is 333 K. An appropriate convection coefficient is calculated for each heat pipe unit based on operating temperature. The convection coefficient is calculated using the properties of carbine dioxide, since the atmosphere of Mars is predominantly composed of $CO_2$. When the radiator is located underground heat is rejected by conduction. This scenario was treated as conduction from a flat plate in a semi-infitine solid. The heat rejection was calculated from (Rohsenow and Hartnett, p.3-120):

$$Q = k\, a\, (T_{hp} - T_w)\, 2\pi / (\ln (2\pi x/b))$$

where $k$ = thermal conductivity

$a$ = length of the unit, 4 m

$T_w$ = atmospheric temperature, 333 K

$x$ = depth at which the radiator is buried

$b$ = width of the unit, 0.1 m.

The depth of burial is assumed to be 2 m. Since the thermal conductivity for Martian soil was unavailable the thermal conductivities of sand (0.27 W/mK) and soil (0.52 W/mK) were averaged to obtain an estimate (0.37 W/mK) to be used in the calculations. The resulting expression for energy dissipation was:

$$Q = .00192 \text{ W/K } (T_{hp} - 333)\text{K}.$$

5.4.5.4. Numerical Correlations

Numerical correlations were incorporated as functions in the code. Functions were included to calculate the temperature dependent parameters of specific heat, thermal conductivity, and Nusselt number. The numerical expressions for specific heat and thermal conductivity were obtained by fitting a curve to tabular data (Incropera and DeWitt, p. 768). Expressions for Nusselt number and the Prandtl and Rayleigh numbers necessary to calculate it were found in a heat transfer textbook (Incropera and DeWitt, p. 767-768).

## 5.5. Results

### 5.5.1. Preliminary Results

The specified inlet and outlet temperatures of the radiator were 677 K and 428 K, respectively. The amount of heat to be dissipated was 738 kW. The program was then run under the condition that the environment was space. The resulting mass flow rate was calculated to be 2.43 kg/sec. The number of heat pipes necessary to meet these design criteria was 246. The resulting mass of the radiator was 1870 kg. With the design specifications remaining the same, the program was run under the condition that the environment was on Mars. The number of heat pipes necessary for energy rejection in this case was less that that required in space. The program was then run for the case of the radiator buried underground. The number of heat pipes necessary under this condition was significantly larger than under the other two conditions.

The option of operating the radiator underground on Mars was disregarded because the number of heat pipes necessary for this mode was significantly larger than for either of the other two modes. The limiting case then was operation in space. Since the number of heat pipes required for energy rejection in space was more than that on Mars, the final heat pipe unit numbers and radiator mass are based on this case. The program output is included in Appendix 5.2.

### 5.5.2. Modified Results

The probability of non-failure was calculated to be 0.864 for the heat pipe design (see VII. Space Logistics). The number of heat pipe units necessary to compensate for failure due to micrometeroid penetration was obtained by dividing the number of heat pipes units necessary to dissipate the required amount of heat by 0.864. This resulted in a value of 280 heat pipe units. This made the final mass of the radiator 2130 kg. Due to the addition of heat pipe units to compensate for failure, a valve was inserted between the initially calculated number of heat pipe units, the primary radiator, and the additional heat pipe units, secondary unit. The valve is initially closed but can be opened when failure occurs in the primary radiator unit which warrants additional heat pipe units.

A diagram of the heat pipe radiator unit, including the dimensions of the components, is shown in Figure 5.3. A diagram of the primary radiator system is shown in Figure 5.4. The primary radiator system is 12.3 m long and 8 m wide. The total area of the primary radiator system is 98.4 $m^2$. The secondary radiator system is 0.4 m long and 8 m wide and is 3.2 $m^2$.

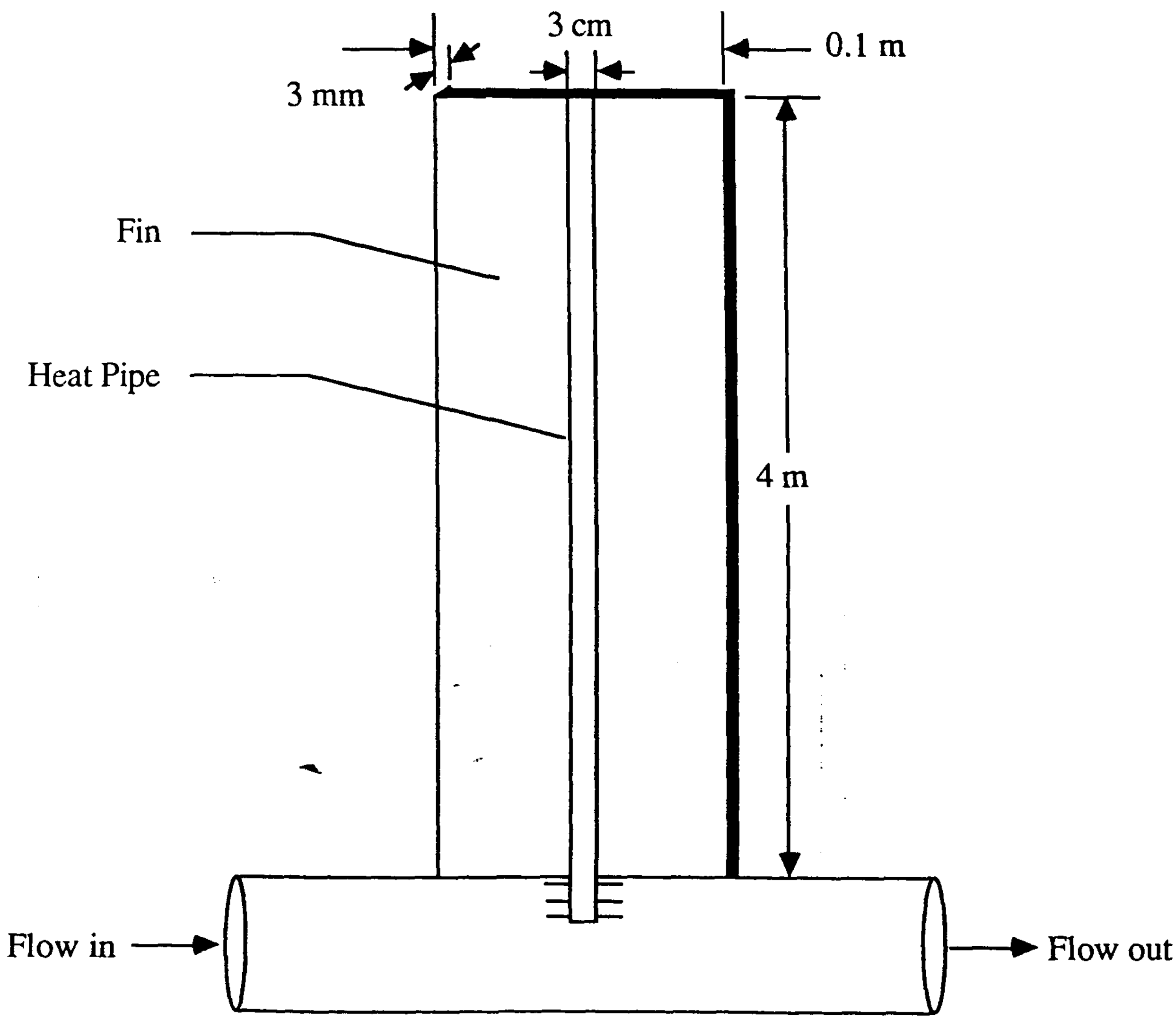


Figure 5.3 - Heat Pipe Unit

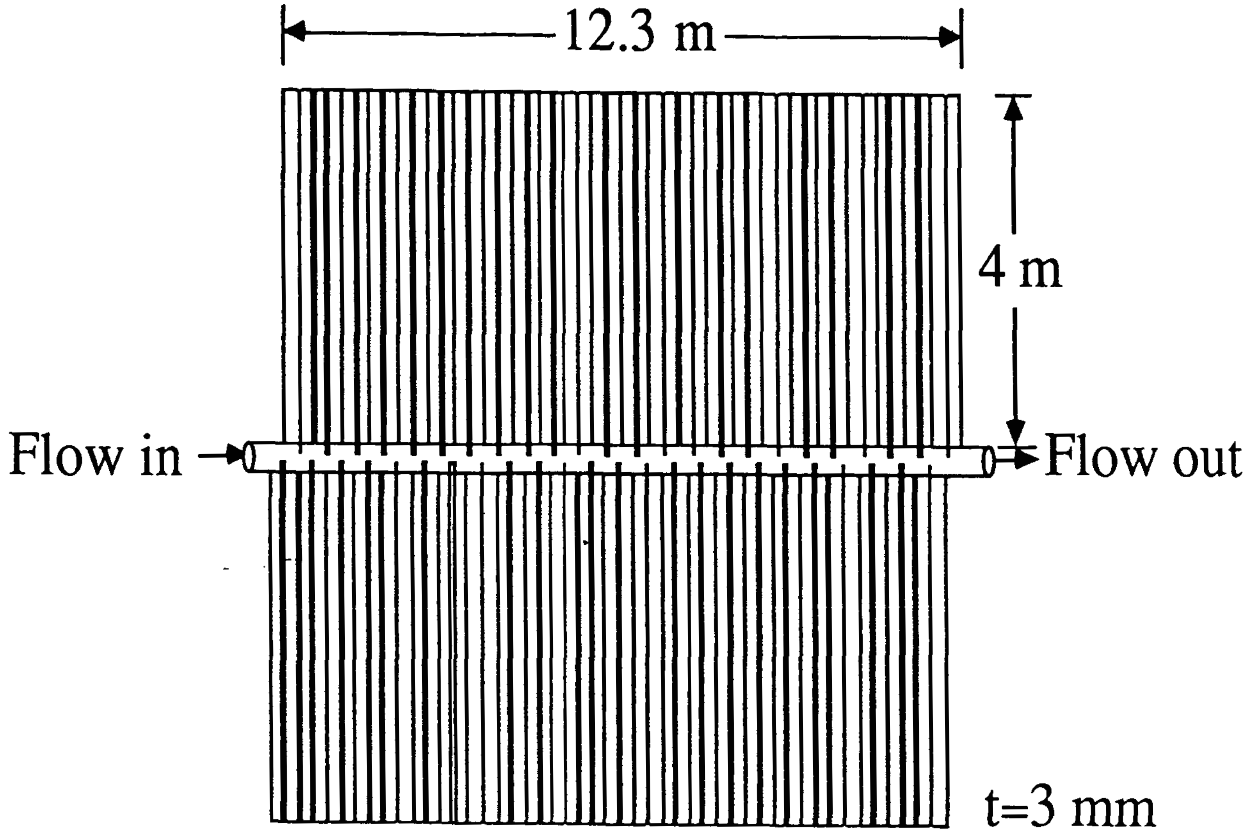


| | |
|---|---|
| • Total Area | 98 $m^2$ |
| • Mass | 1870 kg |
| • Heat Pipes | 246 |
| • Container Material | SS 304 |
| • Coating | $Al_2O_3$ |
| • Working Fluid | Sodium |
| • Fin Material | Aluminum |

Figure 5.4 - Heat Rejection System

## 5.6. **References**

Chi, Heat Pipe Theory and Practice: A Sourcebook, Hemisphere Publishing, Washington, 1976.

Dieckamp, H. M., Nuclear Space Power Systems, Atomics International, Canoga Park, 1967.

Dunn, P. D. and D. A. Reay, Heat Pipes, First Edition, Pergamon Press, New York, 1976.

Incropera, F. P. and D. P. DeWitt, Fundamentals of Heat and Mass Transfer, Second Edition, John Wiley & Sons, New York, 1985.

Pearson, R. and D. Dabrowski, "Optimization of Heat Rejection Subsystem for Solar Dynamic Brayton Cycle Power System," Document Number 860999, Grumman Aerospace Corp., Bethpage, NY.

Rohsenow, W. M. and J. P. Hartnett, Editors, Handbook of Heat Transfer, McGraw-Hill Book Company, New York, 1973.

# Appendix 5.1 - Program Listing

```
C*********************************************************************
C*********************************************************************
C
C                   HEAT PIPE RADIATOR CALCULATIONS
C
C                           Sandra M. Sloan
C                       Nuclear Engineering 410
C                           Design Project
C
C*********************************************************************
C*********************************************************************
C
C  The purpose of this program is to calculate the necessary set of
C  parameters to design a heat pipe radiator.  The program calculates
C  the operating temperature of and heat dissipated by each heat pipe
C  which is necessary to meet the design conditions. Based on these
C  calculations, the number of heat pipes necessary to dissipate the
C  required amount of heat is known.
C
C  Numerical correlations are used for heat transfer constants such
C  as Nu,c,etc.  They are incorporated into the program as functions.
C
C*********************************************************************
C
C  THE PARAMETERS OF THE SYSTEM
C
C*********************************************************************
C
C     TI = heat pipe radiator inlet temperature
C     TO = heat pipe radiator outlet temperature
C     QRAD = heat to be dissipated in the radiator
C     Q = heat dissipated in the heat pipe
C     QTOT = total amount of heat dissipated in the radiator
C     MFLOW = mass flow rate
C     MASS = mass of unit (heat pipe and fin)
C     SYSMAS = mass of radiator system
C     NUSSLT = Nusselt number
C     C = specific heat
C     RK = k, thermal conductivity
C     H = h, convective heat transfer coefficient
C     ENVIR = environment in which the radiator operates
C
C*********************************************************************
C
C  DECLARE VARIABLES AND OPEN DATA FILES
C
C*********************************************************************
C
      REAL MASS,MFLOW
      INTEGER ENVIR
C
      OPEN(UNIT=10,FILE='HEATPIPE1.OUT',STATUS='NEW')
      OPEN(UNIT=12,FILE='HEATPIPE2.OUT',STATUS='NEW')
      OPEN(UNIT=15,FILE='HEATPIPE3.OUT',STATUS='NEW')
C
      PRINT*,'INLET TEMPERATURE(K)?'
      READ*,TI
      PRINT*,'OUTLET TEMPERATURE(K)?'
      READ*,TO
      PRINT*,'HEAT TO BE DISSIPATED(KW)?'
      READ*,QRAD
```

```
C************************************************************************
C
C  If the environment is the MARTIAN ATMOSPHERE, then the radiator
C  rejects heat by radiation and convection.
C
60    DO 80 I=1,300
C
         H=NUSSLT(TOLD)*RK(TOLD)/0.20
C
         Q=3.74E-11*(TOLD**4-1.23E10)+H*0.80*(TOLD-333)
C
         PRINT*,I,Q,TOLD
         WRITE(12,*)I,Q,TOLD
C
         TNEW=(-1.0*Q/MFLOW/C(TOLD))+TOLD
C
         QTOT=QTOT+Q
C
         ERRORT=TOLD-TO
         ERRORQ=QTOT-QRAD
C
         IF(ERRORT.LT.O.OR.ERRORQ.GT.O)THEN
         PRINT*,QTOT
         WRITE(12,*)QTOT
         GO TO 100
         ENDIF
C
         TOLD=TNEW
C
80    CONTINUE
C
      GO TO 100
C
C************************************************************************
C
C  If the heat pipe system is UNDERGROUND, it rejects heat by conduc-
C  tion to the surrounding soil.
C
120   DO 140 I=1,350
C
      Q=.00192*(TOLD-333)
      PRINT*,I,Q,TOLD
      WRITE(15,*)I,Q,TOLD
C
      TNEW=(-1.0*Q/MFLOW/C(TOLD))+TOLD
C
      QTOT=QTOT+Q
C
      ERRORT=TOLD-TO
      ERRORQ=QTOT-QRAD
C
      IF(ERRORT.LT.O.OR.ERRORQ.GT.O)THEN
      PRINT*,QTOT
      WRITE(15,*)QTOT
      GO TO 100
      ENDIF
C
      TOLD=TNEW
C
140   CONTINUE
C
```

```
      NUSSLT=(0.825+NUM/DENOM)**2.0
C
      RETURN
      END
C
C***********************************************************************
C***********************************************************************
```

# Appendix 5.2 - Program Output

ENVIRONMENT IS SPACE

| No. | Q(z) | T(z) |
|---|---|---|
| 1 | 7.856449 | 677.0000 |
| 2 | 7.742754 | 674.5373 |
| 3 | 7.631761 | 672.1068 |
| 4 | 7.523382 | 669.7078 |
| 5 | 7.417531 | 667.3397 |
| 6 | 7.314126 | 665.0016 |
| 7 | 7.213094 | 662.6932 |
| 8 | 7.114356 | 660.4136 |
| 9 | 7.017840 | 658.1622 |
| 10 | 6.923476 | 655.9385 |
| 11 | 6.831200 | 653.7419 |
| 12 | 6.740946 | 651.5718 |
| 13 | 6.652653 | 649.4277 |
| 14 | 6.566266 | 647.3091 |
| 15 | 6.481723 | 645.2154 |
| 16 | 6.398973 | 643.1461 |
| 17 | 6.317961 | 641.1008 |
| 18 | 6.238640 | 639.0790 |
| 19 | 6.160957 | 637.0803 |
| 20 | 6.084868 | 635.1041 |
| 21 | 6.010328 | 633.1500 |
| 22 | 5.937291 | 631.2177 |
| 23 | 5.865718 | 629.3068 |
| 24 | 5.795566 | 627.4167 |
| 25 | 5.726798 | 625.5472 |
| 26 | 5.659375 | 623.6978 |
| 27 | 5.593261 | 621.8682 |
| 28 | 5.528422 | 620.0581 |
| 29 | 5.464821 | 618.2670 |
| 30 | 5.402427 | 616.4947 |
| 31 | 5.341210 | 614.7408 |
| 32 | 5.281138 | 613.0049 |
| 33 | 5.222180 | 611.2869 |
| 34 | 5.164309 | 609.5862 |
| 35 | 5.107497 | 607.9028 |
| 36 | 5.051715 | 606.2361 |
| 37 | 4.996940 | 604.5861 |
| 38 | 4.943145 | 602.9523 |
| 39 | 4.890307 | 601.3345 |
| 40 | 4.838403 | 599.7325 |
| 41 | 4.787410 | 598.1461 |
| 42 | 4.737303 | 596.5748 |
| 43 | 4.688063 | 595.0185 |
| 44 | 4.639669 | 593.4769 |
| 45 | 4.592101 | 591.9499 |
| 46 | 4.545338 | 590.4371 |
| 47 | 4.499364 | 588.9384 |
| 48 | 4.454157 | 587.4535 |
| 49 | 4.409702 | 585.9822 |
| 50 | 4.365982 | 584.5243 |
| 51 | 4.322977 | 583.0796 |
| 52 | 4.280675 | 581.6479 |
| 53 | 4.239056 | 580.2289 |
| 54 | 4.198108 | 578.8226 |
| 55 | 4.157814 | 577.4287 |
| 56 | 4.118161 | 576.0470 |

| | | |
|---|---|---|
| 118 | 2.500220 | 508.4832 |
| 119 | 2.483212 | 507.6163 |
| 120 | 2.466396 | 506.7547 |
| 121 | 2.449770 | 505.8986 |
| 122 | 2.433331 | 505.0477 |
| 123 | 2.417075 | 504.2021 |
| 124 | 2.401000 | 503.3617 |
| 125 | 2.385103 | 502.5264 |
| 126 | 2.369381 | 501.6962 |
| 127 | 2.353832 | 500.8711 |
| 128 | 2.338453 | 500.0509 |
| 129 | 2.323241 | 499.2357 |
| 130 | 2.308193 | 498.4254 |
| 131 | 2.293309 | 497.6199 |
| 132 | 2.278584 | 496.8192 |
| 133 | 2.264017 | 496.0232 |
| 134 | 2.249604 | 495.2319 |
| 135 | 2.235345 | 494.4453 |
| 136 | 2.221236 | 493.6632 |
| 137 | 2.207276 | 492.8857 |
| 138 | 2.193462 | 492.1128 |
| 139 | 2.179792 | 491.3442 |
| 140 | 2.166264 | 490.5801 |
| 141 | 2.152876 | 489.8204 |
| 142 | 2.139626 | 489.0650 |
| 143 | 2.126511 | 488.3138 |
| 144 | 2.113531 | 487.5670 |
| 145 | 2.100683 | 486.8243 |
| 146 | 2.087965 | 486.0858 |
| 147 | 2.075376 | 485.3514 |
| 148 | 2.062912 | 484.6211 |
| 149 | 2.050574 | 483.8948 |
| 150 | 2.038358 | 483.1725 |
| 151 | 2.026265 | 482.4543 |
| 152 | 2.014290 | 481.7399 |
| 153 | 2.002434 | 481.0294 |
| 154 | 1.990695 | 480.3229 |
| 155 | 1.979070 | 479.6201 |
| 156 | 1.967558 | 478.9211 |
| 157 | 1.956159 | 478.2259 |
| 158 | 1.944869 | 477.5344 |
| 159 | 1.933688 | 476.8466 |
| 160 | 1.922614 | 476.1624 |
| 161 | 1.911647 | 475.4819 |
| 162 | 1.900783 | 474.8049 |
| 163 | 1.890022 | 474.1315 |
| 164 | 1.879363 | 473.4616 |
| 165 | 1.868805 | 472.7953 |
| 166 | 1.858346 | 472.1323 |
| 167 | 1.847984 | 471.4728 |
| 168 | 1.837719 | 470.8167 |
| 169 | 1.827549 | 470.1640 |
| 170 | 1.817472 | 469.5146 |
| 171 | 1.807489 | 468.8685 |
| 172 | 1.797597 | 468.2256 |
| 173 | 1.787796 | 467.5861 |
| 174 | 1.778084 | 466.9498 |
| 175 | 1.768460 | 466.3166 |
| 176 | 1.758922 | 465.6866 |
| 177 | 1.749471 | 465.0598 |
| 178 | 1.740105 | 464.4361 |

| | | |
|---|---|---|
| 240 | 1.289566 | 430.9164 |
| 241 | 1.283948 | 430.4463 |
| 242 | 1.278370 | 429.9780 |
| 243 | 1.272833 | 429.5116 |
| 244 | 1.267336 | 429.0471 |
| 245 | 1.261879 | 428.5845 |
| 246 | 1.256461 | 428.1237 |

QTOT = 739.2075 kW
SYSMAS = 1871.322 kg

ENVIRONMENT IS MARTIAN ATMOSPHERE

| No. | Q(z) | T(z) |
|---|---|---|
| 1 | 8.981834 | 677.0000 |
| 2 | 8.831504 | 674.1845 |
| 3 | 8.685153 | 671.4117 |
| 4 | 8.542637 | 668.6805 |
| 5 | 8.403819 | 665.9899 |
| 6 | 8.268565 | 663.3390 |
| 7 | 8.136749 | 660.7267 |
| 8 | 8.008252 | 658.1523 |
| 9 | 7.882959 | 655.6147 |
| 10 | 7.760760 | 653.1132 |
| 11 | 7.641548 | 650.6469 |
| 12 | 7.525225 | 648.2150 |
| 13 | 7.411695 | 645.8168 |
| 14 | 7.300862 | 643.4515 |
| 15 | 7.192644 | 641.1183 |
| 16 | 7.086950 | 638.8167 |
| 17 | 6.983700 | 636.5457 |
| 18 | 6.882819 | 634.3049 |
| 19 | 6.784231 | 632.0936 |
| 20 | 6.687865 | 629.9112 |
| 21 | 6.593650 | 627.7570 |
| 22 | 6.501520 | 625.6305 |
| 23 | 6.411414 | 623.5311 |
| 24 | 6.323268 | 621.4582 |
| 25 | 6.237024 | 619.4113 |
| 26 | 6.152626 | 617.3899 |
| 27 | 6.070017 | 615.3934 |
| 28 | 5.989150 | 613.4215 |
| 29 | 5.909972 | 611.4736 |
| 30 | 5.832431 | 609.5491 |
| 31 | 5.756485 | 607.6478 |
| 32 | 5.682088 | 605.7692 |
| 33 | 5.609193 | 603.9127 |
| 34 | 5.537763 | 602.0780 |
| 35 | 5.467754 | 600.2647 |
| 36 | 5.399128 | 598.4724 |
| 37 | 5.331849 | 596.7007 |
| 38 | 5.265877 | 594.9492 |
| 39 | 5.201180 | 593.2176 |
| 40 | 5.137723 | 591.5055 |
| 41 | 5.075475 | 589.8126 |
| 42 | 5.014402 | 588.1384 |
| 43 | 4.954474 | 586.4828 |
| 44 | 4.895660 | 584.8453 |
| 45 | 4.837935 | 583.2256 |
| 46 | 4.781269 | 581.6235 |
| 47 | 4.725634 | 580.0386 |
| 48 | 4.671005 | 578.4707 |
| 49 | 4.617360 | 576.9194 |
| 50 | 4.564669 | 575.3845 |
| 51 | 4.512913 | 573.8657 |
| 52 | 4.462068 | 572.3628 |
| 53 | 4.412112 | 570.8754 |
| 54 | 4.363023 | 569.4034 |
| 55 | 4.314780 | 567.9464 |
| 56 | 4.267364 | 566.5043 |

| | | |
|---|---|---|
| 118 | 2.386726 | 498.6860 |
| 119 | 2.367563 | 497.8533 |
| 120 | 2.348632 | 497.0268 |
| 121 | 2.329927 | 496.2064 |
| 122 | 2.311446 | 495.3922 |
| 123 | 2.293184 | 494.5840 |
| 124 | 2.275138 | 493.7818 |
| 125 | 2.257305 | 492.9855 |
| 126 | 2.239680 | 492.1950 |
| 127 | 2.222261 | 491.4103 |
| 128 | 2.205045 | 490.6314 |
| 129 | 2.188027 | 489.8581 |
| 130 | 2.171205 | 489.0903 |
| 131 | 2.154576 | 488.3281 |
| 132 | 2.138137 | 487.5714 |
| 133 | 2.121885 | 486.8201 |
| 134 | 2.105817 | 486.0741 |
| 135 | 2.089930 | 485.3334 |
| 136 | 2.074220 | 484.5980 |
| 137 | 2.058686 | 483.8677 |
| 138 | 2.043326 | 483.1426 |
| 139 | 2.028135 | 482.4226 |
| 140 | 2.013112 | 481.7076 |
| 141 | 1.998253 | 480.9975 |
| 142 | 1.983558 | 480.2924 |
| 143 | 1.969022 | 479.5921 |
| 144 | 1.954644 | 478.8967 |
| 145 | 1.940422 | 478.2060 |
| 146 | 1.926352 | 477.5201 |
| 147 | 1.912434 | 476.8388 |
| 148 | 1.898664 | 476.1621 |
| 149 | 1.885040 | 475.4901 |
| 150 | 1.871560 | 474.8225 |
| 151 | 1.858223 | 474.1595 |
| 152 | 1.845026 | 473.5009 |
| 153 | 1.831966 | 472.8467 |
| 154 | 1.819043 | 472.1968 |
| 155 | 1.806254 | 471.5513 |
| 156 | 1.793597 | 470.9100 |
| 157 | 1.781070 | 470.2730 |
| 158 | 1.768672 | 469.6402 |
| 159 | 1.756401 | 469.0115 |
| 160 | 1.744255 | 468.3869 |
| 161 | 1.732232 | 467.7664 |
| 162 | 1.720330 | 467.1499 |
| 163 | 1.708548 | 466.5374 |
| 164 | 1.696884 | 465.9289 |
| 165 | 1.685337 | 465.3242 |
| 166 | 1.673905 | 464.7235 |
| 167 | 1.662586 | 464.1266 |
| 168 | 1.651378 | 463.5335 |
| 169 | 1.640281 | 462.9442 |
| 170 | 1.629293 | 462.3586 |
| 171 | 1.618412 | 461.7767 |
| 172 | 1.607637 | 461.1985 |
| 173 | 1.596966 | 460.6239 |
| 174 | 1.586399 | 460.0529 |
| 175 | 1.575933 | 459.4855 |
| 176 | 1.565568 | 458.9216 |
| 177 | 1.555302 | 458.3612 |
| 178 | 1.545133 | 457.8043 |

```
       240   1.063363       428.9617
       241   1.057457       428.5735
       242   1.051597       428.1873
QTOT = 738.8571 kW
SYSMAS = 1840.894 kg
```

ENVIRONMENT IS UNDERGROUND

| No. | Q(z) | T(z) |
|---|---|---|
| 1 | 0.6604800 | 677.0000 |
| 2 | 0.6600825 | 676.7930 |
| 3 | 0.6596852 | 676.5861 |
| 4 | 0.6592880 | 676.3792 |
| 5 | 0.6588911 | 676.1725 |
| 6 | 0.6584944 | 675.9658 |
| 7 | 0.6580978 | 675.7593 |
| 8 | 0.6577015 | 675.5529 |
| 9 | 0.6573052 | 675.3465 |
| 10 | 0.6569093 | 675.1403 |
| 11 | 0.6565135 | 674.9341 |
| 12 | 0.6561179 | 674.7281 |
| 13 | 0.6557225 | 674.5222 |
| 14 | 0.6553274 | 674.3163 |
| 15 | 0.6549323 | 674.1106 |
| 16 | 0.6545375 | 673.9050 |
| 17 | 0.6541429 | 673.6994 |
| 18 | 0.6537484 | 673.4940 |
| 19 | 0.6533542 | 673.2886 |
| 20 | 0.6529601 | 673.0834 |
| 21 | 0.6525662 | 672.8782 |
| 22 | 0.6521726 | 672.6732 |
| 23 | 0.6517791 | 672.4683 |
| 24 | 0.6513858 | 672.2634 |
| 25 | 0.6509927 | 672.0587 |
| 26 | 0.6505998 | 671.8541 |
| 27 | 0.6502071 | 671.6495 |
| 28 | 0.6498145 | 671.4451 |
| 29 | 0.6494222 | 671.2407 |
| 30 | 0.6490301 | 671.0365 |
| 31 | 0.6486381 | 670.8323 |
| 32 | 0.6482463 | 670.6283 |
| 33 | 0.6478548 | 670.4244 |
| 34 | 0.6474634 | 670.2205 |
| 35 | 0.6470722 | 670.0168 |
| 36 | 0.6466811 | 669.8131 |
| 37 | 0.6462904 | 669.6096 |
| 38 | 0.6458998 | 669.4061 |
| 39 | 0.6455093 | 669.2028 |
| 40 | 0.6451191 | 668.9995 |
| 41 | 0.6447290 | 668.7964 |
| 42 | 0.6443391 | 668.5933 |
| 43 | 0.6439495 | 668.3904 |
| 44 | 0.6435601 | 668.1876 |
| 45 | 0.6431708 | 667.9848 |
| 46 | 0.6427817 | 667.7822 |
| 47 | 0.6423928 | 667.5796 |
| 48 | 0.6420041 | 667.3771 |
| 49 | 0.6416156 | 667.1748 |
| 50 | 0.6412272 | 666.9725 |
| 51 | 0.6408391 | 666.7704 |
| 52 | 0.6404511 | 666.5683 |
| 53 | 0.6400633 | 666.3663 |
| 54 | 0.6396758 | 666.1645 |
| 55 | 0.6392884 | 665.9627 |
| 56 | 0.6389012 | 665.7610 |

| | | |
|---|---|---|
| 118 | 0.6152640 | 653.4500 |
| 119 | 0.6148887 | 653.2545 |
| 120 | 0.6145135 | 653.0591 |
| 121 | 0.6141385 | 652.8638 |
| 122 | 0.6137637 | 652.6686 |
| 123 | 0.6133893 | 652.4736 |
| 124 | 0.6130148 | 652.2786 |
| 125 | 0.6126406 | 652.0837 |
| 126 | 0.6122666 | 651.8889 |
| 127 | 0.6118928 | 651.6942 |
| 128 | 0.6115190 | 651.4995 |
| 129 | 0.6111456 | 651.3050 |
| 130 | 0.6107723 | 651.1106 |
| 131 | 0.6103992 | 650.9163 |
| 132 | 0.6100263 | 650.7220 |
| 133 | 0.6096535 | 650.5279 |
| 134 | 0.6092810 | 650.3339 |
| 135 | 0.6089087 | 650.1400 |
| 136 | 0.6085365 | 649.9461 |
| 137 | 0.6081645 | 649.7524 |
| 138 | 0.6077927 | 649.5587 |
| 139 | 0.6074211 | 649.3652 |
| 140 | 0.6070498 | 649.1718 |
| 141 | 0.6066785 | 648.9784 |
| 142 | 0.6063075 | 648.7852 |
| 143 | 0.6059366 | 648.5920 |
| 144 | 0.6055659 | 648.3989 |
| 145 | 0.6051954 | 648.2059 |
| 146 | 0.6048251 | 648.0131 |
| 147 | 0.6044550 | 647.8203 |
| 148 | 0.6040850 | 647.6276 |
| 149 | 0.6037153 | 647.4351 |
| 150 | 0.6033457 | 647.2426 |
| 151 | 0.6029763 | 647.0502 |
| 152 | 0.6026071 | 646.8578 |
| 153 | 0.6022381 | 646.6656 |
| 154 | 0.6018692 | 646.4736 |
| 155 | 0.6015006 | 646.2816 |
| 156 | 0.6011322 | 646.0897 |
| 157 | 0.6007638 | 645.8978 |
| 158 | 0.6003957 | 645.7061 |
| 159 | 0.6000279 | 645.5145 |
| 160 | 0.5996602 | 645.3230 |
| 161 | 0.5992926 | 645.1316 |
| 162 | 0.5989252 | 644.9402 |
| 163 | 0.5985581 | 644.7490 |
| 164 | 0.5981911 | 644.5579 |
| 165 | 0.5978243 | 644.3668 |
| 166 | 0.5974577 | 644.1759 |
| 167 | 0.5970913 | 643.9850 |
| 168 | 0.5967250 | 643.7943 |
| 169 | 0.5963590 | 643.6036 |
| 170 | 0.5959931 | 643.4131 |
| 171 | 0.5956274 | 643.2226 |
| 172 | 0.5952619 | 643.0322 |
| 173 | 0.5948966 | 642.8420 |
| 174 | 0.5945314 | 642.6518 |
| 175 | 0.5941665 | 642.4617 |
| 176 | 0.5938017 | 642.2717 |
| 177 | 0.5934371 | 642.0818 |
| 178 | 0.5930727 | 641.8920 |

| | | |
|---|---|---|
| 240 | 0.5708356 | 630.3102 |
| 241 | 0.5704827 | 630.1264 |
| 242 | 0.5701299 | 629.9427 |
| 243 | 0.5697773 | 629.7590 |
| 244 | 0.5694249 | 629.5755 |
| 245 | 0.5690727 | 629.3920 |
| 246 | 0.5687206 | 629.2087 |
| 247 | 0.5683687 | 629.0254 |
| 248 | 0.5680171 | 628.8422 |
| 249 | 0.5676655 | 628.6591 |
| 250 | 0.5673141 | 628.4761 |
| 251 | 0.5669631 | 628.2933 |
| 252 | 0.5666121 | 628.1105 |
| 253 | 0.5662614 | 627.9278 |
| 254 | 0.5659108 | 627.7452 |
| 255 | 0.5655603 | 627.5627 |
| 256 | 0.5652100 | 627.3802 |
| 257 | 0.5648600 | 627.1979 |
| 258 | 0.5645101 | 627.0157 |
| 259 | 0.5641604 | 626.8336 |
| 260 | 0.5638108 | 626.6515 |
| 261 | 0.5634615 | 626.4695 |
| 262 | 0.5631123 | 626.2877 |
| 263 | 0.5627633 | 626.1059 |
| 264 | 0.5624145 | 625.9242 |
| 265 | 0.5620658 | 625.7426 |
| 266 | 0.5617174 | 625.5612 |
| 267 | 0.5613691 | 625.3798 |
| 268 | 0.5610211 | 625.1985 |
| 269 | 0.5606732 | 625.0173 |
| 270 | 0.5603254 | 624.8362 |
| 271 | 0.5599779 | 624.6552 |
| 272 | 0.5596305 | 624.4742 |
| 273 | 0.5592833 | 624.2934 |
| 274 | 0.5589363 | 624.1127 |
| 275 | 0.5585895 | 623.9320 |
| 276 | 0.5582428 | 623.7515 |
| 277 | 0.5578963 | 623.5710 |
| 278 | 0.5575500 | 623.3906 |
| 279 | 0.5572038 | 623.2103 |
| 280 | 0.5568579 | 623.0302 |
| 281 | 0.5565121 | 622.8500 |
| 282 | 0.5561665 | 622.6700 |
| 283 | 0.5558210 | 622.4901 |
| 284 | 0.5554758 | 622.3103 |
| 285 | 0.5551307 | 622.1306 |
| 286 | 0.5547858 | 621.9509 |
| 287 | 0.5544410 | 621.7714 |
| 288 | 0.5540965 | 621.5919 |
| 289 | 0.5537522 | 621.4126 |
| 290 | 0.5534080 | 621.2333 |
| 291 | 0.5530640 | 621.0542 |
| 292 | 0.5527202 | 620.8751 |
| 293 | 0.5523766 | 620.6962 |
| 294 | 0.5520331 | 620.5173 |
| 295 | 0.5516899 | 620.3385 |
| 296 | 0.5513468 | 620.1598 |
| 297 | 0.5510039 | 619.9812 |
| 298 | 0.5506611 | 619.8027 |
| 299 | 0.5503186 | 619.6243 |
| 300 | 0.5499762 | 619.4459 |

## 6. RADIATION SHIELDING

The proposed design is for an unmanned mission to Mars followed by six years of operation on Mars. Consequently, radiation shielding for the mission was determined to be on the order of that required for the SNAP reactor nuclear power systems with doses on the order of the SP-100 mission to the equipment. The specifications for the SP-100 dose rates for an instrument-rated mission are $10^{13}$ neutrons/cm$^2$ and $5 \times 10^5$ rads for gamma rays over a 7.3 year full power lifetime at a 4.5 meter diameter dose plane that is 22.5 meters from the center of the reactor. This results in $5.1 \times 10^5$ rads over the system lifetime at the dose plane (1).

Utilizing the weight scaling factors developed by Hedgecock and German (2) for instrument-rated shadow shields similar to that of SNAP reactor nuclear power systems the shielding weight was determined. Reactor power, dose rate, and principle overall dimensions make up seven weight scaling factors ($w_A$, $w_B$, $w_C$, . . . ,$w_G$) that are multiplied by the base case shielding weight ($m_o$)

$$m = m_o \times (w_A \times w_B \times w_C \times w_D \times w_E \times w_F \times w_G) \qquad (6.1)$$

to find the resulting weight (m) as in Equation 1. The instrument-rated shadow shield parameters are determined according to Figure 6.1 and the weight scaling factors are determined using the parameters and Figure 6.2. For the instrument-rated shadow shield the base case weight is 844 pounds while the other base case parameters are listed with the actual parametric values and resulting weight scaling factors in Table 6.1. This results in a shield mass of 1122 pounds or 509 kilograms.

The shielding is comprised of tungsten to attenuate the gamma rays and lithium hydride to absorb and moderate neutrons. The total neutron shield weight was taken equal to 1.39 times the weight of the lithium hydride neutron shield material alone to allow for the weight of structural members.

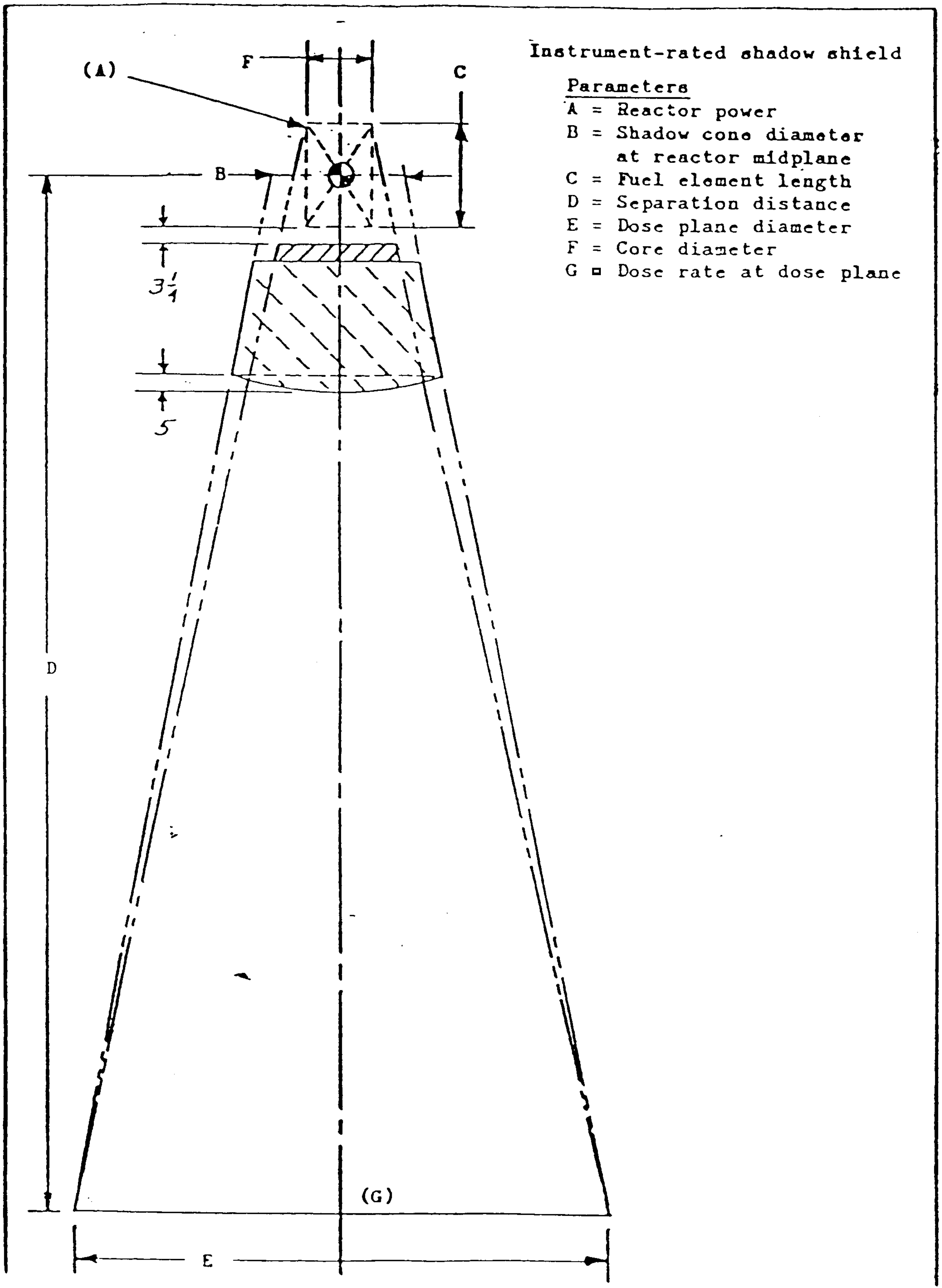


Figure 6.1 Reactor Radiation Shielding Design and Parameters

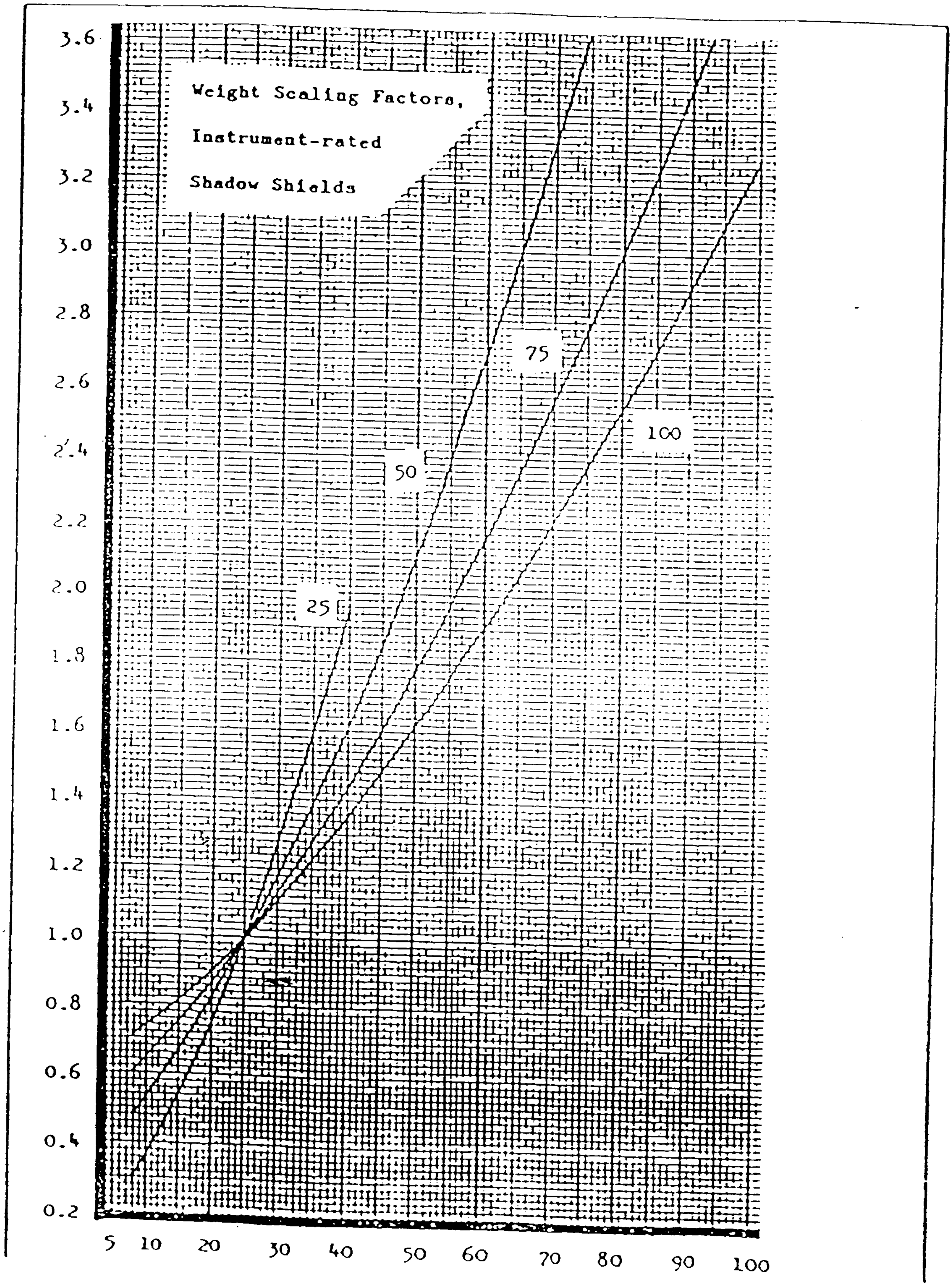


Figure 6.2 Weight Scaling Factors (1 of 3)

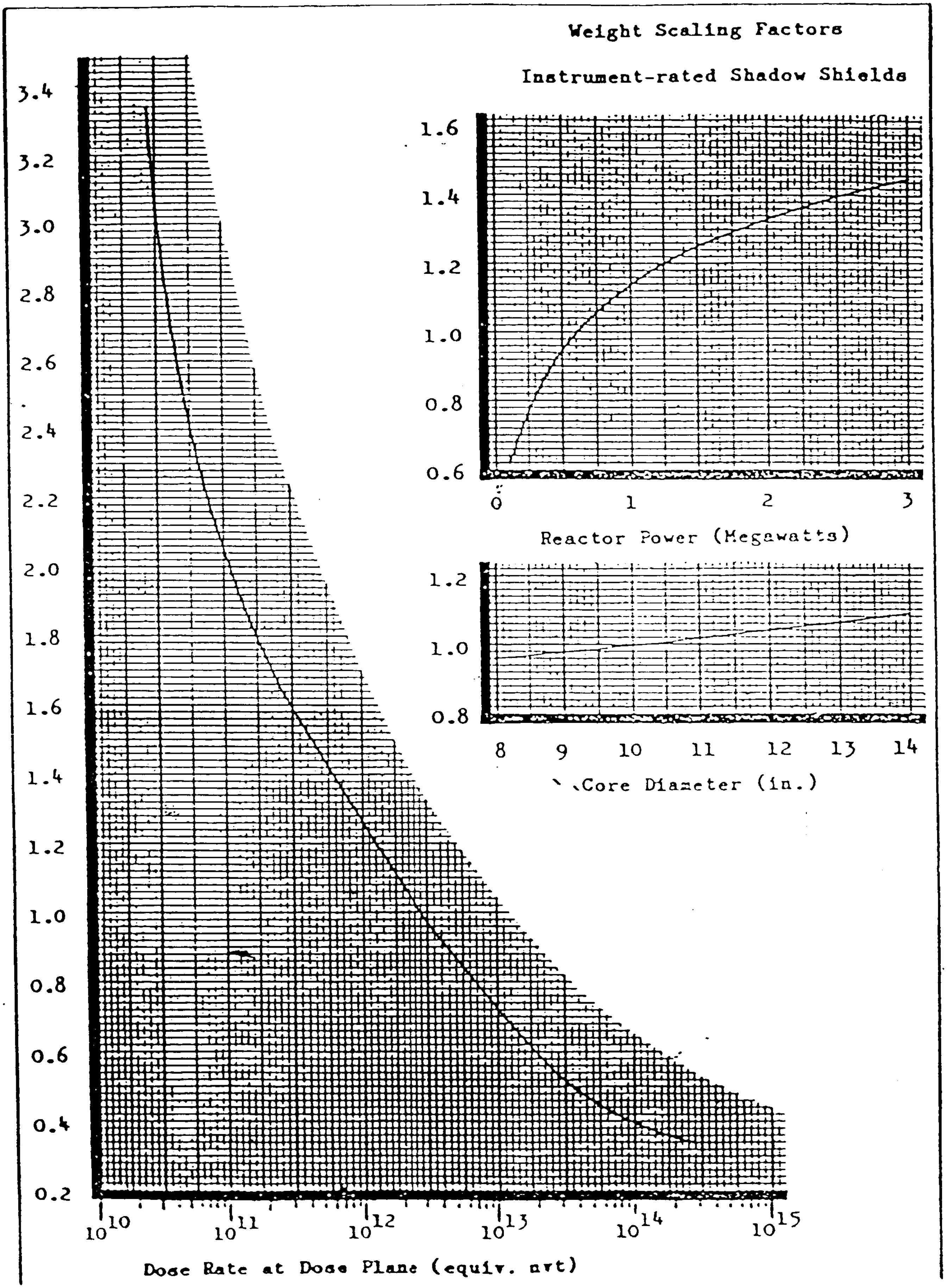


Figure 6.2 Weight Scaling Factors (2 of 3)

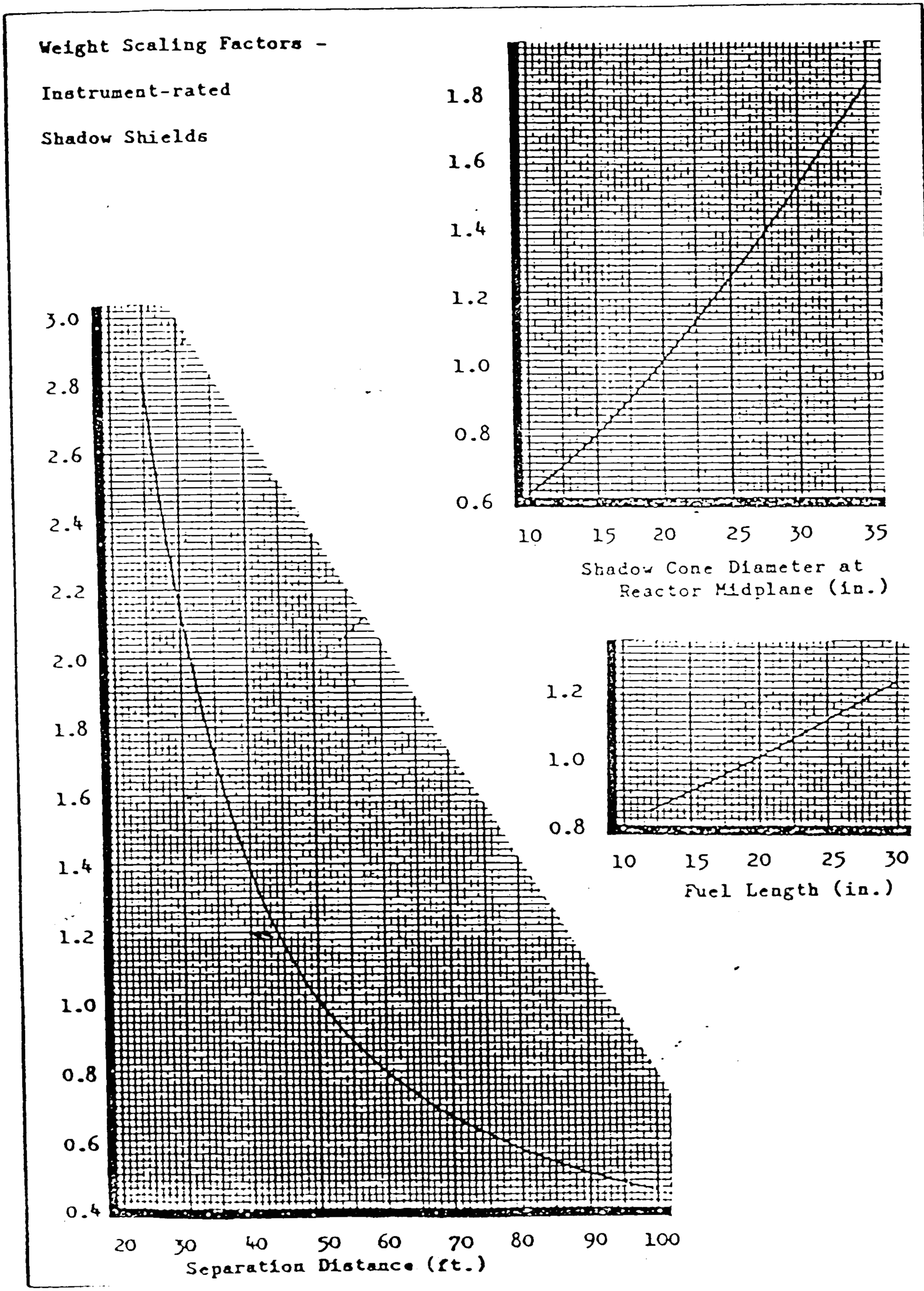


Figure 6.3 Weight Scaling Factors (3 of 3)

Table 6.1

Instrument-Rated Shadow Shield

| Parameter | Base Case Value (2) | Actual Value | Weight Scaling Factor |
|---|---|---|---|
| A=Reactor Power | 600 kWe | 300kWe | 0.81 |
| B=Shadow cone diameter at reactor midplane | 20 in. | 47.2 in. | 2.61 |
| C=Fuel element length | 20 in. | 11.8 in. | 0.84 |
| D=Separation Distance | 50 ft. | 73.8 ft. | 0.62 |
| E=Dose plane diameter | 25 ft. | 14.8 ft. | 0.72 |
| F=Core diameter | 10 in. | 23.6 in. | 1.29 |
| G=Dose rate at dose plane | $2.8\times10^{12}$ nvt. eq. | $9.15\times10^{11}$ nvt. eq. | 1.30 |

## References


1. General Electric Sp-100 Reference Design. GE TM-73219, Jun. 1986.

2. Hedgecock, J. L. ; and German, G. E. : Weight Scaling Factors for SNAP Reactor Shields. Atomic International TDR 11971, Jun. 1966.

## 7. SPACE LOGISTICS

### Mission trajectory

The mission will be initiated with the launch of the MPR-300 aboard one of the space shuttles. Maximum payloads for this launch vehicle are estimated at 35 metric tonnes (MT). Assuming the dimensions of the MPR-300 are compatible with those of the shuttle cargo bay, a single launch would deliver the 8,000-10,000 kg craft into low earth orbit (LEO = 320km). There, the craft would be deployed and cast away from the shuttle. In preparation of obtaining escape conditions from the Earth's gravitation, a chemical booster rocket attachment would be ignited. The transport from one orbit to another for the case of a tangential thrust is described by the following relation:

Equation 7.1 $$t = \frac{WR}{F\sqrt{g_c}}\,(1/r_0 - 1/r) \qquad [1]$$

where F/W = thrust to weight ratio

R = Earth's radius

$g_0$ = 9.81 $m/s^2$

$r_0$ = initial orbit radius

r = orbit radius at time t

With a 100 N chemical thruster, a 10 MT craft has a thrust-to-weight ratio of $1.02 \times 10^{-3}$; to obtain a geosynchronous orbital radius from an initial orbit 320 km in altitude, the craft requires 100 N constant tangential thrust for about 38.8 days. Alternatively, this task could be accomplished using the MPR-300's main propulsion system which was designed for the interplanetary portion of the flight. The main thrusters provide a thrust-to-weight ratio of $3.67 \times 10^{-5}$; although there is some atmospheric drag in LEO, its effect only becomes significant below altitudes of 200 km and thrust-to-weight ratios of $10^{-6}$ are sufficient to compensate for this effect. Using this in Equation 7.1 yields an orbit transfer time of 1077 days or about 36 months. The reason for choosing a chemical rocket booster is obvious: mission objectives require a total flight time of approximately 6 months and so 38.8 days is acceptable for LEO to GEO orbit transfer while 1077 days is not.

The next portion of the flight is that from high Earth orbit to Mars orbit. The flight mechanics involved were highly simplified by assuming the craft is far enough from the Earth to neglect its gravitation. This assumption is reasonable considering the previously described orbit transfer. The spaceraft never really approaches a stable geosynchronous orbit (35,870 km) but a highly eccentric one which allows it to eventually escape Earth orbit. In addition, the flight distance was computed from the average radii of revolution about the sun for the Earth and Mars: this implies the necessity of good timing for a rendezvous with Mars on its closest approach to Earth. To further simplify the mission, a "crow flight" path was assumed as well as constant acceleration and craft mass throughout the flight.

Taking all the simplifications into consideration yields a simple equation for rough estimates of flight time and propellant consumption (see Equation 7.2). Although this formulation

Equation 7.2 $$t = [2mx/T]^{1/2}$$

where $m$ = total craft mass

$x$ = flight distance

$t$ = flight time

$T$ = total thrust

neglects gravitational effects while near the earth, it also neglects decreasing system mass due to propellant consumption (a large percentage of the total mass) and initial velocity: both of these effects would shorten the flight. With these considerations, Equation 7.2 should yield a conservative estimate of flight time and thus propellant consumption.

Once having reached Mars, the MPR-300 craft will implement aerobraking in the Martian upper atmosphere to slow itself and approach a stable orbit of about 320 km in altitude. This will keep the craft sufficiently high to avoid significant atmospheric drag losses over long periods. The craft will then initiate entry into the Martian atmosphere with retroactive bursts of the main thrusters. An ablative heat shield on the ship's fore end will protect the craft in the entry stage. Shortly thereafter, parachutes will be deployed to slow the descent to less than 20 fps [2]. As a reference, 30 fps is a typical parachute letdown of a man; the more sensitive reactor system would probably tolerate only less than this. It is therefore necessary to have a damping mechanism to absorb the shock of touchdown.

## Propulsion

The main propulsion system consists of an array of MPD (magnetoplasmadynamic) thrusters, 4 operating simultaneously. These thrusters were selected from a variety of electrically driven ion thrusters on the basis of high efficiency, high specific impulse (see Table 7.1), and compact size (each is less than 12" long and 6" in diameter). Also, the unit's small power requirements allow for modular fitting to the supplied power. Ammonia was chosen over argon and hydrogen as the propellant for the MPD's based on experimental data [3] which showed it to be the most efficient of any studied. For the operation parameters given in Table 7.1, the MPD produces a thrust of 0.9 N. Power supply limitations restrict the number of units, to be operated simultaneously, to 4 for a total thrust of 3.6 N and power consumption of 296 $kw_e$. To insure reliability, a total of 13 thrusters were included in the design based on a unit life of 3 months for similar ion thrusters [3].

Table 7.1

MPD Thruster Parameters [3]

| | |
|---|---|
| current | : 2000 A |
| voltage | : 37.0 V |
| thrust | : 0.9 N |
| propellant consumtion rate | : 0.015 g/s |

| | |
|---|---|
| specific impulse | : 6140 s |
| efficiency | : 36.6% |

Using Equation 7.2 and parameters from Table 7.1, a 10 MT craft with 4 MPD's operating would travel to Mars in 242 days and consume 1257 kg of $NH_3$. For reasons of improving reliability, an extra $NH_3$ propellant tank has been added to the final design.

The MPD thruster operates in a pseudo steady state mode and requires a pulsed current with a large DC component. The unusually high currents necessary to operate them are readily supplied by homopolar generators. These devices, although used only experimentally at present, are capable of producing large currents in the pulse mode for extended periods [4]. For their inclusion in this design it was assumed that current work on modularization of these generators has been successful and that homopolar generators are a scalable power source. Advantages of using these devices, as opposed to ordinary generators, is the omission of transformers and wave rectification equipment.

**Propellant tank design considerations**

Proper analysis of pressurized tanks in a space environment requires detailed consideration of radiative heat transfer. While free space behaves as a blackbody radiating at 3 K, objects in space do not necessarily approach this condition since they are continually being irradiated by a variety of celestial bodies such as the sun and planets. By evaluating the impact of each radiation source on pressurized tanks of cryogenic fluid it is possible to determine the minimal design specifications necessary for their survivability in a stellar environ.

First, consider a spherical tank one astronomical unit from the sun and orbiting about the Earth. To determine the tank wall thickness required to contain the pressurized $NH_3$ it is first necessary to calculate the equilibrium temperature. Performing an energy balance on the tank

Equation 7.3 $$\alpha G A_S - \varepsilon \sigma T_S^4 A_S = M c_p \, dT_S/dt$$

where $\alpha$ = total hemispherical absorptivity

$G$ = total irradiation ($W/m^2$)

$A_s$ = surface area

$\varepsilon$ = total hemispherical emissivity

$\sigma$ = Stephan-Boltzmann constant

$T_s$ = surface temperature

$M$ = mass of tank

$c_p$ = specific heat of tank material

For the given orbit, the total solar irradiation $G_{solar}$ is 1353 $W/m^2$ and its spectral dependence may be approximated as if it had been emitted by a blackbody radiating at 5800 K. For the Earth, its contribution at low orbits is a total irradiation $G_{earth}$ of 340 $W/m^2$; it may be modeled as a blackbody emitting at 280 K. The spectral dependence of blackbody emitters is well known (see Figure 7.1), having first been determined by Planck, and is tabulated along with other blackbody radiation functions [5].

The tank model consists of a sphere continually and diffusely irradiated over one entire hemisphere while the other side remains in complete darkness. Because the irradiation consists of essentially parallel rays, the actual irradiation varies sinusoidally over the spheres surface (see Figure 7.2a). For conservatism, the tanks will assume the maximum irradiation over the whole hemisphere as shown in Figure 7.2b. Another important consideration of this model is the thermal properties of the tank material and content; if the material used has a sufficiently high thermal conductivity and tank size is small, the tank's dark side will radiate at approximately the same temperature as the irradiated side.

The initial scoping calculation was based on a plain stainless steel tank with a lightly oxidized surface. The spectral absorption for this surface was approximated using the following equation and the data in Figure 7.3.

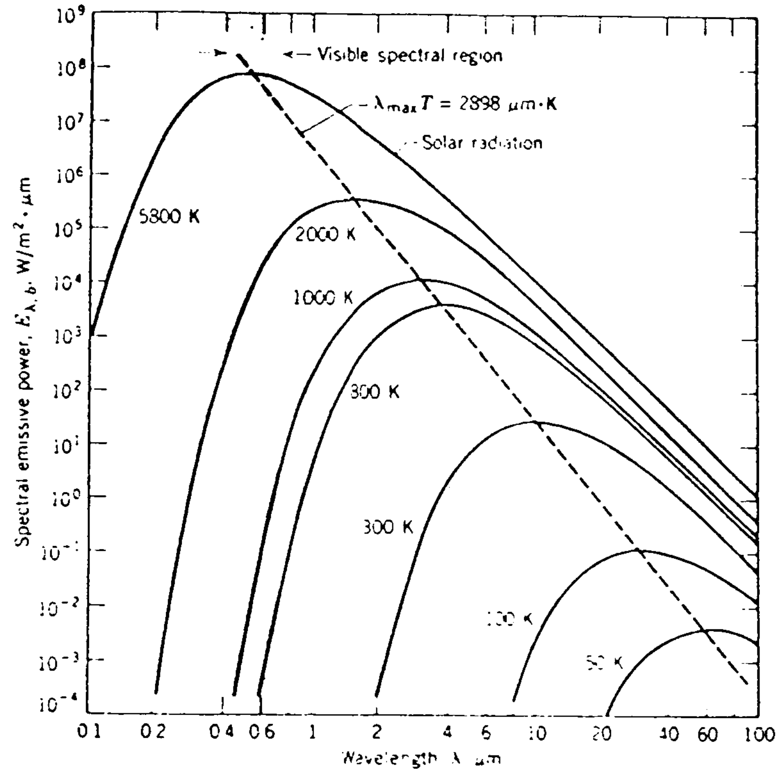


Spectral blackbody emissive power.

**Figure 7.1**

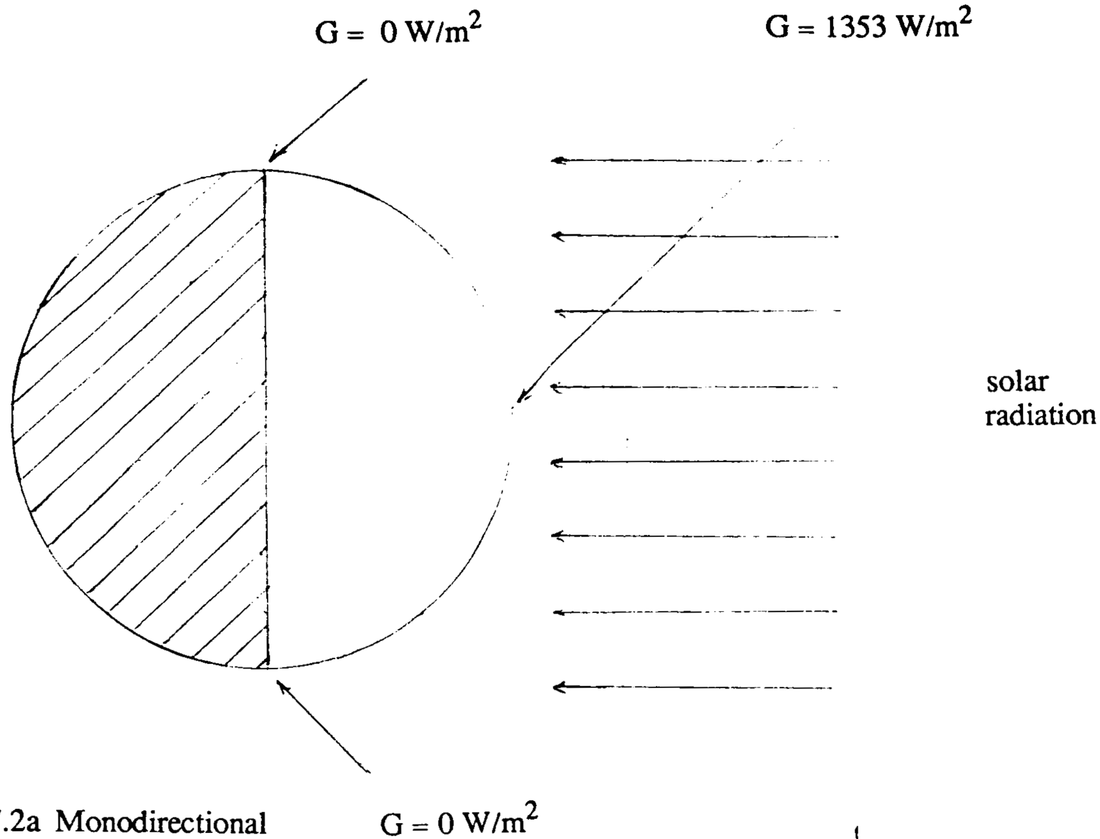


Figure 7.2a Monodirectional irradiation.

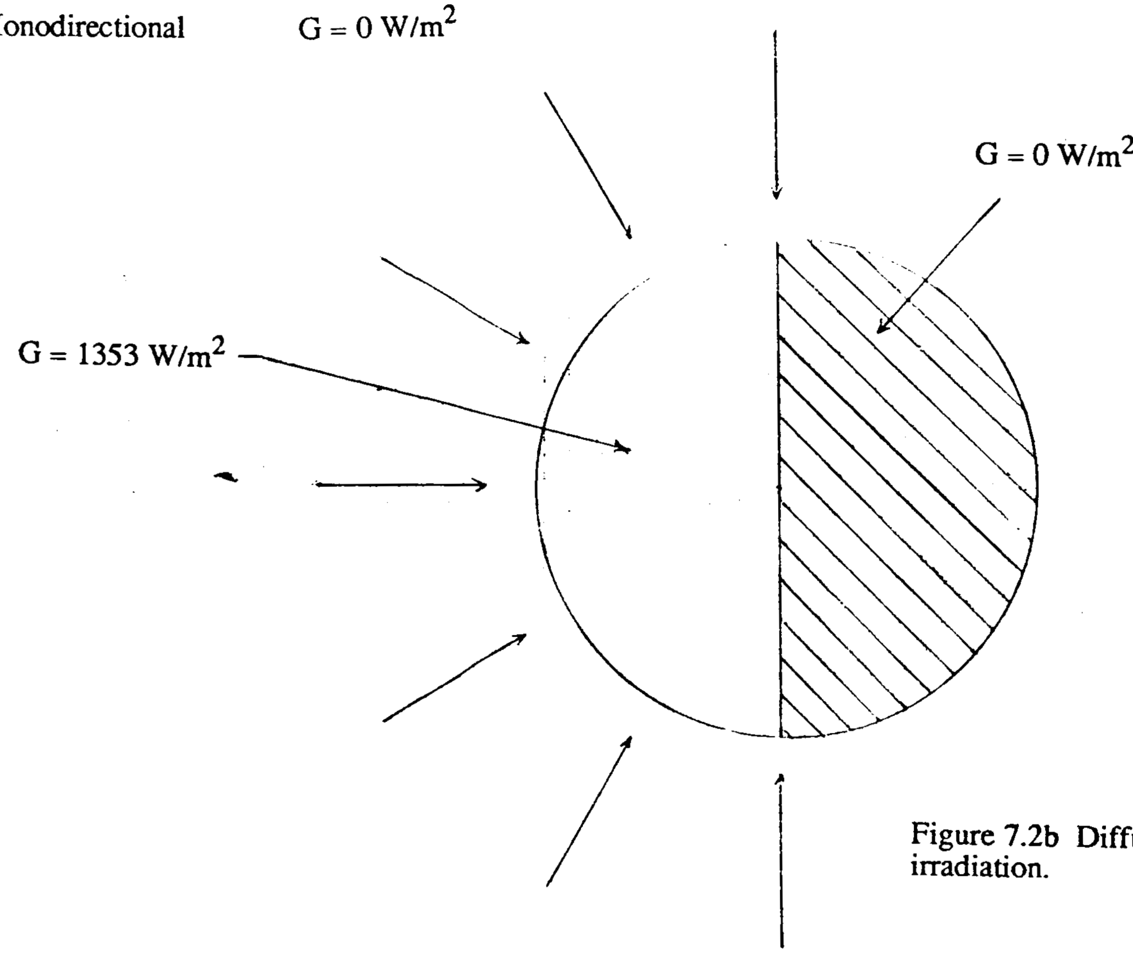


Figure 7.2b Diffuse irradiation.

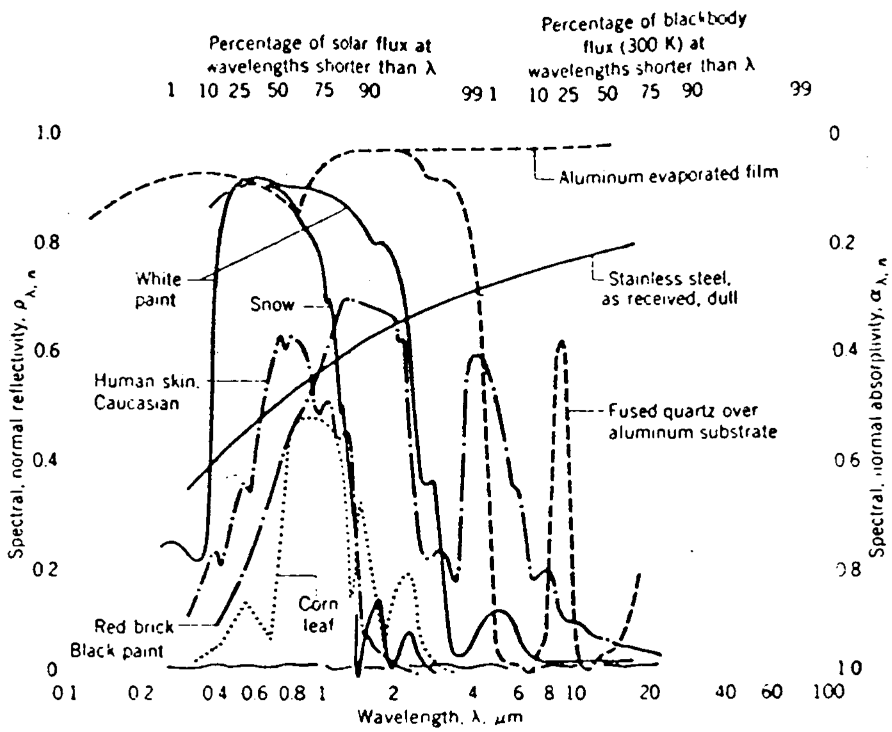


Figure 12.23 Spectral dependence of the spectral, normal absorptivity $\alpha_{\lambda,n}$ and reflectivity $\rho_{\lambda,n}$ of selected materials.

Figure 7.3

Equation 7.4 $$\rho_\lambda + \alpha_\lambda + \tau_\lambda = 1$$

where $\rho_\lambda$ = spectral reflectivity

$\alpha_\lambda$ = spectral absorptivity

$\tau_\lambda$ = spectral transmissivity

Since the tank material will almost invariably be opaque, the transmissivity will be zero. Thus, knowledge of $\rho_\lambda$ implies knowledge of $\alpha_\lambda$. The absorptivity of stainless steel used in the calculations was made consistently higher than the actual value. Its spectral dependence was approximated as follows:

$$\alpha_\lambda = \begin{cases} 0.65 & 0\mu m < \lambda < 1\mu m \\ 0.40 & 1\mu m < \lambda < 4\mu m \\ 0.30 & 4\mu m < \lambda < \infty\mu m \end{cases}$$

The relationship between the total hemispherical absorptivity, $\alpha$, in Equation 7.3 and the spectral absorptivity is as follows:

Equation 7.5 $$\alpha \cong \frac{\int \alpha_\lambda(\lambda) E_{\lambda,b}(\lambda,T)\, d\lambda}{\int E_{\lambda,b}(\lambda,T)\, d\lambda}$$

where $E_{\lambda,b}(\lambda,T)$ = spectral emissive power of a blackbody at temperature T

The value of the integral in the denominator of Equation 7.5 is tabulated for bounds of 0 to $\lambda$ where $\lambda$ takes on many incremental values; this is the radiation function $F_{(0-\lambda)}$. The radiation function gives the ratio of the total emission from a blackbody at a prescribed temperature for the wavelength interval 0-$\lambda$. Assuming $\alpha_\lambda(\lambda)$ is constant over certain intervals allows for their removal from the integral in Equation 7.5. Total absorptivity may then be found as follows:

Equation 7.6 $\alpha = \alpha_{\lambda_1} F_{(0-\lambda_1)} + \alpha_{\lambda_2} (F_{(0-\lambda_2)} - F_{(0-\lambda_1)}) + \ldots$

$$\alpha_{\lambda_n} (F_{(0-\infty)} - F_{(0-\lambda_{n-1})})$$

Evaluation of $\alpha_{solar}$ in this way yields 0.579 for the solar absorptivity. Multiplying $\alpha_{solar}$ and the total solar irradiation $G_{solar}$ (=1353W/m$^2$) yields $G_{abs}$ = 783.4 W/m$^2$. Analyzing the irradiation from the Earth in a similar manner reveals $G_{abs}$= 102.0 W/m$^2$ for the Earths radiation. Now, assuming the whole tank is radiating at one temperature, then the tank's emissive power must be half that of the total $G_{abs}$(=885.4w/m$^2$) since only one half of the tank is being irradiated while both are emitting. Thus is is necessary to find the temperature at which stainless steel has an emissive power of 885.4 W/m$^2$. This may be found from Equation 7.1 by assuming steady state conditions and taking into consideration the temperature dependence of the emissivity $\varepsilon$ ; $\alpha$ is a weak funtion of temperature. Figure 7.4 illustrates the effect of increasing tank temperature on emissive power. The necessary operating temperature is slightly less than 500 K.

Since an approximate equilibrium temperature for the propellant tanks is now known, the minimum required tank thickness for assured integrity may now be computed. For stainless steel $\sigma_{yield}$ = 69,000 psi [6] and from Figure 7.5 the vapor pressure of $NH_3$ at 500 K is well above 1000 psi [7].

Equation 7.7 $t = p_0 R / 2\sigma$

where t = tank wall thickness

$p_0$ = interior pressure

$\sigma$ = design stress of tank material

R = tank radius

Using a design stress of 34,500 psi in Equation 7.7, one obtains a tank wall thickness of 7.25 mm for a 1 m diameter tank. This corresponds to a tank mass of 176.5 kg each; at 500 K this would

Emissive Power vs. Temperature for Lightly Oxidized Stainless Steel

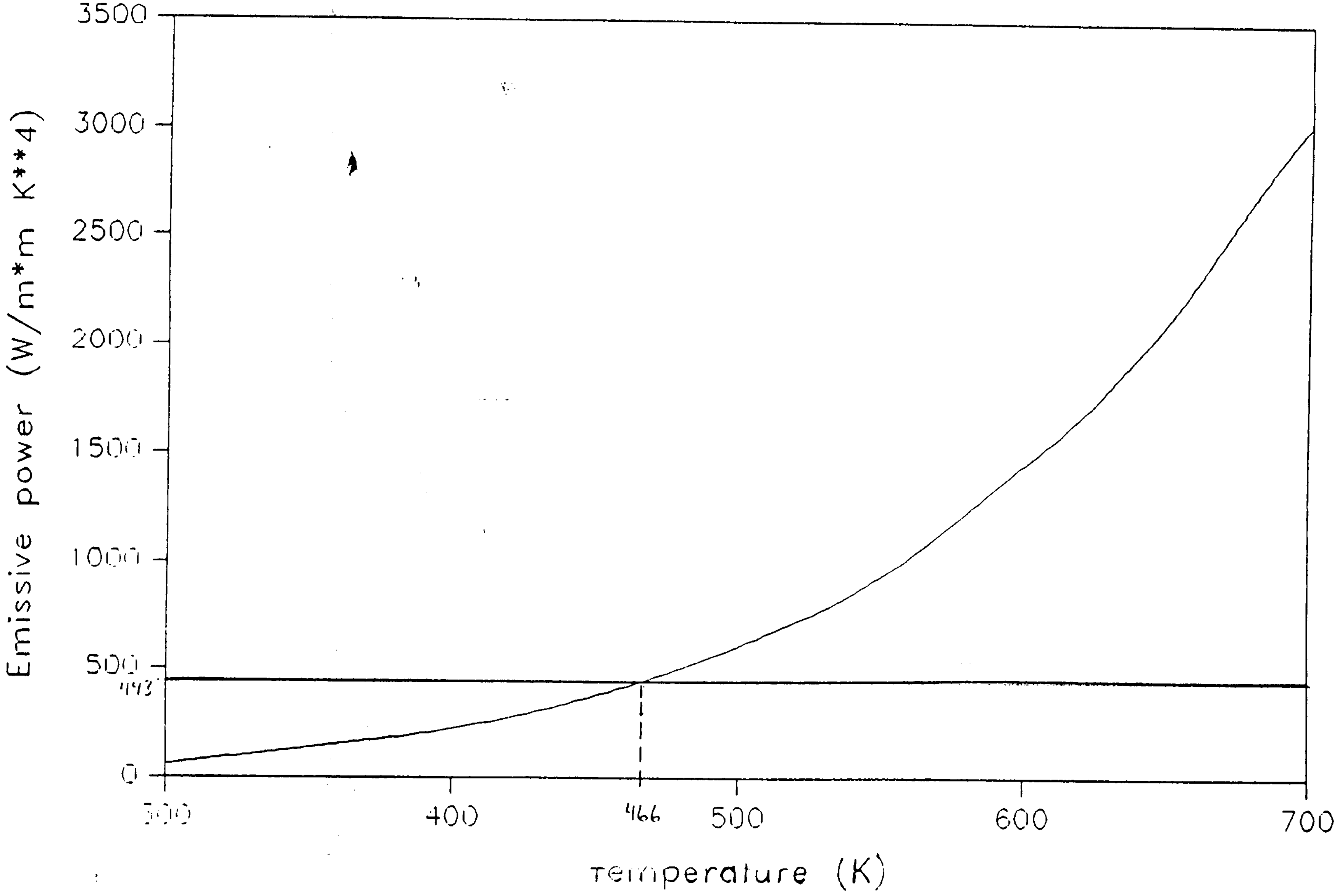


Figure 7.4

require more than 5 tanks (=882 kg) for the MPR-300 transport. This is a rather large mass and the problem deserves further investigation to reduce the tank temperature and pressure, and hence, propellant tank mass.

Upon investigation of the radiative heat transfer characteristics of other materials, a more viable solution was found. The new design requires one additional assumption: that the propellant tanks are always oriented with a highly reflective side toward the sun. The new tank is, as before, constructed from stainless steel; however, one half of each tank is to be coated with an evaporated aluminum film, the other side is to be heavily oxidized. This kind of system is desirable since the aluminum film provides a very high reflectivity while the oxidized stainless steel has a large emissivity. Handling the radiation absorption analysis as before (with the additional assumption), the total irradiation absorbed from the sun and Earth are 139.7 $W/m^2$ and 17.0$W/m^2$ respectively for a total of 156.7 $W/m^2$ absorbed. Since the emissivity data for aluminum film is available only at 300 K ($\mathcal{E}$ = 0.03 [5]), the energy balance equation (Equation 7.3) will be evaluated at this temperature. From the second term of Equation 7.3, the emissive power of the Al film is13.78 $W/m^2$. The oxidized side of the tank, however, has an emissive power of 252.6 $W/m^2$. With these figures it is apparent that the tank - if initially above 300 K - would tend to decrease its temperature until an equilibrium condition was achieved at some temperature below 300 K.

Knowing that the tank temperatures can be maintained below 300 K allows for reevaluation of propellant vapor pressures and thus the required tank wall thickness, from Figure 7.5a, the ammonia vapor pressure at 300 K is 166 psi. Using Equation 7.7 for a tank 1 m in diameter, the necessary tank wall thickness is 1.20 mm. This is a marked improvement over 7.25 mm from the prior design; the new tank mass is thus 29.2 kg per unit. The density of $NH_3$ at 300 K is 37.2 $lb_m/ft^3$ (595 $kg/m^3$, see Figure 7.5b). The required propellant mass of 1257 kg will therefore need about 4 tanks for a total propellant tank mass of 116.8 kg: a reduction in total tank mass by a factor of 8 over the first design!

Reiterating some of the conservative approximations: when the tanks are in orbit about the Earth they are being subjected to the most intense irradiation of the entire flight: the idea being

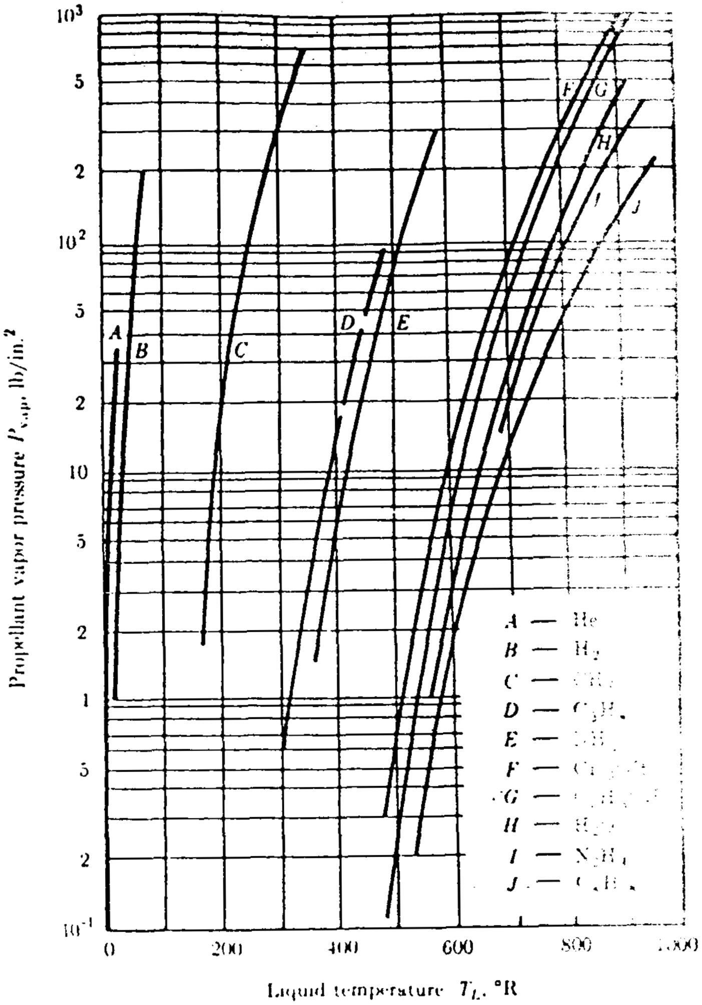


Vapor pressure of various liquid propellants

Figure 7.5a (7)

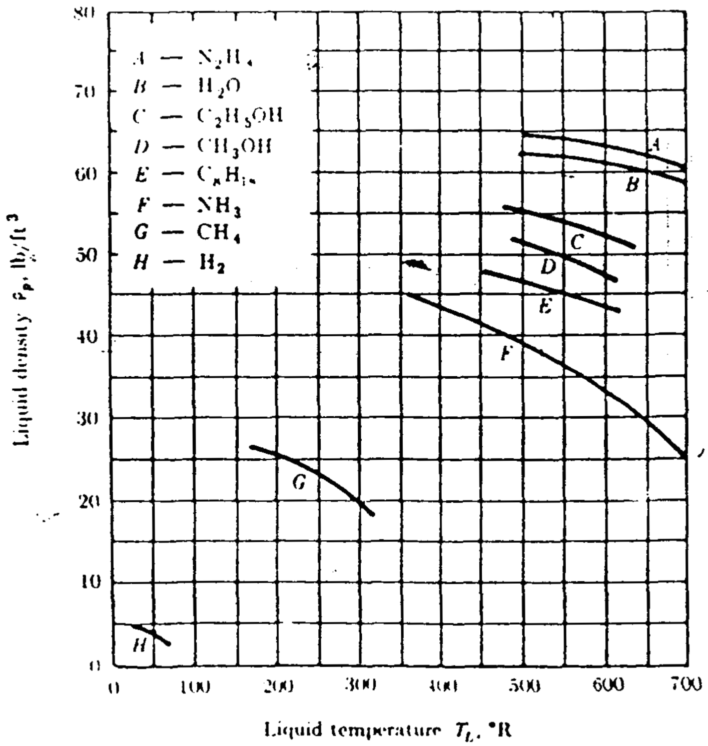


Density of various liquid propellants.

Figure 7.5b (7)

survivability under the most harsh conditions, the actual absorptivities are smaller than those used in the analysis and so the actual total irradiation absorbed $G_{abs}$ is less, the energy balance showed that the system at 300 K would tend to decrease its temperature and hence actual tank wall thicknesses are larger than necessary to meet pressure requirements at 300 K. Although this design is purely conceptual, the analysis used does present conservative estimates for the pressure tank parameters in a space environ. More importantly, it characterizes the advantages to be had in careful selection of materials.

### Micrometeoroid damage and failure probabilities

The vast regions between stellar systems, typically referred to as voids, are infact not devoid of matter. Although much has yet to be resolved, the existence of particulates and micrometeoroids in space is known and they seriously compromise the survivability of space systems. Careful consideration of micrometroroid effects is therefore necessary to safegaurd against potentially debilitating damage otherwise incurred.

Three principle mechanisms by which meteoroids cause damage are: erosion, spalling, and puncture. The abrasive action of meteoroids on metal surfaces may exceed $2x10^{-4}$ cm/yr [1]. Meteoroid fluxes may, therefore, lead to significant attrition of a radiators emissive coating over long periods and result in reducing its radiative power; additional radiator area would then be necessary to accomodate this reduction in radiator effectiveness. In addition, solar protons may erode another $10^{-3}$ - $10^{-4}$ cm/yr from exposed surfaces; this effect, however, quickly diminishes as the inverse square of the distance from the sun. Highly reflective surfaces are effected in a similar manner since they are typically either polished metals or an evaporated film. Evaporated films may be on the order of several atomic diameters thick and thus its degradation below the acceptable limits of performance may occur in much less than a years time. Thickening of the film layer may sufficiently extend performance life.

Spalling, the process by which small metal chips are expelled from an interior surface due to an external impact, may cause problems in the power conversion system if the metal chips reach the turbine or bearings. Due to the large size of the hear pipe radiator in the MPR-300 system, the majority of the spalling is expected to occur there. The radiator modules, however, do not carry primary coolant but their own working fluid. Thus, spalling would have its most serious effect on the heat pipe manifold and other piping in the power conversion cycle, all of which carry primary coolant.

The puncture of sytem piping by micrometeoroids also poses a serious problem. The resulting holes in piping and tanks allows the slow release of coolant and propellant respectively. This implies the necessity of a reserve coolant supply as well as extra propellant and redundant heat pipes. Since only sparse knowledge of the meteoroid environment in space exists, it is difficult to establish protection criteria. However, the meteoroid penetration theory developed by Summers and Charters [8] provides a means of calculating the probability of no system failure due to meteoroid damage ($P_0$) as a function of exposed area, exposure time, and target material properties ( see Figure 7.6 and Table 7.2). With these data it is possible to view the required propellant tank wall thickness from another design perspective as well as provide an estimate of the additional heat pipe modules necessary to accomodate failures.

Considering a propellant temperature of 300 K, the required tank wall thickness was found to be 1.2 mm stainless steel. From Table 7.2 and Figure 7.6, this yields a $P_0$ of 0.968 for all 4 propellant tanks in a nine month flight. For reliability, an additional tank of $NH_3$ was included in the design. Computation of the appropriate number of redundant heat pipes was carried out similarly. The heat pipe walls are composed of stainless steel 1.5 mm thick and the sensitive area is 29.5 $m^2$; a nine month flight yields $P_0 = 0.864$. Subsequently, about 13.6% more heat pipes were added to the design to replace the number of expected module failures.

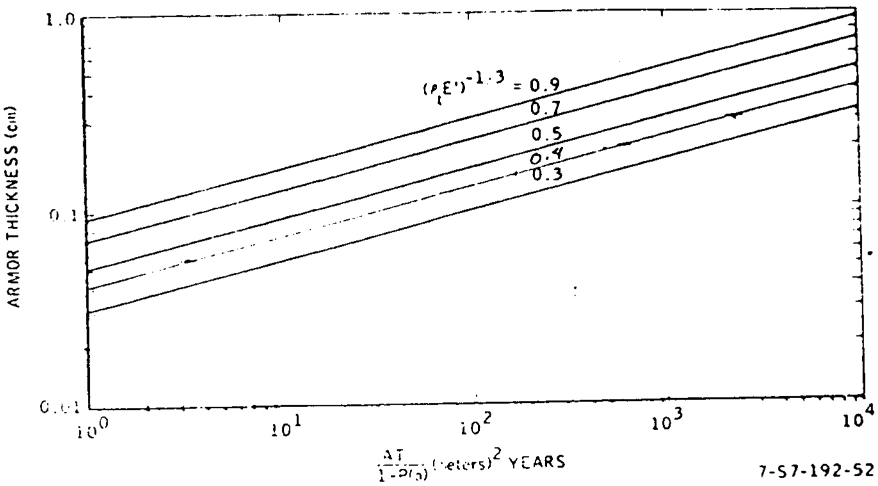


Meteoroid Armor Thickness Requirements

Figure 7.6 [8]

METEOROID ARMOR MATERIAL PROPERTIES

| Material | Density (g/cc) | E x $10^{-6}$ (kg/cm$^2$) | $\rho_t E'^{-1/3}$ | $\rho_t^{2/3} E'^{-1/3}$ |
|---|---|---|---|---|
| Beryllium | 1.85 | 2.9 | 0.57 | 1.1 |
| Aluminum | 2.7 | 0.63 | 0.83 | 2.2 |
| Iron | 7.9 | 2.1 | 0.39 | 3.1 |
| Molybdenum | 10.2 | 3.3 | 0.31 | 3.2 |
| Stainless Steel | 7.9 | 1.9 | 0.4 | 3.2 |
| Copper | 8.9 | 1.1 | 0.46 | 4.1 |

1 kg/cm$^2$ = 14.4 psi

Table 7.2 [8]

## References


1. W. R. Corliss, "Propulsion Systems for Space Flight", pp 19-62, McGraw-Hill Book Company, Inc., New York, Toronto, London, 1960.

2. H. F. Crouchy, "Nuclear Space Propulsion", chapter 12, Astronuclear Press, Granada Hills, California, 1965.

3. R. Jahn, "Physics of Electric Propulsion", chapter 8, pp 240-246, McGraw-Hill Book Company, Inc., 1968.

4. E. K. Inall, "High Power High Energy Pulse Production and Application", chapter 1, ANU Press Canberra, 1978.

5. F. P. Incropera, D. P. DeWitt, "Fundamentals of Heat and Mass Transfer", chapter 12, John Wiley & Sons, New York, Chichester, Brisbane, Toronto, Singapore, 1985.

6. J. H. Rust, "Nuclear Power Plant Engineering", chapter 8, S. W. Holland Company, Atlanta, Georgia, 1979.

7. R. W. Bussard, R. D. DeLauer, "Fundamentals of Nuclear Flight", pp 360-367, McGraw-Hill Book Company, New York, St. Louis, San Francisco, London, Sydney, 1967.

8. H. M. Dieckamp, "Nuclear Space Power Systems", pp 112-123, Atomics International (a division of North American Aviation, Inc.), Canoga Park, Califoria, 1967.

## IV. Conclusions and Recommendations

Several aspects of the design project should be further examined and a more detailed analysis performed. Additional neutronics work could include two dimensional and multigroup computations and examining the possibility of reducing the core size by increasing the enrichment of the fuel. Thermal hydraulics calculations could be modified by introducing radial conduction into the model which would lead to two dimensional computations. Changes in the Brayton cycle would consist of including an intercooler and regenerator to improve cycle efficiency. Modifications in the heat rejection system design would be performing a finite difference analysis on the fins and devising a mechanism so that the radiator system could be collapsed for entry into the Martian atmosphere. Additional propulsion analysis should include a more detailed calculation of trajectory, a more specific entry and landing plan such as aerobraking, and reduction of trip time. Overall areas which could be more closely examined are pressure losses and materials. A more realistic piping diagram should be developed and piping losses calculated for the system. Also, the pressure drop across the grid plate of the reactor needs to be reanalyzed. A materials search needs to be performed to identify materials compatible with carbon dioxide at high temperatures and identify a material for the turbine/compressor shaft.

## V. Summary

### Overall Hardware Layout

The layout of the pebble bed nuclear space reactor and associated equipment can be seen in Figure V.1 which is a spacecraft conceptual configuration. A more detailed configuration of the power system can be observed in Figure V.2. Note the jet engine type design where the turbine, reactor, and compressor are welded together. The reactor configuration can be seen in Figure V.3. Also note that the heat pipe radiators complete the power configuration loop but are not shown.

### System Schematic:

The thermodynamic cycle can be seen in Figure V.4. This is a Brayton cycle consisting of $CO_2$ gas coolant and the reactor, turbine, heat pipe radiator, and compressor loop. The four state points on the figure will be referred to later.

### Final Design Description:

The final design description can be observed in Tables V.1 through V.7. The only parameters not listed in the previous tables are the total mass of the $CO_2$ coolant which is 17.2 kg and the mass flow rate of 2.43 kg/s.

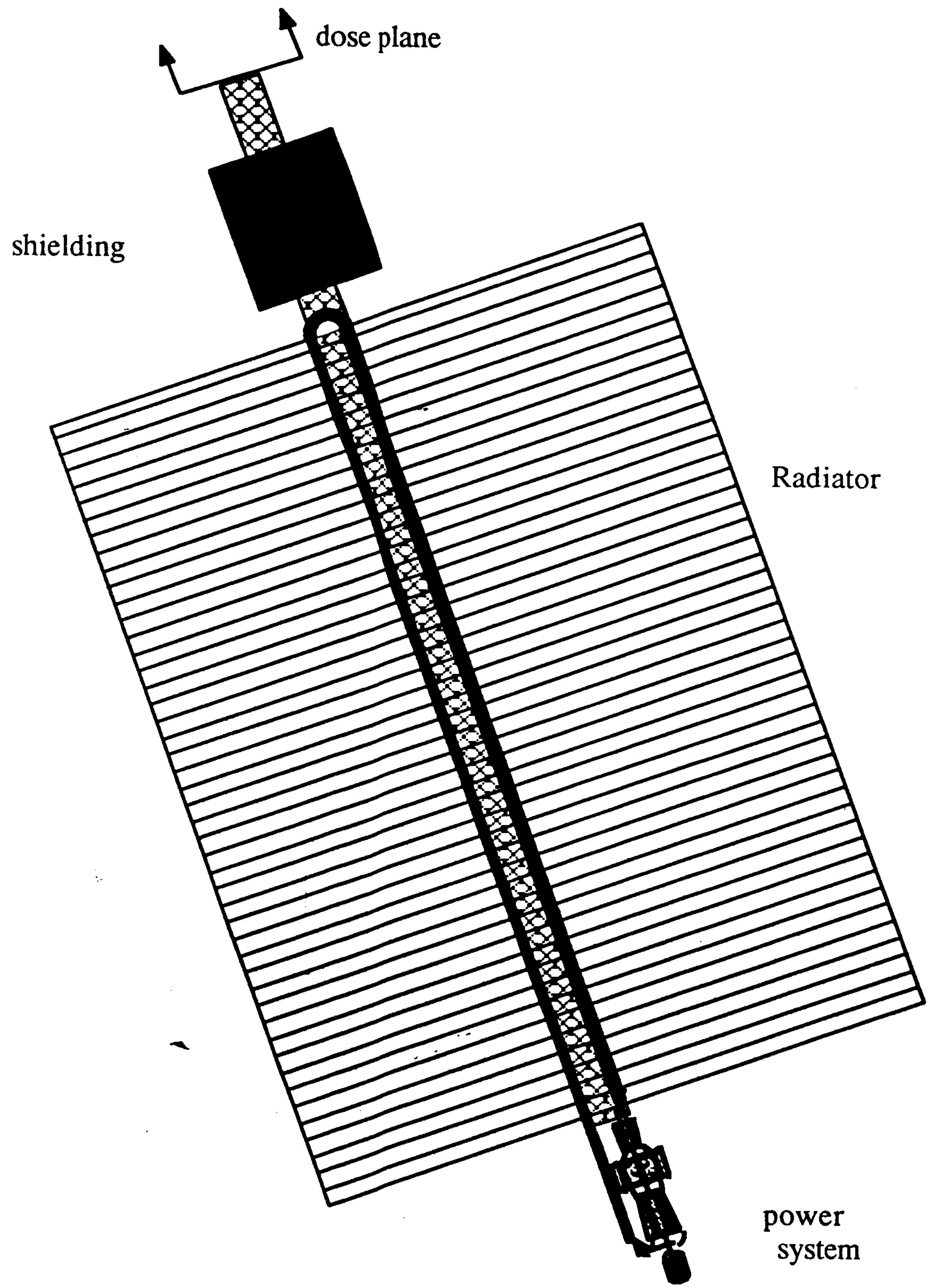


Figure V.3 Space Craft Configuration

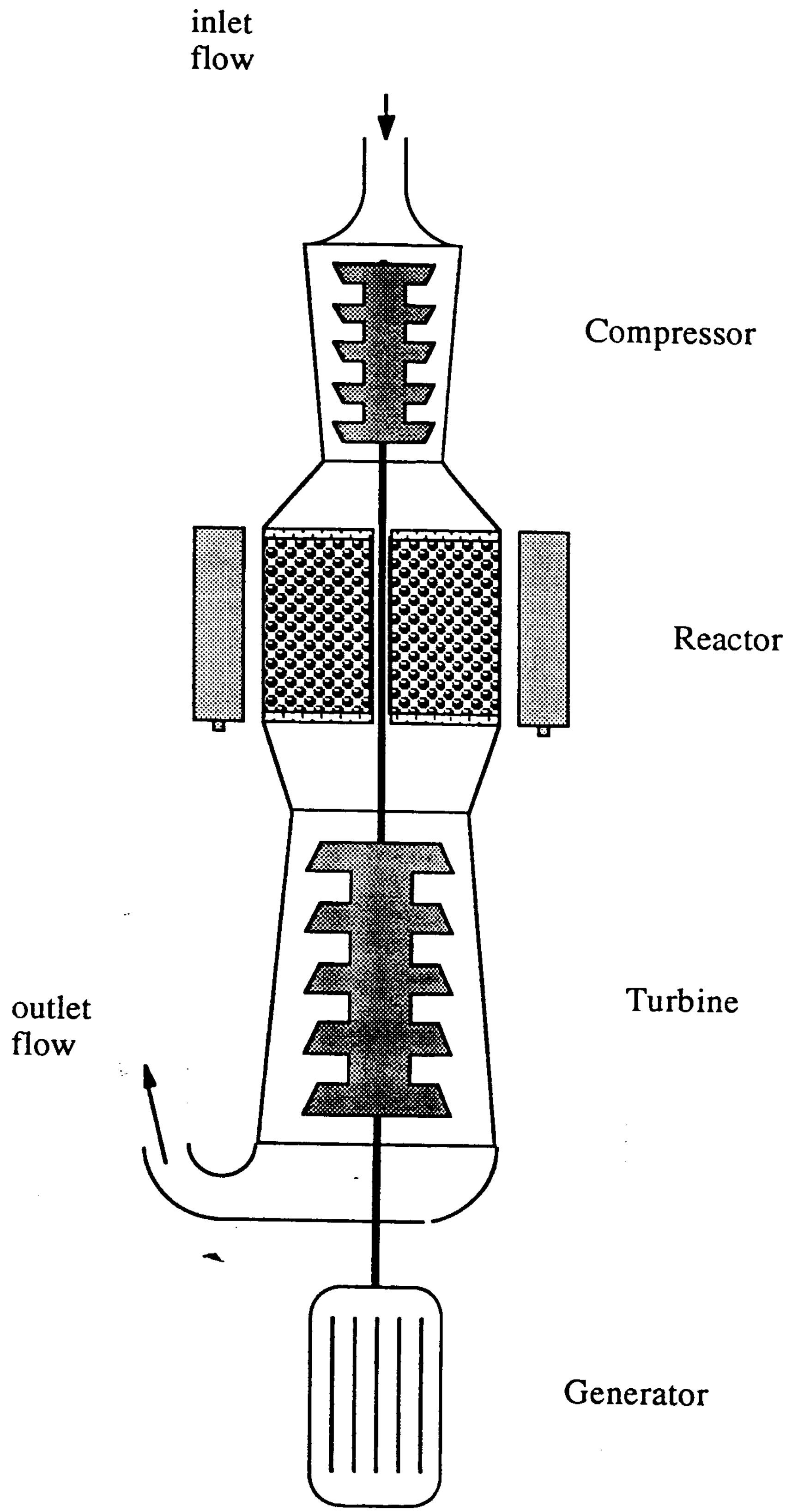


Figure V.2 Power System

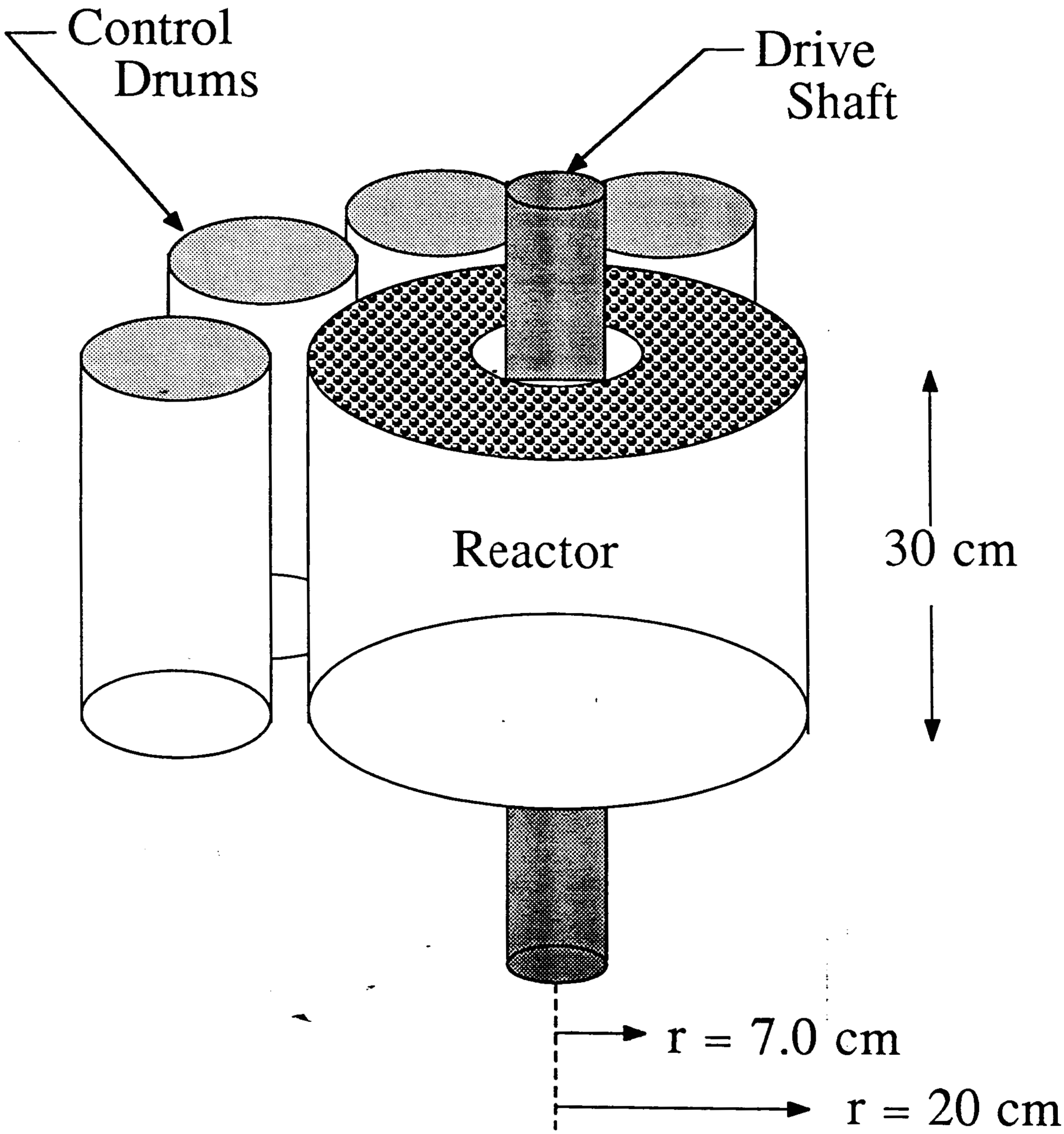


Figure V.3 Conceptual Reactor Design

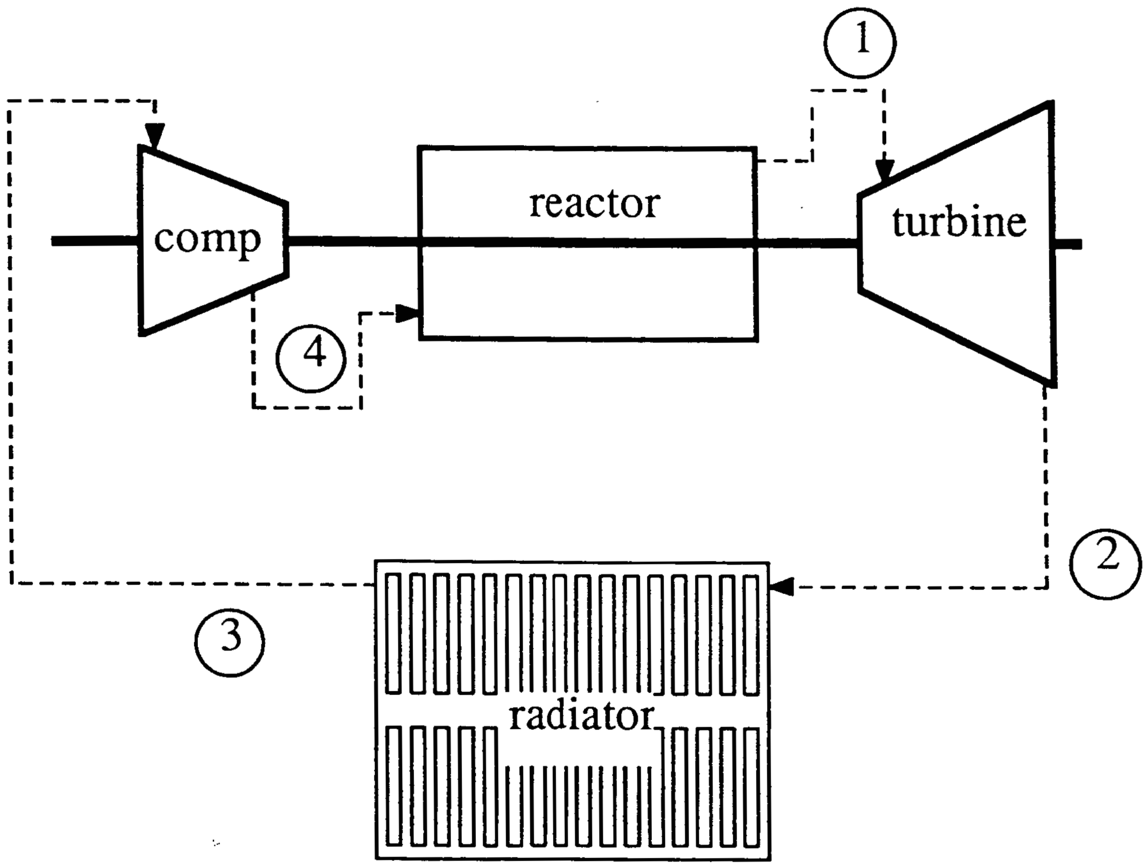


Figure V.4 System Brayton Cycle

Table V.1: Reactor parameters

| | |
|---|---|
| Thermal Output | 1 MWt |
| Electrical Output | 300 kWe |
| Power Density | 3.1 W/cm$^3$ |
| Active Core Volume | 32,330 cm$^3$ |
| CO2 fraction | 0.37 |
| UN fraction | 0.315 |
| PyC fraction | 0.315 |
| Peak to Average Flux Ratio | 1.12 |
| Power Production | |
| Thermal Flux | 91% |
| Fast Flux | 9% |
| Control Drum Diameter | 10 cm |
| Reactor core annular radius | 12.8 cm |
| Central Shaft Diameter | 6 cm |
| Reactor Vessel Wall Diameter | |
| inner | 4 cm |
| outer | 3 cm |
| Peak Fluxes | |
| thermal | 4.7E13 |
| fast | 7.3E14 |
| Reactor Height | 30 cm |
| Height to diameter ratio | 0.81 |

Table V.2 Fuel Parameters

| | |
|---|---|
| UN Fuel Mass | 145.7 kg |
| Fuel Enrichment | 8.0% |
| Mass of U-235 | 10.8 kg |
| critical mass at startup | 7.6 kg |
| fuel burnup | 3.2 kg |
| Specific Power | 6.86 kW/kg UN |
| # of Fuel Pebbles | 180,000 |
| Pebble Diameter | 0.602 cm |

Table V.3 System Thermodynamic States*

| State | Temperature (K) | Pressure (MPa) |
|---|---|---|
| 1 | 850 | 6.58 |
| 2 | 677 | 3.76 |
| 3 | 428 | 3.63 |
| 4 | 500 | 6.90 |

Table V.4 System Energy Balance

$Q_{in}$ = 1038 kW

$Q_{out}$ = 738 kW

$W_T$ = 513 kW

$W_C$ = 213 kW

h = 28.9 %

* Refer to Figure V.3 for the state points.

Table V.5 - Heat Rejection System

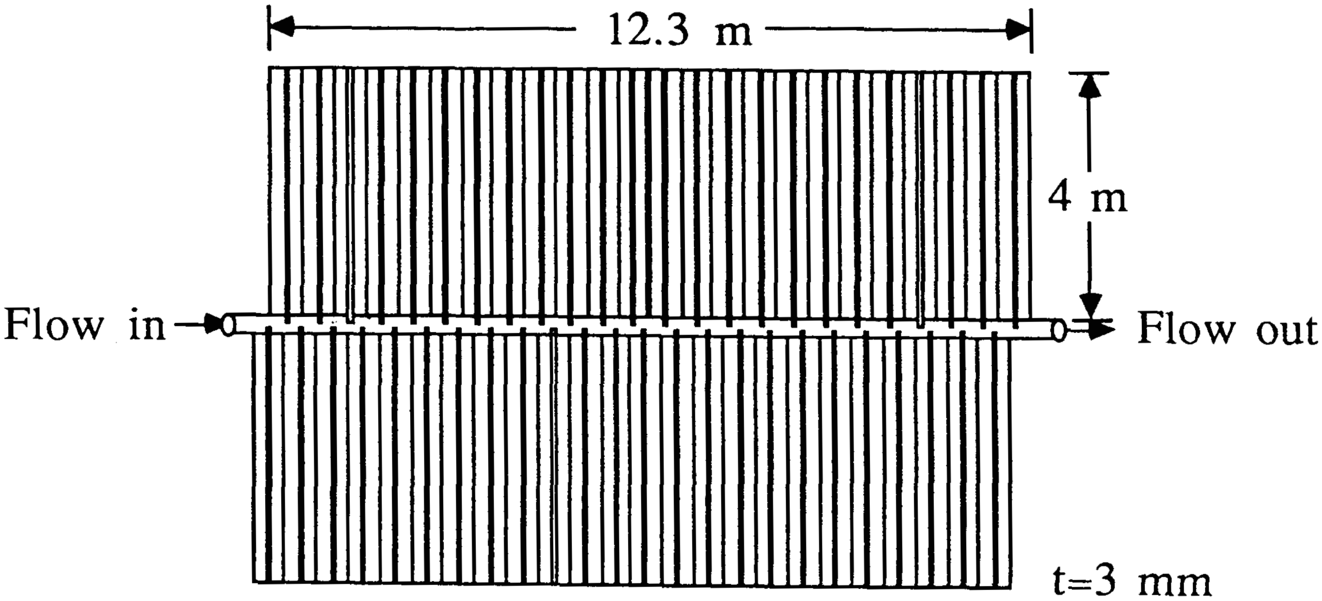


| | |
|---|---|
| • Total Area | 98 $m^2$ |
| • Mass | 1870 kg |
| • Heat Pipes | 246 |
| • Container Material | SS 304 |
| • Coating | $Al_2O_3$ |
| • Working Fluid | Sodium |
| • Fin Material | Aluminum |

Table V.6 Propulsion

| | |
|---|---|
| • MPD Thrusters | 13 units |
| • Total Craft Mass | 8000 kg |
| • Total Thrust | 3.6 N |
| • Propellant | $NH_3$ |
| Mass | 1571 kg |
| • Flight Time | 242 days |
| • MPD power | 296 kW |
| • Specific Impulse | 6140 seconds |

Table V.7 Masses

| | |
|---|---|
| • Propulsion | 2350 kg |
| • Reactor system and shield | 1029 kg |
| • Rotating machinery | 565 kg |
| • Ducting and structure | 700 kg |
| • Heat pipes | 2130 kg |
| • Miscellaneous | 480 kg |
| • Total Mass | 7254 kg |